UNIVERSITY OF CALIFORNIA,
IRVINE

Investigating the Interactions of Neuromodulators: A Computational Modeling, Game Theoretic, Pharmacological, Embodiment, and Neuroinformatics Perspective

DISSERTATION

submitted in partial satisfaction of the requirements
for the degree of

DOCTOR OF PHILOSOPHY

in Psychology-Cognitive Neuroscience

by

Andrew Zaldivar

Dissertation Committee:
Professor Jeffrey L. Krichmar, Chair
Professor Emily Grossman
Professor Kourosh Saberi

2014

TABLE OF CONTENTS

LIST OF FIGURES

LIST OF TABLES

ACKNOWLEDGEMENTS

The writing of this dissertation has been one of the most significant academic challenges I have ever had to face. Without the support, patience and guidance of the following people, this body of research would not have been completed. It is to them that I owe my deepest gratitude.

- My advisor and committee chair, and who I express my deepest appreciation towards, Professor Jeffrey L. Krichmar. He has the attitude and the substance of a genius. Without his guidance and persistent help, all the way back from when I first stumbled upon his office as an undergraduate, this dissertation would not have been possible.
- My committee, Professor Emily Grossman and Professor Kourosh Saberi. Their wisdom, knowledge, and commitment to the highest standards motivated me.
- The Intelligence Advanced Research Projects Activity (IRAPA), National Science Foundation (NSF), Office of Naval Research (ONR), and the Eugene-Cota Robles Diversity Fellowship for their financial support.
- My colleagues: Brian Cox, Michael Wei, Jayram Moorkanikara Nageswaran, Michael Avery, Chelsea Guthrie, Micah Richert, James Benvenuto, Grant Vousden-Dishington, Derrik Asher, Nicolas Oros, Michael Beyeler, Nikil Dutt, Feng Rong, Kristofor Carlson, Liam Bucci, Ting-Shuo Chou, Alexis Craig, and Emily Rounds. Without their support, life in the Cognitive Anteater Robotics Laboratory would not have been so joyous and inspiring.
- My friends and family for encouraging me in all of my pursuits and influencing me to follow my dreams. I am especially grateful to my father, Rolando Zaldivar. Even when circumstances were bleak, I always knew that you believed in me and wanted the best for me. Thank you for teaching me, day by day, that my job in life is to learn, to be happy, and to know and understand myself.

CURRICULUM VITAE

Andrew Zaldivar

EDUCATION

University of California, Irvine
Ph.D., Psychology-Cognitive Neuroscience, 2014

M.S., Psychology-Cognitive Neuroscience, 2012

B.A., Honors Psychology-Cognitive Sciences, 2009
Minor: Informatics

PUBLICATIONS

Zaldivar, A. and J. L. Krichmar (2014). "Allen Brain Atlas-Driven Visualizations: a web-based gene expression energy visualization tool." Frontiers in Neuroinformatics. 8:51.

Zaldivar, A. and J. L. Krichmar (2013). "Interactions between the neuromodulatory systems and the amygdala: exploratory survey using the Allen Mouse Brain Atlas." Brain Structure & Function 218(6): 1513-1530.

*****Asher, D. E., *****Craig, A. B., ***Zaldivar, A.**, et al. (2013). "A dynamic, embodied paradigm to investigate the role of serotonin in decision-making." Frontiers in Integrative Neuroscience 7: 78. (*****Contributed equally to this work.)

Asher, D. E., **Zaldivar, A**., et al. (2012). "Reciprocity and Retaliation in Social Games With Adaptive Agents." IEEE Transactions on Autonomous Mental Development 4(3): 226-238.

Asher, D. E., S. Zhang, **Zaldivar, A.**, Lee, M. D., & Krichmar, J. L. (2012). "Modeling Individual Differences in Socioeconomic Game Playing." Proceedings of the 34th Annual Conference of the Cognitive Science Society.

Chelian, S. E., N. Oros, **Zaldivar, A.**, Krichmar, J. L., & Bhattacharyya, R. (2012). "Model of the Interactions Between Neuromodulators and Prefrontal Cortex During a Resource Allocation Task." 2012 IEEE International Conference on Development and Learning and Epigenetic Robotics (ICDL). (Best paper award.)

Zaldivar, A., D. E. Asher, et al. (2010). "Simulation of How Neuromodulation Influences Cooperative Behavior." From Animals to Animats 11 6226: 649-660.

Ross, J., Irani, L., Silberman, M. S., **Zaldivar, A.**, & Tomlinson, B. (2010). "Who are the crowdworkers?: shifting demographics in mechanical turk." CHI '10 Extended

Abstracts on Human Factors in Computing Systems. Atlanta, Georgia, USA, ACM: 2863-2872.

Patterson, D. J., Ding, X., Kaufman, S. J., Liu, K. & **Zaldivar, A**. (2009). "An Ecosystem for Learning and Using Sensor-Driven IM Status Messages." IEEE Pervasive Computing 8(4): 42-49.

AWARDS

Associate Dean's Fellowship, 2013
Travel Grant to Participate in the Allen Institute for Brain Science Hackathon in Seattle, Washington, 2012
Eugene Cota-Robles Diversity Fellowship for Graduate Studies, 2009
Scholar of Distinction & Order of Merit, 2009
Outstanding Transfer Student Scholarship, 2009
Undergraduate Research Opportunities Program Honorary Fellowship, 2008
Psychology Honors Program, 2008
Summer Undergraduate Research Fellowship in Information Technology, 2008

ABSTRACT OF THE DISSERTATION

Investigating the Interactions of Neuromodulators: A Computational Modeling, Game Theoretic, Pharmacological, Embodiment, and Neuroinformatics Perspective

By

Andrew Zaldivar

Doctor of Philosophy in Psychology-Cognitive Neuroscience

University of California, Irvine, 2014

Professor Jeffrey L. Krichmar, Chair

Neuromodulatory systems originate in nuclei localized in the subcortical region of the brain and control fundamental behaviors by interacting with many areas of the central nervous system. Much is known about neuromodulators, but their structural and functional implications in fundamental behavior remain unclear. This dissertation set out to investigate the interaction of neuromodulators and their role in modulating behaviors by combining methodologies in computational modeling, game theory, embodiment, pharmacological manipulations, and neuroinformatics. The first study introduces a novel computational model that predicts how dopamine and serotonin shape competitive and cooperative behavior in a game theoretic environment. The second study adopted the model from the first study to gauge how humans react to adaptive agents, as well as measuring the influence of embodied agents on game play. The third study investigates functional activity of these neuromodulatory circuits by

exploring the expression energy of neuromodulatory receptors using the Allen Brain Atlas. The fourth study features a web application known as the Allen Brain Atlas-Drive Visualization, which provides users with a quick and intuitive way to survey large amounts of expression energy data across multiple brain regions of interest. Finally, the last study continues exploring the interaction of dopamine and serotonin by focusing specifically on the reward circuit using the Allen Brain Atlas. The first two studies provide a more behavioral understanding of how dopamine and serotonin interacts, what that interaction might look like in the brain, and how those interactions transpire in complex situations. The remaining three studies uses a neuroinformatics approach to reveal the underlying empirical structure and function behind the interactions of dopamine, serotonin, acetylcholine and norepinephrine in brain regions responsible for the behaviors discussed in the first two studies. When combined, each study provides an additional level of understanding about neuromodulators. This is of great importance because neuroscience simply cannot be explained through one methodology. It is going to take a multifaceted effort, like the one presented in this dissertation, to obtain a deeper understanding of the complexity behind neuromodulators and their structural and functional relationship with each other.

INTRODUCTION

Neuromodulatory systems, composed of relatively small nuclei of neurons, are located in the sub-cortical region of the brain and control fundamental behaviors through interactions with board areas of the nervous system (Briand, Gritton et al. 2007; Krichmar 2008). When a biological organism experiences an important event in the environment, the activation of neuromodulatory systems contributes to the organism's ability to commit an action accordingly. These actions include mitigating responses to risks, rewards, attentional effort and novelty. Thus, it is important to understand the underlying structures of these neuromodulatory systems because they have an important role in higher-order cognition and in an organism's survival.

The nuclei of each neuromodulatory system contain neurons that produce specific neurotransmitters, which then project to broad and extensive areas in the nervous system. Serotonin (5-HT, 5-hydroxytryptamine or serotonergic) originates in the raphe nuclei of the brainstem, which projects to almost all forebrain areas. In particular, the cortex, ventral striatum, hippocampus and amygdala are amongst brain areas that are heavily innervated by raphe nuclei efferents (Harvey 2003; Meneses and Perez-Garcia 2007). It has been suggested that serotonin influences a broad range of decision-based functions such as reward assessment, cost assessment, impulsivity, harm aversion, and anxious states (Asher, Craig et al. 2013). Dopamine (DA or dopaminergic) is produced by two groups of cell bodies in the mesencephalon: the substantia nigra and the ventral tegmental area. The

ventral tegmental area projects to various subcortical and cortical regions that mediate reward related behaviors (Hyman, Malenka et al. 2006). The substantia nigra is the source of dopamine in the basal ganglia, which may contribute to their diverse roles in reward, addiction and movement (Ungless and Grace 2012). Acetylcholine (ACh or cholinergic) originates in the basal forebrain, which sends efferent projections to the cortex, amygdala, and hippocampus. Basal forebrain cholinergic neurons appear to modulate attention and optimize information processing (Baxter and Chiba 1999; Sarter, Hasselmo et al. 2005). Cholinergic neurons also originate in the brainstem pedunculopontine and laterodorsal tegmental nuclei and have projections to the amygdala, basal forebrain the ventral tegmental area (Semba and Fibiger 1992; Holmstrand and Sesack 2011). Norepinephrine (NE or noradrenergic) in the central nervous system is produced in the locus coeruleus, which projects to virtually all brain regions with the exception of basal ganglia (Berridge and Waterhouse 2003). The nucleus of the solitary tract (NTS) is another source of norepinephrine. There is a feedback loop in which the amygdala affects stress hormones, then the stress hormones act on the NTS, which then acts on the locus coeruleus, resulting in the release of norepinephrine in the amygdala. Activation of norepinephrine in the amygdala helps to consolidate and modulate memory in other brain regions (McGaugh 2004).

While much is known about the sources of these neurotransmitters, their projections and function in fundamental behavior, understanding how these neuromodulatory systems interact in order to give rise to decision-making and

adaptive behaviors remains elusive. To illuminate the intricacies of neuromodulators, a series of studies were conducted to explore the interaction between these neuromodulatory systems. This dissertation utilizes a multifaceted approach to better understand the interacting neuromodulatory mechanisms that give rise to adaptive behaviors.

Chapter 1 explores the roles of dopamine and serotonin during decision-making in games of conflict. A computational model of neuromodulation and action-selection was implemented for this study based on the assumption that dopamine activity is linked to incentive salience and "wanting" of a reward (Berridge 2004), referred to as expected reward (Schultz, Dayan et al. 1997), and serotonin activity is linked to cognitive control of stress, social interactions, and risk taking behavior (Millan 2003; Crockett, Clark et al. 2008), referred to as expected cost. With these assumptions, an agent, which is an autonomous entity in a simulated model whose behavior the neural model guided, played a game called Hawk-Dove, where players must choose between confrontational and cooperative actions (Axelrod and Hamilton 1981; Maynard Smith 1982). Game theory has had a long and productive history of predicting and describing human behavior in cooperative and competitive situations (Maynard Smith 1982; Nowak and Sigmund 1993; Nowak, Page et al. 2000; Skyrms and Pemantle 2000). Game theoretic approaches have also been used to illuminate the neural basis of economic and social decision-making (Lee 2008; Yamagishi, Horita et al. 2009; Rilling and Sanfey 2011). By building upon these dopamine and serotonin assumptions with a game theoretic approach, this

computational model can predict how neuromodulatory activity shapes behavior under various environmental and competitive situations.

Building upon this computational model of neuromodulation and action selection, Chapter 2 goes a step further by embedding this model in both simulated and embodied neural agents to investigate reciprocal social interactions in games of cooperation and conflict with human subjects. In this study, alongside Hawk-Dove, another game called Chicken (Rapoport and Chammah 1966) was used to analyze competitive situations in terms of expected rewards (dopamine activity) and costs (serotonin activity). Chicken forced players to decide on an action quickly without knowledge of the opponent's choice, as players do not know the decision their opponent has made until the outcome. Besides the addition of having both simulated and embodied neural agents play Hawk-Dove and Chicken against human subjects, this study also manipulated levels of serotonin in human subjects using an acute tryptophan depletion (ATD) procedure. ATD is a dietary reduction of tryptophan, an amino acid precursor of serotonin, which causes a rapid decrease in the synthesis and release of central serotonin in human brain, thus affecting behavioral control (Nishizawa, Benkelfat et al. 1997). Altering serotonin levels via ATD has been shown to influence a subject's ability to resist a small immediate reward over a larger delayed reward (Schweighofer, Bertin et al. 2008; Tanaka, Shishida et al. 2009), as well as predicting punishment or harm aversion (Crockett, Clark et al. 2009; Seymour, Daw et al. 2012). Manipulating levels of serotonin helps

test the influence of embodiment and serotonin on decisions where there is a tradeoff between cooperation and competition.

Moving away from computational modeling, game theory and dietary manipulation, Chapter 3 takes explores other techniques of investigating neurmodulation by surveying receptor gene expression data of neuromodulatory systems retrieved from neuroinformatics resources to better understand the organization of brain circuitry involved with neuromodulators. Because neuromodulatory systems have distinct sources, one can infer connectivity by assuming that there are projections from the source to sites where specific neuromodulatory receptors are expressed. Gene expression is a molecular process where a gene, a segment of DNA, is turned into a protein or RNA structure. Gene expression is often visualized through fluorescence in situ hybridization (ISH), a technique that uses a labeled complementary RNA strand to localize a specific RNA sequence in a section of tissue. With ISH, detecting specific mRNA sequences can localize elements important to neuronal processing, such as receptors, transporters and growth factors. The ability to identify these essential components of brain and behavior encouraged organizations to put together publicly accessible neuroinformatics resources that contain massive amounts of gene expression data for other researchers to conduct scientific work. Neuroinformatics is an emerging field that is concerned with the management and sharing of neuroscience data. The Allen Mouse Brain Atlas (ABA) project from the Allen Institute for Brain Science is one such neuroinformatics resource that contains public data sets of extensive gene

expression and neuroanatomical data with a suite of search and viewing tools (Hawrylycz, Lein et al. 2012; Sunkin, Ng et al. 2013). By data mining the ABA, the gene expression profile of serotonin, dopamine, cholinergic and adrenergic receptor genes were characterized within anatomical origins of these neuromodulatory systems, as well as in the amygdala, which is important for cognitive behavior and has known interactions with all the neuromodulatory systems (McGaugh 2004; Bouret and Sara 2005; Lee, Wheeler et al. 2011).

Influenced by methodology used in Chapter 3 to retrieve expression data, Chapter 4 details a web application created for other researchers to conduct analysis on other neural systems with characteristics similar to those discussed in Chapter 3, but without dealing with the complexities of interfacing with raw neuroinformatics resources. The web application, called the Allen Brain Atlas-Driven Visualization (ABADV), is a publicly accessible tool created to retrieve and visualize expression energy data from the ABA ISH mouse data set across multiple genes and brain structures. When studying gene expression, researchers analyze changes in the expression of a particular gene or set of genes by quantifying the amount of its gene-specific transcript. Researchers use gene expression data in various ways, such as investigating profiles or patterns of expression across several genes, cross-species comparisons, searching for biomarkers, validating various data modalities, correlating gene expression to neuroanatomy, and other large-scale data analysis (Jones, Overly et al. 2009). The ability to measure and localize these gene-specific transcripts in the nervous system enables researchers to investigate a broad

range of brain-related phenomena. While the ABA takes care of measuring and localizing these gene-specific transcripts, their sophisticated tools to navigate their large data set come with a steep learning curve (Hawrylycz, Lein et al. 2012; Sunkin, Ng et al. 2013). Using the ABA application programming interface (API), ABADV programmatically retrieves mouse gene expression data across brain structures specified by users and generates visualizations using Data-Driven Documents (D3), a programming library that uses data to drive the creation and control of visualizations in web browsers (Bostock, Ogievetsky et al. 2011). To demonstrate the effectiveness of ABADV, a query was performed using both ABADV and Brain Explorer 2, which is a desktop application the Allen Institute for Brain Science created for viewing their reference atlases and gene expression data (Sunkin, Ng et al. 2013). A comparison of these tools highlighted the ease of visualization through ABADV.

Using ABADV, Chapter 5 continues to explore the comprehensive ABA ISH mouse data set, this time surveying genes that encode dopamine and serotonin receptors within brain structures associated with the reward processing (Nakamura 2013; Russo and Nestler 2013). The reward circuit, which is comprised of several subcortical and cortical brain structures forming a network responsible for mediating various aspects of reward processing, is a key component for driving incentive-based learning and developing goal-directed behaviors (Haber and Knutson 2010). Reward not only refers to a pleasant stimulus, but also the active processes in the brain that responds to a stimulus rather than the stimulus itself.

These responses include the 'liking' or the actual pleasure component of a reward, the 'wanting' or the motivation for acquiring a reward, and the 'learning' or the associations about future rewards based on experience. (Berridge and Kringelbach 2008). Though studies have identified dopamine neurons originating in the ventral tegmental area having a primary role in modulating learning and activity in reward processing (Hyman, Malenka et al. 2006), other studies also suggest that serotonin neurons of the dorsal raphe nucleus have a pivotal role in the emotional, motivational and cognitive aspects of reward representation, in addition to its role in modulating the behavioral response to threats and risks (Nakamura, Matsumoto et al. 2008; Kranz, Kasper et al. 2010). Understanding the complex interactions between dopamine and serotonin continues to pose a hurdle in understanding reward mechanisms, one that the comprehensive ABA may help in illuminating the underlying mechanisms of the reward circuit by profiling dopamine and serotonin receptor genes.

By using computational modeling, game theory, embodiment, pharmacological manipulation and neuroinformatics in novel ways, these studies have contributed to clarifying the interaction of neuromodulatory systems and their role in modulating fundamental behaviors. Using multiple techniques, instead of a single approach, to draw conclusions about the neuromodulatory system may enable the research community to make stronger predictions about the neuroscience that ties together these neuromodulators to brain behavior.

References

Asher, D. E., A. B. Craig, et al. (2013). "A dynamic, embodied paradigm to investigate the role of serotonin in decision-making." Front Integr Neurosci 7.

Axelrod, R. and W. D. Hamilton (1981). "The evolution of cooperation." Science 211(4489): 1390-1396.

Baxter, M. G. and A. A. Chiba (1999). "Cognitive functions of the basal forebrain." Curr Opin Neurobiol 9(2): 178-183.

Berridge, C. W. and B. D. Waterhouse (2003). "The locus coeruleus-noradrenergic system: modulation of behavioral state and state-dependent cognitive processes." Brain Res Brain Res Rev 42(1): 33-84.

Berridge, K. C. (2004). "Motivation concepts in behavioral neuroscience." Physiol Behav 81(2): 179-209.

Berridge, K. C. and M. L. Kringelbach (2008). "Affective neuroscience of pleasure: reward in humans and animals." Psychopharmacology (Berl) 199(3): 457-480.

Bostock, M., V. Ogievetsky, et al. (2011). "D^3 Data-Driven Documents." Visualization and Computer Graphics, IEEE Transactions on 17(12): 2301-2309.

Bouret, S. and S. J. Sara (2005). "Network reset: a simplified overarching theory of locus coeruleus noradrenaline function." Trends Neurosci 28(11): 574-582.

Briand, L. A., H. Gritton, et al. (2007). "Modulators in concert for cognition: Modulator interactions in the prefrontal cortex." Prog Neurobiol 83(2): 69-91.

Crockett, M. J., L. Clark, et al. (2009). "Reconciling the role of serotonin in behavioral inhibition and aversion: acute tryptophan depletion abolishes punishment-induced inhibition in humans." J Neurosci 29(38): 11993-11999.

Crockett, M. J., L. Clark, et al. (2008). "Serotonin modulates behavioral reactions to unfairness." Science 320(5884): 1739.

Haber, S. N. and B. Knutson (2010). "The Reward Circuit: Linking Primate Anatomy and Human Imaging." Neuropsychopharmacology 35(1): 4-26.

Harvey, J. A. (2003). "Role of the serotonin 5-HT2A receptor in learning." Learn Mem 10(5): 355-362.

Hawrylycz, M. J., S. Lein, et al. (2012). "An anatomically comprehensive atlas of the adult human brain transcriptome." Nature 489(7416): 391-399.

Holmstrand, E. C. and S. R. Sesack (2011). "Projections from the rat pedunculopontine and laterodorsal tegmental nuclei to the anterior thalamus and ventral tegmental area arise from largely separate populations of neurons." Brain Structure & Function 216(4): 331-345.

Hyman, S. E., R. C. Malenka, et al. (2006). "Neural mechanisms of addiction: the role of reward-related learning and memory." Annu Rev Neurosci 29: 565-598.

Jones, A. R., C. C. Overly, et al. (2009). "The Allen Brain Atlas: 5 years and beyond." Nat Rev Neurosci 10(11): 821-828.

Kranz, G. S., S. Kasper, et al. (2010). "Reward and the serotonergic system." Neuroscience 166(4): 1023-1035.

Krichmar, J. L. (2008). "The Neuromodulatory System – A Framework for Survival and Adaptive Behavior in a Challenging World." Adaptive Behavior 16: 385-399.

Lee, D. (2008). "Game theory and neural basis of social decision making." Nat Neurosci 11(4): 404-409.

Lee, H. J., D. S. Wheeler, et al. (2011). "Interactions between amygdala central nucleus and the ventral tegmental area in the acquisition of conditioned cue-directed behavior in rats." European Journal of neuroscience 33(10): 1876-1884.

Maynard Smith, J. (1982). Evolution and the theory of games, Cambridge University Press.

McGaugh, J. L. (2004). "The amygdala modulates the consolidation of memories of emotionally arousing experiences." Annu Rev Neurosci 27: 1-28.

Meneses, A. and G. Perez-Garcia (2007). "5-HT1A receptors and memory." Neurosci Biobehav Rev 31(5): 705-727.

Millan, M. J. (2003). "The neurobiology and control of anxious states." Prog Neurobiol 70(2): 83-244.

Nakamura, K. (2013). "The role of the dorsal raphe nucleus in reward-seeking behavior." Front Integr Neurosci 7: 60.

Nakamura, K., M. Matsumoto, et al. (2008). "Reward-dependent modulation of neuronal activity in the primate dorsal raphe nucleus." J Neurosci 28(20): 5331-5343.

Nishizawa, S., C. Benkelfat, et al. (1997). "Differences between males and females in rates of serotonin synthesis in human brain." Proceedings of the National Academy of Sciences of the United States of America 94(10): 5308-5313.

Nowak, M. and K. Sigmund (1993). "A strategy of win-stay, lose-shift that outperforms tit-for-tat in the Prisoner's Dilemma game." Nature 364(6432): 56-58.

Nowak, M. A., K. M. Page, et al. (2000). "Fairness versus reason in the ultimatum game." Science 289(5485): 1773-1775.

Rapoport, A. and A. M. Chammah (1966). "The game of chicken." American Behavioral Scientist 10(3): 10-28.

Rilling, J. K. and A. G. Sanfey (2011). "The neuroscience of social decision-making." Annu Rev Psychol 62: 23-48.

Russo, S. J. and E. J. Nestler (2013). "The brain reward circuitry in mood disorders." Nat Rev Neurosci 14(9): 609-625.

Sarter, M., M. E. Hasselmo, et al. (2005). "Unraveling the attentional functions of cortical cholinergic inputs: interactions between signal-driven and cognitive modulation of signal detection." Brain Res Brain Res Rev 48(1): 98-111.

Schultz, W., P. Dayan, et al. (1997). "A neural substrate of prediction and reward." Science 275(5306): 1593-1599.

Schweighofer, N., M. Bertin, et al. (2008). "Low-serotonin levels increase delayed reward discounting in humans." J Neurosci 28(17): 4528-4532.

Semba, K. and H. C. Fibiger (1992). "Afferent connections of the laterodorsal and the pedunculopontine tegmental nuclei in the rat: a retro- and antero-grade transport and immunohistochemical study." Journal of Comparative Neurology 323(3): 387-410.

Seymour, B., N. D. Daw, et al. (2012). "Serotonin selectively modulates reward value in human decision-making." J Neurosci 32(17): 5833-5842.

Skyrms, B. and R. Pemantle (2000). "A dynamic model of social network formation." Proc Natl Acad Sci U S A 97(16): 9340-9346.

Sunkin, S. M., L. Ng, et al. (2013). "Allen Brain Atlas: an integrated spatio-temporal portal for exploring the central nervous system." Nucleic Acids Res 41(Database issue): D996-D1008.

Tanaka, S. C., K. Shishida, et al. (2009). "Serotonin affects association of aversive outcomes to past actions." J Neurosci 29(50): 15669-15674.

Ungless, M. A. and A. A. Grace (2012). "Are you or aren't you? Challenges associated with physiologically identifying dopamine neurons." Trends Neurosci 35(7): 422-430.

Yamagishi, T., Y. Horita, et al. (2009). "The private rejection of unfair offers and emotional commitment." Proc Natl Acad Sci U S A 106(28): 11520-11523.

CHAPTER 1: Simulation of Dopamine, Serotonin and Their Influences on Cooperative and Competitive Behavior

This study explores the research question of how the interplay between cost and reward could lead to appropriate decision-making under varying conditions in a game theoretic environment. To test this question, several predictions as to how the activity of a reward and cost function leads to appropriate action selection in competitive and cooperative environments were computationally modeled. This computational model was based on the assumptions that dopaminergic activity increases as expected reward increases, and serotonergic activity increases as the expected cost of an action increases.

Game Theory and Hawk-Dove

Game theory is a toolbox utilized in a multitude of disciplines for its ability to quantitatively measure and predict behavior in situations of cooperation and competition (Maynard Smith 1982; Nowak, Page et al. 2000; Skyrms 2001). It operates on the principle that organisms will balance reward with effort while acting in self-interest to obtain the optimal result in a given situation. Game theory is especially valuable as a way to study human behavior because it provides a replicable, predictable, and controlled environment with defined boundaries. These elements are essential when introducing computer agents as opponents.

The computational model created for this study played a game called Hawk-Dove, where players must choose between confrontational and cooperative tactics against a computer algorithm with fixed strategies (Maynard Smith and Parker

1973; Axelrod and Hamilton 1981). In this study's variant of Hawk-Dove (Figure 1.1), players were contesting over a resource in an area referred to as the territory of interest (TOI).

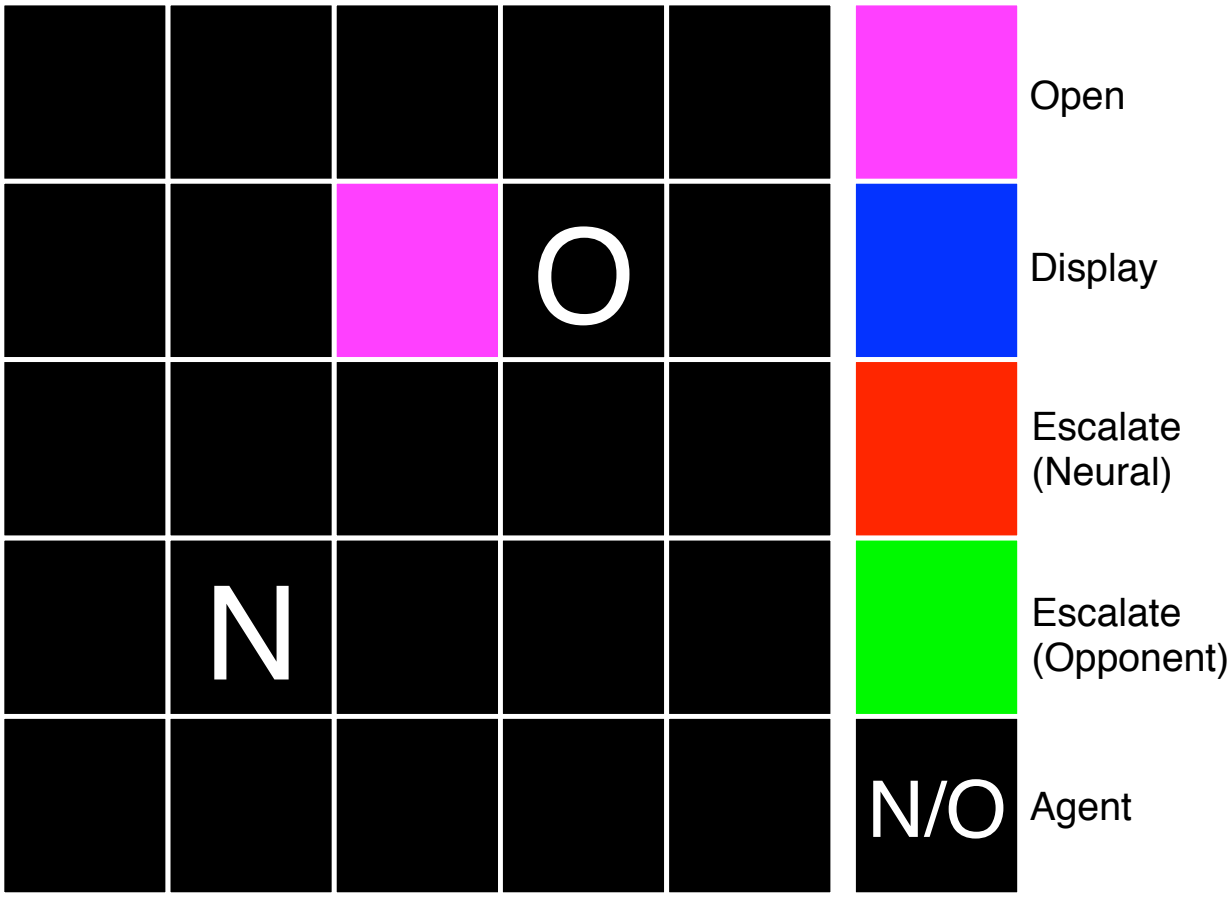

Figure 1.1. Game Diagram for Hawk-Dove. In Hawk-Dove, two players must compete for a territory, deciding either to be submissive (display) or aggressive (escalate), avoiding or risking injury in hopes of a larger payoff, respectively. The game board included a 5 × 5 grid of squares, upon which a territory was marked and the human and neural agent players were placed. The color of the territory reflected the state of the players' actions.

At the start of every game of Hawk-Dove, each player and the TOI were randomly placed inside an environment. Once a player reached the TOI, the player had to choose between two actions: escalate (an aggressive, confrontational tactic) or display (a nonviolent, cooperative tactic). If both players chose to escalate, they fought, resulting in an injury or penalty, which could either be serious or mild. If

only one player chose to escalate, then the escalating player received the total value of the TOI, and the other player received nothing. If both players chose to display, then there was a tie, and both players split the value of the TOI. The variant of Hawk-Dove used in this study also modified the harshness of the environment in certain experimental conditions by increasing the likelihood of receiving a serious injury when escalating. Thus, players must choose between a high-risk, high-payoff option, and a low-risk, low payoff option.

Two agents played this study's variant of Hawk-Dove: one agent was a computer model, whose actions were guided by either a rigid strategy or probabilities (*Opponent*), the other agent was a neural network model that mimicked the effects of serotonin and dopamine on action selection and learning (*Neural*). After each game, payoff was calculated and plastic connections were updated based on outcome (Table 1.1). The computational model played a total of 100 series, where each series consisted of 100 games.

Table 1.1 Payoff Matrix for Hawk-Dove. V is the value of the resource and is set to 0.60. D is the damage incurred when both players escalate. D is set to 1.60 for serious injury and 0.62 for a scratch. The probability of a serious injury is 0.25 or 0.75.

	B. Escalate	**B. Display**
A. Escalate	A: (V–D)÷2, B: (V–D)÷2	A: V, B: 0
A. Display	A: 0, B: V	A: V÷2, B: V÷2

At the start of each series, the neural network was initialized and the *Neural* agent was considered "naïve", that is, the weights of the network were set to their initial values. For each series, the two agents played Hawk-Dove with a randomly selected parameter set that dictated which of one the three opponents the *Neural* was going to play against or the harshness of the environment (e.g., whether the

probability of serious injury or escalation from the *Opponent* agent was going to be low, which is 0.25, or high, which is 0.75).

Opponent Agent

The *Opponent* agent followed one of three strategies. In one strategy, referred to as the *Statistical* model, the agent had a probability of escalation independent of the *Neural* agent's tactics, which was set at the beginning of the game to 0.25 or 0.75. In the second strategy, referred to as Tit-For-Tat (TT), the computer model repeated the *Neural* agent's previous action. The only exception to this rule was if the *Opponent* agent reached the TOI first in the opening game, in which the *Opponent* agent opened with a Display. TT is a straight-forward, yet effective strategy in game theory, which has shown to be successful in game playing tournaments (Axelrod and Hamilton 1981). In the third strategy, referred to as Win-Stay, Lose-Shift (WSLS), the *Opponent* agent would win and stay with the same action in the following situations: the *Opponent* agent's Escalate is met with the *Neural* agent's *Display* or the *Opponent* agent's *Display* is matched by a *Neural* agent's *Display*, otherwise the *Opponent* agent resorted to a lose and shift action (Nowak and Sigmund 1993). As with the TT strategy, the WSLS opponent would open with a *Display* action if it arrived at the TOI first on the first game.

Neural Agent

To control the behavior of the *Neural* agent playing Hawk-Dove, a neural network-based computational model inspired by an organisms' central nervous system was implemented. The neural network comprised of three areas: *TOI-State*,

Action, and *Neuromodulatory* (Figure 1.2). The *TOI-State* included three neurons that corresponded to the possible states of the TOI the *Neural* agent may observe: 1) *Open*. The *Neural* agent reached the TOI first. 2) *Escalate*. The opponent reached the TOI first and escalated a conflict. 3) *Display*. The opponent reached the TOI first but did not start a conflict.

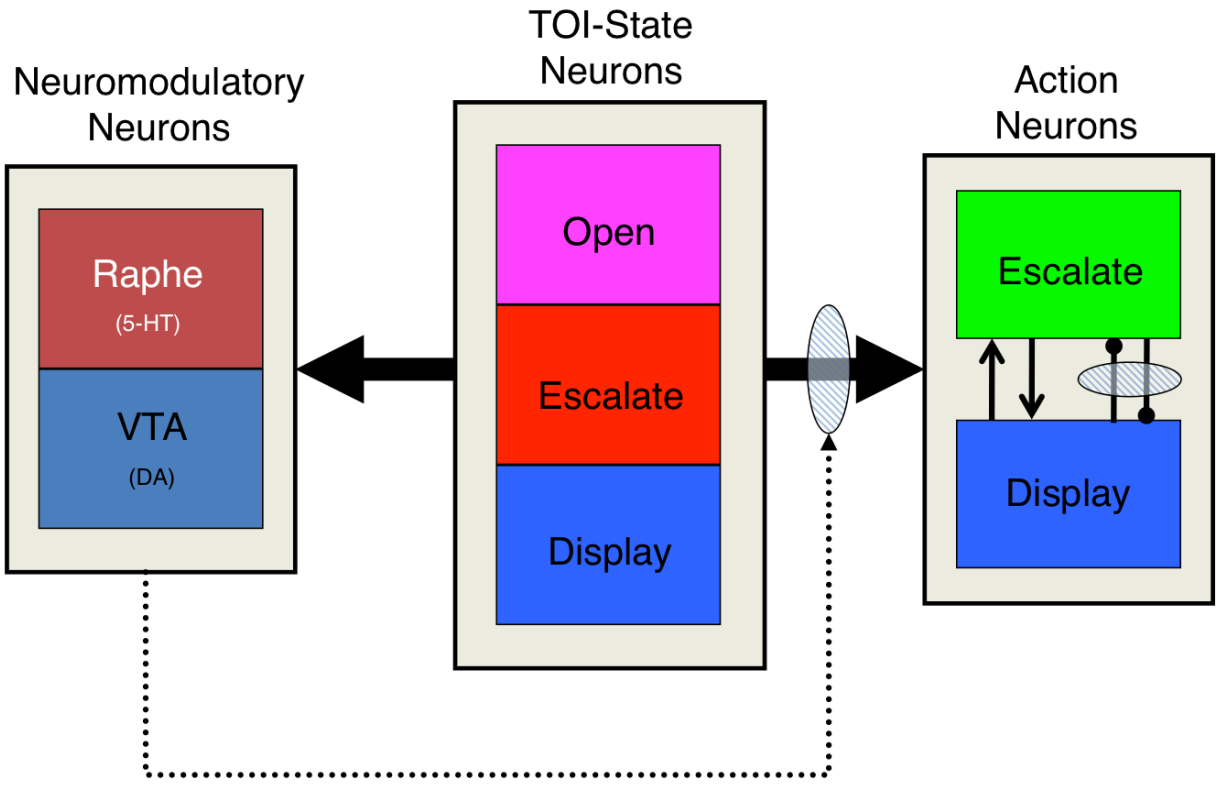

Figure 1.2. Neural Network Architecture for Hawk-Dove. The thick arrows represent all-to-all connections. The dotted arrows with the shaded oval represent modulatory plastic connections. Within the *Action* area, neurons with excitatory reciprocal connections are represented as arrow-ended lines, and neurons with reciprocal inhibitory connections are represented as dot-ended lines overlaid by a shaded oval, which denotes plasticity.

The equation for the activity of each of these neurons (n_i) was set based on the current state of the TOI:

$$n_i = \begin{cases} 0.75 + rnd(0.0,0.25), & i = TOI\text{-}State \\ rnd(0.0,0.25), & \text{Otherwise} \end{cases}$$

where $rnd(0.0,0.25)$ was a random number uniformly distributed between 0.0 and

0.25. The *Action* area included two neurons: 1) *Escalate*. The *Neural* agent escalated a conflict. 2) *Display*. The *Neural* agent did not start a conflict or retreated if the opponent escalated. The neural activity was based on input from *TOI-State* and neuromodulation. Lastly, the *Neuromodulatory* area included two neurons: 1) *Raphe*. A simulated raphe nucleus, which is the source of serotonergic neuromodulation. 2) *VTA*. A simulated ventral tegmental area, which is the source of dopaminergic neuromodulation. The synaptic connectivity of the network is shown in Figure 1.2 and in Table 1.2, and is all-to-all. Some of these connections were subject to synaptic plasticity and phasic neuromodulation, where the activity of *Neuromodulatory* neurons affected the synaptic efficacy.

Table 1.2. Synaptic Connections Between Neural Areas for Hawk-Dove.

From	To	Initial Weight	Plastic	Phasic Neuromodulation
TOI-State	*Action*	0.1	Y	Y
TOI-State	*Neuromodulator*	0.1	Y	N
Action	*Action*	0.1	N	N
Action	*Action*	-0.1	N	Y

The neural activity was simulated by a mean firing rate neuron model, where the firing rate of each neuron ranged continuously from 0 (quiescent) to 1 (maximal firing). The equation for the mean firing rate neuron model was:

$$s_i(t) = \rho_i s_i(t-1) + (1-\rho_i)\left(\frac{1}{1+\exp\left(-5I_i(t)\right)}\right)$$

where t was the current time step, s_i was the activation level of neuron i, ρ_i was a constant set to 0.1 and denoted the persistence of the neuron, and I_i was the synaptic input. The synaptic input of the neuron was based on pre-synaptic neural

activity, the connection strength of the synapse, and the amount of neuromodulatory activity:

$$I_i(t) = rnd(-0.5, 0.0) + \Sigma_j nm(t-1) w_{ij}(t-1) s_j(t-1)$$

where $w_{ij}$was the synaptic weight from neuron j to neuron i, and nm was the level of neuromodulator at synapse ij. Phasic neuromodulation had a strong effect on action selection and learning. During phasic neuromodulation, synaptic projections from sensory systems and inhibitory neurons are amplified relative to recurrent or associational connections (Hasselmo and McGaughy 2004). In this computational model, the *TOI-State* to *Action* neurons represented sensor connections and the excitatory *Action-to-Action* neurons represented the associational connections. To simulate the effect of phasic neuromodulation, inhibitory and sensory connections were amplified by setting nm to ten times the combined average activity of the simulated *Raphe* and *VTA* neurons. Otherwise, nm was set to 1 for recurrent or association connections. The last column of Table 1.2 lists connections amplified by phasic neuromodulation. In simulation studies (Krichmar 2008) and robotic experiments (Cox and Krichmar 2009), this mechanism was shown effective in making the network exploitive when neuromodulation levels were high and exploratory when neuromodulation levels were low.

Action selection depended on the summed activity of the *Action* neurons after the *Neural* agent reached the TOI. When the *Neural* agent reached the TOI, neural activities of the *Action* and *Neuromodulator* neurons were calculated for ten time-steps. The *Action* neuron with the largest total activity during those ten time-steps

dictated the action taken (e.g., if the total *Display* activity was greater than *Escalate*, then the *Neural* agent displayed).

After both the *Neural* agent and the opponent chose a tactic, a learning rule, which depended on the current activity of the pre-synaptic neuron, the post-synaptic neuron, the overall activity of the neuromodulatory systems and the payoff from the game, was applied to the equation for the plastic connections (Table 1.2):

$$\Delta w_{ij} = \alpha * nm(t-1)s_j(t-1)\big(s_i(t-1)\big) * R$$

where s_j was the pre-synaptic neuron activity level, s_i was the post-synaptic neuron activity level, α was a learning rate set to 0.1, nm was the average activity of all neuromodulatory neurons, and R was the level of reinforcement based on payoff and cost. The pre-synaptic neuron was the most active *TOI-State* neuron. The post-synaptic neuron could either be the most active *Action*, *Raphe*, or *VTA* neuron. Weights were normalized by the square root of sum of squared weights. The level of reinforcement was:

$$R = \begin{cases} (Reward - VTA) - (Cost - Raphe), & \textit{TOI-State}\rightarrow\textit{Action} \\ Reward - VTA, & \textit{TOI-State}\rightarrow\textit{VTA} \\ Cost - Raphe, & \textit{TOI-State}\rightarrow\textit{Raphe} \end{cases}$$

where the *Reward* was the payoff the *Neural* agent received as specified in Table 1.1 divided by the maximum possible reward. It was assumed that serotonin plasticity was based on the predicted cost of an action and dopamine plasticity was based on the predicted reward of an action. If there was an error in this prediction, weights changed according to the plastic connections and level of reinforcement. If *Raphe* or *VTA* accurately predicted the respected cost or payoff of an action, then

learning ceased. The cost was 1 if the *Neural* agent received a serious injury, the ratio of scratch to serious injury (0.3875, Table 1) if scratched, or zero otherwise. The reward received when the *Neural* agent won the resource is 1, 0.5 if split, and zero otherwise.

Neural Agent's Performance in Simulations

During the course of a series, the *Neural* agent learned to adopt various strategies depending on the chance of serious injury and its opponent's strategy. To ensure that these strategies did not occur by chance, 100 randomly behaving agents played against all three *Opponent* agents. The random *Neural* agents had lesions (i.e., activity set to zero) of both the simulated *VTA* and *Raphe*, which resulted in no learning occurring. The 95% confidence interval was used as the cutoff for gauging non-random behavior in the random agents. This cutoff corresponded to the probability of selecting a particular action in response to a given *TOI-State* greater than 65% or less than 35% of the time.

The *Neural* agent adapted its behavior depending on its opponent's strategy and environmental conditions (Figure 1.3). In response to a given *TOI-State*, the *Neural* agent could respond randomly (i.e., within the 95% confidence), or significantly tend toward escalation or displaying. There are a total of 27 possible outcomes the *Neural* agent can take with respect to the three different states of the TOI. Only a few of these outcomes emerged in the simulations, and these outcomes are represented in Figure 1.3 as a triplet pairing (i.e., EEE, DDE, UDE, etc.). The first value in the triplet pairing corresponds to the expected action when the *TOI-*

State was *Open*. The second represents the anticipated action when the *TOI-State* was *Escalate*. The third value denotes the expected outcome when the *TOI-State* was *Display*. These triplets are associated with a color spectrum, where aggressive outcomes ('E' in the triplet) are denoted red, passive outcomes ('D' in the triplet) are denoted in blue, and values that do not fall within either outcome ('U' in the triplet) are denoted in yellow.

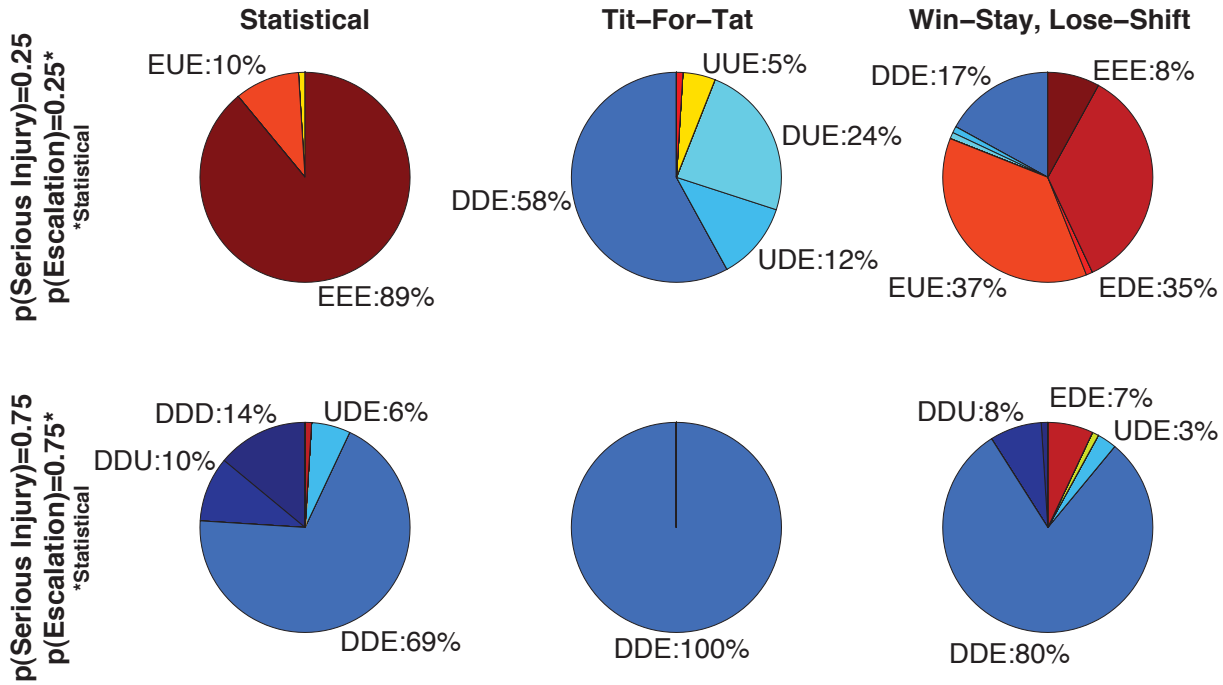

Figure 1.3. Proportion of Probable Neural Agent Actions. There are three *TOI-State* areas (*Open*, *Escalate*, and *Display*), and three outcomes the *Neural* agent can commit to: *Escalate* (E), *Display* (D) or *Undecided* (U). *Undecided* represents random choice between 'E' and 'D'. The labels represent the *Neural* agent's response to the three *TOI-State* areas. Strategies that are Dove-like are displayed in blue, Hawk-like are displayed in red, and arbitrary strategies displayed in yellow.

Against all three opponents, the *Neural* agent adopted Hawk-like behavior in "safe" environments, where the probability of serious injury was 0.25 (top row, Figure 1.3), and Dove-Like behavior in "harsh" environments, where the probability of serious injury was 0.75 (bottom row, Figure 1.3). As the probability of serious

injury or an opponent escalating increases, the adoption of 'DDE' strategy (*Neural* agent displayed when the *TOI-State* was *Open* and *Escalate*, and escalated when the *TOI-State* was *Display*) increases as well (Figure 1.3). In situations where the *Neural* agent was in a competitive, antagonistic environment, the *Neural* agent tended to behave in a Dove-like way (displaying a large proportion of the games in a series). Conversely, as the probability of serious injury or opponent escalating decreases, aggressive strategies (escalating when the *TOI-State* is *Open*, *Escalate* or *Display*) increases (Figure 1.3). In circumstances where the *Neural* agent was in a cooperative, forgiving environment, it tended to adopt more Hawk-like behavior (escalating in a larger proportion of the games in a series).

Simulated lesion experiments were carried out to test the effect of neuromodulation on behavior. An intact neuromodulatory system was necessary for appropriate behavior (Table 1.3). When the simulated *Raphe* area was lesioned, the *Neural* agent's behavior became more Hawk-like, even when the chance of serious injury was high (*Harsh* column in Table 1.3). When the simulated *VTA* area was lesioned, the *Neural* agent's behavior became more Dove-like (fewer escalations) in all environments.

Table 1.3. Percentage of Escalation for the Neural Agent.

	Control		**Raphe Lesion**		**VTA Lesion**	
	Safe	*Harsh*	*Safe*	*Harsh*	*Safe*	*Harsh*
Statistical	97.65%	10.00%	99.06%	92.86%	34.79%	7.14%
TT	34.15%	13.64%	81.82%	81.82%	24.74%	12.50%
WSLS	93.22%	9.09%	96.88%	96.88%	20.93%	8.22%

The *Neural* agent adapted its behavior to its opponent's strategy. Against the TT opponent, the *Neural* agent oscillated between escalating and displaying in

successive games. In essence, the *Neural* agent learned to adopt a TT strategy against this opponent, which yielded approximately equal reward to both agents. The oscillating neuromodulatory activity corresponded to the alternating actions taken by both agents (Figure 1.4A). Against the WSLS opponent, the *Neural* agent created opportunities for high payoffs. The high-expected cost and reward were reflected in the serotonergic and dopaminergic activity when both agents escalated (see Figure 1.4B: bottom plot, games 79, 82, or 86). In these examples, the *Neural* agent escalated first and its opponent escalated second (Figure 1.4B: top plot, games 79, 82, or 86). The *Neural* agent learned that this tactic caused the *Opponent* agent to 'lose-shift' towards *Display* in the following game, which could be taken advantage of by escalating (Figure 1.4B: top plot, games 80, 83, or 87). This tactic resulted in a maximal reward to the *Neural* agent but caused the *Opponent* agent to 'lose-shift' back to *Escalate* in the following game (see Figure 1.4B: top plot, games 81, 84, or 88).

The neural response of the simulated neuromodulators appears to govern the *Neural* agent's actions (Figure 1.4). When the *VTA* activity dropped below the *Raphe* activity, the *Neural* agent displayed. That is, *Raphe* activity may be acting as a threshold for the expected cost of upcoming actions, whereas the *VTA* activity rises and falls based on the expected reward. When the expected reward is lower than the expected cost, the *Neural* agent tended to display. For example, when a *Neural* agent behaved Dove-like, serotonin activity was high relative to dopamine

activity because the expected reward from displaying was low (Figure 1.4: games 78-80).

In addition, the oscillatory *Neural* agent actions (Figure 1.4A: games 84-99) are exactly matched by oscillatory *VTA* neuromodulatory activity (Figure 1.4: games 84-99) rising above and falling below the *Raphe* neuromodulatory activity. The low fluctuation in *Raphe* values from one game to the next in Figure 1.4A result from the precision of predicted cost when playing a highly predictable opponent using the TT strategy. Predicted cost was not as regular for the *Neural* agent when playing against the WSLS opponent, which is why the *Raphe* neuromodulatory activity fluctuated more in Figure 1.4b (bottom plot). Although the *Raphe* activity fluctuated more when playing against the WSLS opponent, the *Neural* agent actions were consistent with the neuromodulatory activity. Thus, the results from the simulated neuromodulatory activity in Figure 1.4 suggest that the *Raphe* neural activity acts as a threshold for aggressive (escalate) or non-aggressive (display) *Neural* agent actions.

Discussion

In this study, an agent, whose behavior was guided by a computational model of the neuromodulatory system, played Hawk-Dove against simulated opponents and learned to adjust its strategy appropriately depending on environmental conditions and its opponent's strategy. The model makes several predictions on how the activity of neuromodulatory systems can lead to appropriate action selection in competitive and cooperative environments.

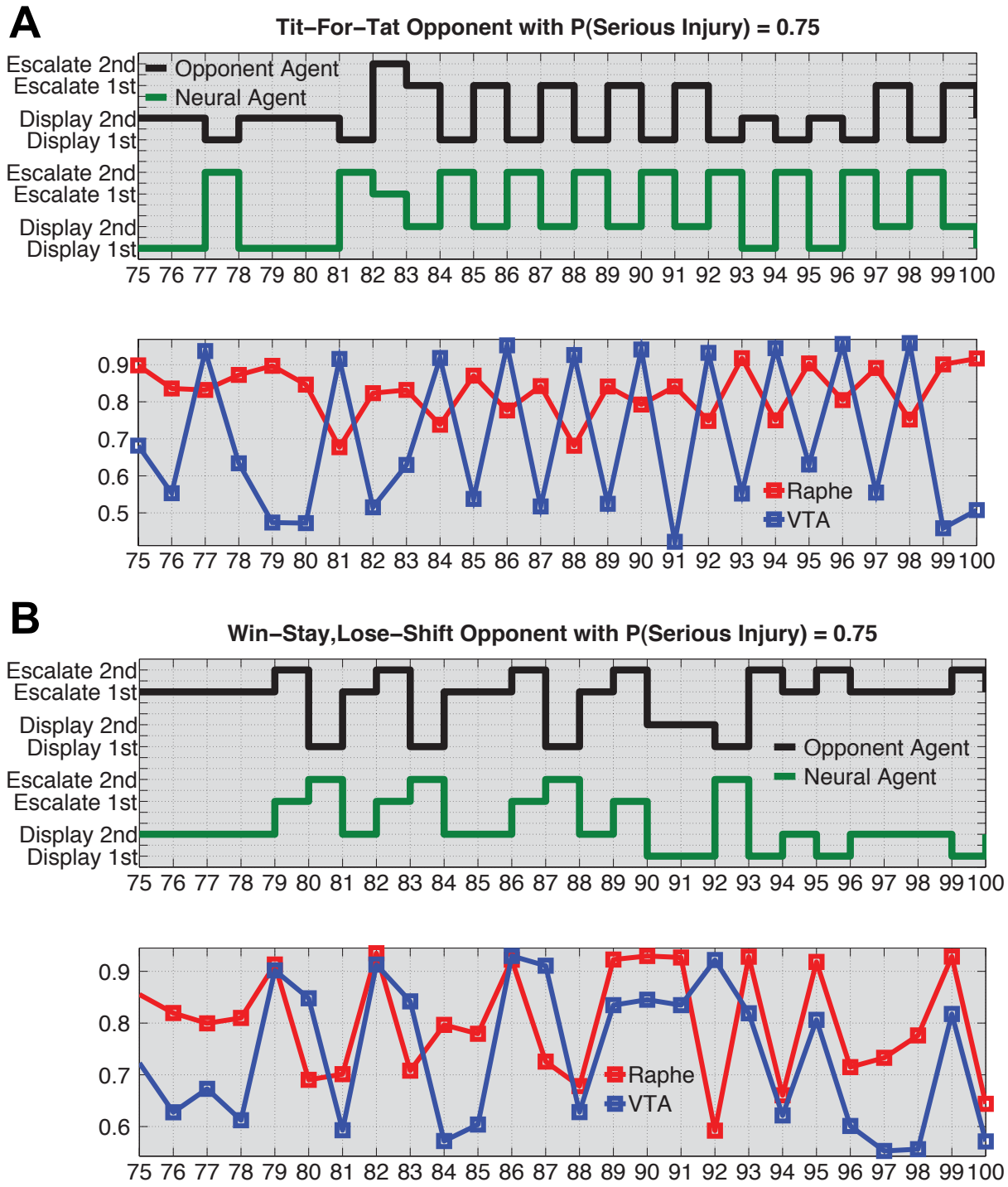

Figure 1.4. Actions and Neuromodulatory Activity of Agents. *Neural* and *Opponent* agent actions taken during the last 25 games of a single series, along with corresponding neuromodulatory activity for the *Neural* agent. The stair plots located on the top half of **A** and **B** are the actions taken by both the *Neural* (green) and *Opponent* (black) agents. The line plots located in the bottom half of **A** and **B** represent the neuromodulatory activity for the *Neural* agent during the same 25 games of the same series. The red line represents the *Raphe* activity, and the blue line represents the *VTA* activity. **A.** *Neural* agent versus the TT opponent. **B.** *Neural* agent versus WSLS opponent.

Results from this study verified the prediction that the interaction between the simulated serotonergic neuromodulatory system, associated with the expected cost of a decision, and the simulated dopaminergic system, associated with the expected reward of a decision, would allow for appropriate decision-making in Hawk-Dove (Figure 1.4). The *Neural* agent was more likely to escalate over the resource when activity of the reward system exceeded the activity of the cost system. Conversely, when the reward activity did not exceed the activity of cost, the *Neural* agent displayed. Impairment to either the dopaminergic or serotonergic system lead to perseverant, uncooperative behavior is another prediction verified in this study (Table 1.3). A simulated lesion of the serotonergic system resulted in the *Neural* agent engaging in risk taking (aggressive) behavior, which was similar to the uncooperative behavior seen in human studies where serotonin levels were lowered via ATD while subjects played games such as Prisoner's Dilemma and the Ultimatum game (Wood, Rilling et al. 2006; Crockett, Clark et al. 2008). Impairment of the dopaminergic system resulted in risk-averse behavior (Dove-like) caused by an inability to assess reward, and impairment of the serotonergic system resulted in risk-taking behavior (Hawk-like) because of its inability to assess cost. Although dopamine and serotonin activity appears related to various expectations (e.g., predictive reward, anticipated cost), the action of these neuromodulators on downstream targets is similar in that it governs decision-making. That is, phasic neuromodulation shifts an agent's behavior from random and exploratory to decisive and exploitive through differentially modulating synaptic pathways.

Altogether, results in this study are in agreement with the theoretical work proposed by Boureau and Dayan (Boureau and Dayan 2011), in which the influence of serotonergic and dopaminergic systems in generating an appropriate decision are sometimes in opposition.

The model constructed for this study is based on the notion that all neuromodulators have the same effect on downstream targets (Krichmar 2008). Large, phasic increases in neuromodulator activity cause an organism's behavior to be more exploitive or decisive, whereas lower levels of neuromodulatory activity result in the organism being more exploratory or indecisive. This is in agreement with the idea of cholinergic modulation of attention (Pauli and O'Reilly 2008) and noradrenergic modulation of decision-making (Aston-Jones and Cohen 2005), but extended to dopaminergic and serotonergic systems. The model used in this study differs somewhat from the behavioral and neuroscience literature that suggests the role of dopamine is to calculate the reward prediction error, and that serotonin controls the timescale of the evaluation of delayed rewards in reinforcement learning (Doya 2002; Schweighofer, Tanaka et al. 2007). It may instead be more in agreement with the proposal that neuromodulators, such as dopamine and serotonin are involved with the discovery of new actions to outcome mappings (Redgrave and Gurney 2006).

References

Aston-Jones, G. and J. D. Cohen (2005). "An integrative theory of locus coeruleus-norepinephrine function: adaptive gain and optimal performance." Annu Rev Neurosci 28: 403-450.

Axelrod, R. and W. D. Hamilton (1981). "The evolution of cooperation." Science 211(4489): 1390-1396.

Boureau, Y. L. and P. Dayan (2011). "Opponency Revisited: Competition and Cooperation Between Dopamine and Serotonin." Neuropsychopharmacology 36(1): 74-97.

Cox, B. R. and J. L. Krichmar (2009). "Neuromodulation as a Robot Controller: A Brain Inspired Design Strategy for Controlling Autonomous Robots." IEEE Robotics & Automation Magazine 16(3): 72-80.

Crockett, M. J., L. Clark, et al. (2008). "Serotonin modulates behavioral reactions to unfairness." Science 320(5884): 1739.

Doya, K. (2002). "Metalearning and neuromodulation." Neural Netw 15(4-6): 495-506.

Hasselmo, M. E. and J. McGaughy (2004). "High acetylcholine levels set circuit dynamics for attention and encoding and low acetylcholine levels set dynamics for consolidation." Prog Brain Res 145: 207-231.

Krichmar, J. L. (2008). "The Neuromodulatory System – A Framework for Survival and Adaptive Behavior in a Challenging World." Adaptive Behavior 16: 385-399.

Maynard Smith, J. (1982). Evolution and the theory of games, Cambridge University Press.

Maynard Smith, J. and G. A. Parker (1973). "The Logic of Animal Conflict." Nature 246: 15-18.

Nowak, M. and K. Sigmund (1993). "A strategy of win-stay, lose-shift that outperforms tit-for-tat in the Prisoner's Dilemma game." Nature 364(6432): 56-58.

Nowak, M. A., K. M. Page, et al. (2000). "Fairness versus reason in the ultimatum game." Science 289(5485): 1773-1775.

Pauli, W. M. and R. C. O'Reilly (2008). "Attentional control of associative learning-A possible role of the central cholinergic system." Brain Res 1202: 43-53.

Redgrave, P. and K. Gurney (2006). "The short-latency dopamine signal: a role in discovering novel actions?" Nat Rev Neurosci 7(12): 967-975.

Schweighofer, N., S. C. Tanaka, et al. (2007). "Serotonin and the evaluation of future rewards: theory, experiments, and possible neural mechanisms." Ann N Y Acad Sci 1104: 289-300.

Skyrms, B. (2001). The Stag Hunt. Presidential Address. Pacific Division of the American Philosophical Association.

Wood, R. M., J. K. Rilling, et al. (2006). "Effects of tryptophan depletion on the performance of an iterated Prisoner's Dilemma game in healthy adults." Neuropsychopharmacology 31(5): 1075-1084.

CHAPTER 2: Reciprocity and Retaliation in Social Games With Adaptive Agents, Embodiment, and Pharmacological Manipulation

With the computational model from Chapter 1 providing a means for investigating how neuromodulation may shape behavior during competitive and cooperative situations, this Chapter further tests neuromodulators role in decision-making by embedding a similar model in an embodied (robotic) agent. Hawk-Dove was introduced in Chapter 1 as a socioeconomic game where players choose between competing and sharing a resource. Chicken (Rapoport and Chammah 1966), another game of conflict, was used to investigate competitive situations in terms of expected costs and reward alongside Hawk-Dove. Furthermore, the computational model featured in this Chapter plays against human subjects with manipulated levels of 5-HT through acute tryptophan depletion, a procedure that has been shown to decrease cooperation and lower harm-aversion (Young, Smith et al. 1985; Wood, Rilling et al. 2006; Crockett, Clark et al. 2008).

Chicken

In Chicken, two cars approach each other on a collision course, and players must decide to drive straight for a high-risk, high reward payoff or swerve away (Figure 2.1). If both cars go straight, a stiff penalty is incurred with the collision. If one car goes straight and the other swerves, the driver of the car that went straight receives a reward and the other driver receives nothing. While somewhat similar to Hawk-Dove and Prisoner's Dilemma, Chicken forces players to decide on an action

quickly without knowledge of the opponent's choice. Therefore, players must rely solely on prior game experience to make appropriate decisions.

In this study's version of Chicken, human subjects and *Neural* agents drove their cars along a single lane from opposite directions (Figure 2.1). Both players started simultaneously at the same speed. The human subject had less than a second to decide to swerve or to continue straight and risk a crash. After each game, a payoff was calculated based on the outcome of the game (Table 2.1). If both players drove straight, then the result was a head-on collision with a heavy penalty. If one player swerved (thereby deemed the "chicken"), then the player that continued moving straight on the lane received a high payoff. If both players swerved, then a mutual small payoff was rewarded.

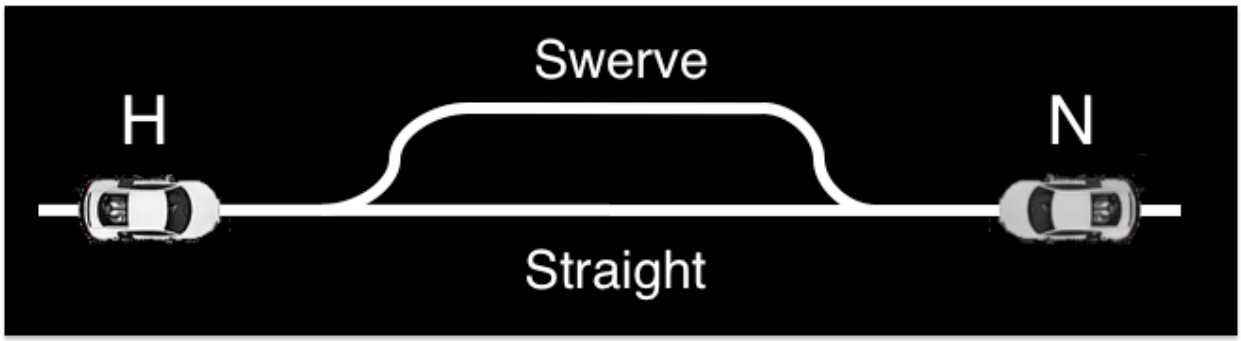

Figure 2.1. Game Diagram for Chicken. In Chicken, two race cars approach each other on a collision course. The human subject (H) controlled one car and the *Neural* agent (N) controlled the other. Players decide whether to swerve onto another lane or stay straight.

Neural Agent

Throughout this study, a neural network controlled the behavior of the *Neural* agent, similar to the one used in Chapter 1 (Asher, Zaldivar et al. 2010; Zaldivar, Asher et al. 2010). The focus of this study was to move past using opponents with fixed strategies and introduce adaptive neural agents. For Hawk–

Dove, this study borrows the same neural network architecture implemented in Chapter 1 (Figure 1.2). For Chicken, the neural network architecture was slightly modified from Hawk-Dove to accommodate for changes specific to the Chicken game (Figure 2.2). In place of the *TOI-State* area in Hawk-Dove (Figure 1.2), Chicken contains a *Previous Action* area featuring four neurons that represented information on possible outcomes performed in the prior game for both itself and the human subject: *Neural Straight*, *Neural Swerve*, *Opponent Straight*, or *Opponent Swerve* (Figure 2.2). Congruent with the Hawk–Dove games, at the start of each condition, the weights of the neural network were set to their initial values (Table 2.2).

Table 2.1 Chicken Payoff Matrix.

	Neural Straight	**Neural Swerve**
Human Straight	H: -4, N: -4	H: 3, N: 0
Human Swerve	H: 0, N: 3	H: 1, N: 1

Table 2.2. Synaptic Connections Between Neural Areas for Chicken.

From	**To**	**Initial Weight**	**Plastic**	**Phasic Neuromodulation**
Previous Action	*Action*	0.1	Y	Y
Previous Action	*Neuromodulator*	0.1	Y	N
Action-Straight	*Action-Swerve*	0.1	N	N
Action-Straight	*Action-Swerve*	-0.1	N	Y
Action-Swerve	*Action-Straight*	0.1	N	N
Action-Swerve	*Action-Straight*	-0.1	N	Y

While the equations for each of the areas implemented in the neural architecture for Chicken are similar to Hawk-Dove (Chapter 1, Neural Agent), there were a few differences. In Chicken, the activity of *Previous Action* area (n_i), which resembles the *TOI-State* area from the Hawk-Dove model (Figure 1.2), was based on what occurred in the previous game:

$$n_i = \begin{cases} 0.45 + rnd(0.0,0.5), & i = PreviousAction \\ rnd(0.0,0.5), & \text{Otherwise} \end{cases}$$

where $rnd(0.0,0.5)$ was a random number uniformly distributed between 0.0 and 0.5. The *Neuromodulatory* area was identical in both games and included two neurons: *Raphe*, a simulated raphe nucleus, which was the source of serotonergic neuromodulation, and *VTA*, a simulated ventral tegmental area, which was the source of dopaminergic neuromodulation. The *Action* area in both games included two neurons, whose activity was based on input from *TOI-State/Previous Action* area and *Neuromodulatory* area, that function in similar ways. For Hawk-Dove, these areas were labeled *Escalate* (the *Neural* agent created a conflict) and *Display* (the *Neural* agent did not create a conflict) (Chapter 1, Neural Agent). For Chicken, the represented neurons in this *Action* area were: *Straight* (the *Neural* agent remained in the same lane) and *Swerve* (the *Neural* agent moved away from the lane) (Figure 2.2). Lastly, $Reward$ and $Cost$ were computed differently for Hawk-Dove and Chicken, as their payoff matrix (Table 1.1 and Table 2.1, respectively) used different values. As such, the following $Reward$ and $Cost$ equations were used when computing the level of reinforcement:

$$Reward = \begin{cases} \frac{\text{Payoff}}{0.60}, & \text{for Hawk-Dove} \\ \frac{\text{Payoff}}{3}, & \text{for Chicken} \end{cases}$$

$$Cost = \begin{cases} \frac{\text{Payoff}}{-0.50}, & \text{for Hawk-Dove} \\ \frac{\text{Payoff}}{-4}, & \text{for Chicken} \end{cases}$$

Identical to the base assumptions for the computational model in Chapter 1 (Neural Agent), serotonin plasticity was based on the predicted cost of an action and dopamine plasticity was based on the predicted reward of an action.

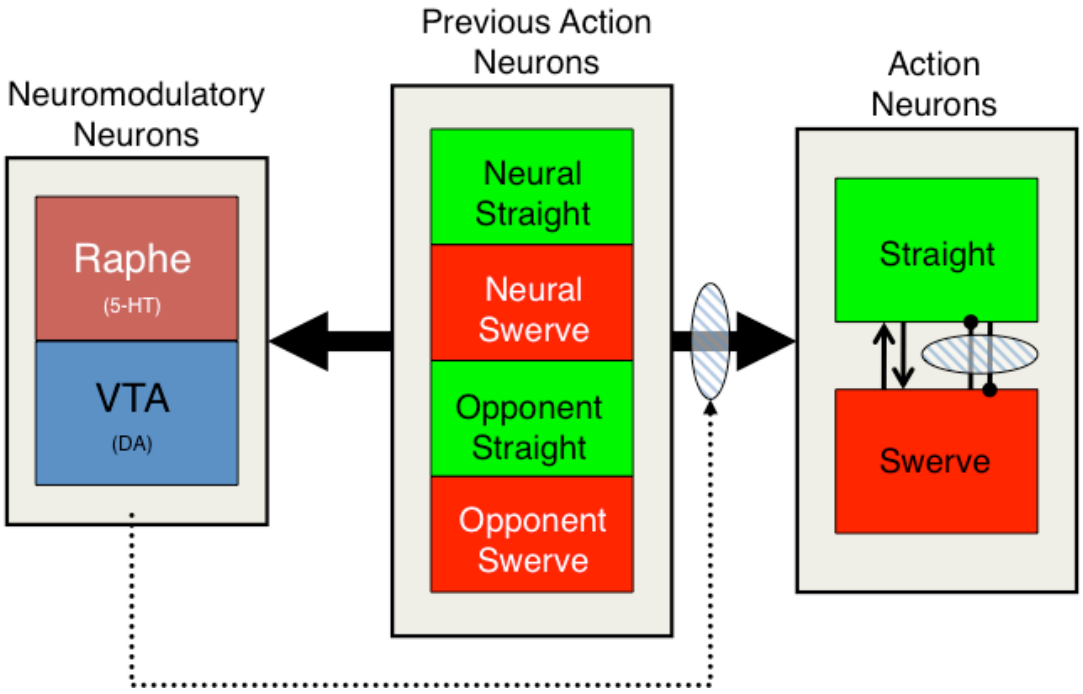

Figure 2.2. Neural Network Architecture for Chicken. The thick arrows represent plastic pathways. The dotted arrows and shaded ovals represent neuromodulatory pathways. Within the *Action* area, neurons with excitatory reciprocal connections are denoted with the lines with an arrow at the end, and neurons with reciprocal inhibitory connections are denoted with lines with a dot at the end. The solid arrows extending from the Previous Action neurons represent all-to-all connections.

Acute Tryptophan Depletion

Several studies of social behavior have used a dietary manipulation, called the acute tryptophan depletion procedure (ATD), to investigate the short-term effects of a decline in serotonin levels on mood in humans (Young, Smith et al. 1985; Wood, Rilling et al. 2006). The goal of ATD is to temporarily alter the levels of serotonin in the brain via a decrease in blood plasma tryptophan, the amino acid precursor to serotonin. Because free blood plasma tryptophan levels vary with the

amount of dietary tryptophan, these levels can be altered by a low protein diet in combination with a specially prepared "protein shake." This "protein shake" contains an amino acid load (lacking tryptophan), which has two effects. First, it stimulates protein synthesis in the liver, which uses up blood plasma tryptophan. Second, the amino acids that are given in the "protein shake" compete with tryptophan for transport across the blood-brain barrier, which restricts entry of tryptophan into the brain and leads to lower levels of serotonin in the brain (Biggio, Fadda et al. 1974; Gessa, Biggio et al. 1974; Bell, Hood et al. 2005; Hood, Bell et al. 2005).

Through ATD, serotonin has also been linked to predicting punishment or harm aversion (Cools, Roberts et al. 2008; Crockett, Clark et al. 2009; Tanaka, Shishida et al. 2009; Crockett, Clark et al. 2012; Seymour, Daw et al. 2012). Cools et al. paired the ATD procedure with a reversal-learning task, demonstrating that subjects under ATD made more prediction errors for punishment-associated stimuli than for reward-associated stimuli (Cools, Roberts et al. 2008). In a related study, Crockett et al. utilized the ATD procedure with a Go/No-Go task to show that lowering serotonin levels resulted in a decrease in punishment-induced inhibition (Crockett, Clark et al. 2009). In a follow up study, they investigated the mechanisms through which serotonin regulated punishment-induced inhibition by using the ATD procedure paired with their Reinforced Categorization task, a variation on the Go/No-Go task (Crockett, Clark et al. 2012). Subjects with lowered serotonin were faster in responding to stimuli predictive of punishments (Crockett,

Clark et al. 2012), indicating a manipulation of some punishment-predicting mechanism associated with standard serotonergic function. Together, these results suggest that serotonin influences the ability to inhibit actions that predict punishment and to avoid harmful circumstances.

Table 2.3. Amino Acid Levels for Acute Tryptophan Depletion Procedure

	Control/Depleted Mixture
L-alanine	5.5g
L-arginine	4.9g
L-cystine	2.7g
glycine	3.2g
histidine	3.2g
L-isoleucine	8.0g
L-leucine	13.5g
L-lysine monohydrochloride	11.0g
L-methionine	3.0g
L-proline	12.2g
L-phenylalanine	5.7g
L-serine	6.9g
L-threonine	6.5g
L-tyrosine	6.9g
L-valine	8.9g
L-tryptophan	**2.3g/0.0g**
Total	**104.4g/102.1g**

In this study, an ATD "protein shake" was prepared for subjects to ingest prior to playing games of conflict against simulated and embodied agents. The ATD "protein shake" contained 15 amino acids (NutraBio, www.nutrabio.com) mixed with approximately 400 ml water and flavoring (Crystal Light, Kraft Foods, Inc.). The amino acids were used in proportions approximating human milk, except for three amino acids (Table 2.3). The ATD Trp- mixture lacks tryptophan, as well as aspartic acid and glutamic acid, which are omitted because of concern about their toxicity at high doses (Young, Smith et al. 1985; Wood, Rilling et al. 2006). The

Tryp- mixture had a total protein content of approximately 100 g. The control mixture, Tryp+ condition, used the same ratio of amino acids, but additionally included 2.3 g of tryptophan. For female participants, the same ratios of amino acids were used, but with approximately 17% reduction in quantity to take into account average lower body weight (Young, Smith et al. 1985).

Embodiment Apparatus for Hawk-Dove

To carry out the embodied version of the Hawk-Dove game, a robot (named CARL) and its interactive floor apparatus was modified from its original conditioning paradigm (Cox and Krichmar 2009). The robot consisted of a two wheeled mobile base equipped with infrared (IR) sensors for obstacle avoidance, a compass for orienting and navigation, a Wi-Fi device server (http://www.sena.com) for communication between the robot and a computer workstation, and a charge-coupled device video camera with a radio frequency transmitter for vision. The model for the *Neural* agent ran on a computer workstation. The workstation received CARL's camera video through radio frequency, CARL's sensor input through serial (RS-232 port) communication, and sent motor commands to CARL through RS-232 communication. The pan and tilt position of the camera was controlled by commands to a pair of servomotors. The base of the robot was 10 inches in diameter and 8.5 inches high. Visual processing was carried out on the workstation using open source Computer Vision (OpenCV) libraries (http://opencv.willowgarage.com/wiki/). A color histogram method was run across image frames to classify salient features (Cox and Krichmar 2009).

The robot's environment consisted of a 10-foot by 10-foot enclosure that contained 25 light panels arranged in a 5-by-5 grid (Figure 2.3). The panel color was set to magenta, red, blue or green through RS-232 communication from the workstation to electronics controlling the panels. All 25 panels had IR transceivers that could communicate position information to the robot when it was directly above the panel. Robot navigation was achieved by combining heading information with visual tracking.

The game proceeded with the human subject and *Neural* agent approaching the TOI and then upon arriving at the TOI, making a decision to choose *Escalate* or *Display*. A human subject sat at a computer workstation with a visual representation that reflected the state of the interactive floor (Figure 2.3). At the start of each game, the TOI was set to the *Open* state by displaying one panel on the human subject's user interface as magenta, and setting the corresponding four panels on CARL's interactive floor to magenta. After the TOI was presented to both players, the human subject and robot moved toward the Open resource. The human subject moved his or her icon by clicking on one adjacent panel at a time using a mouse. A ten-second delay between moves was used to prevent the human from moving toward the TOI faster than the robot. If the human subject's icon was adjacent to the TOI, the human subject was allowed to make a decision. The human subject could *Display* by turning the panel to blue, or *Escalate* by turning the panel to Red. When the robot was at the TOI location, it would make a decision by visually recognizing the light panel's color (i.e., magenta for *Open*, red for *Escalate*,

blue for *Display*). The robot chose *Display* by turning the panel to blue, or *Escalate* by turning the panel to green. The change of state was reflected on the human subject's interactive screen.

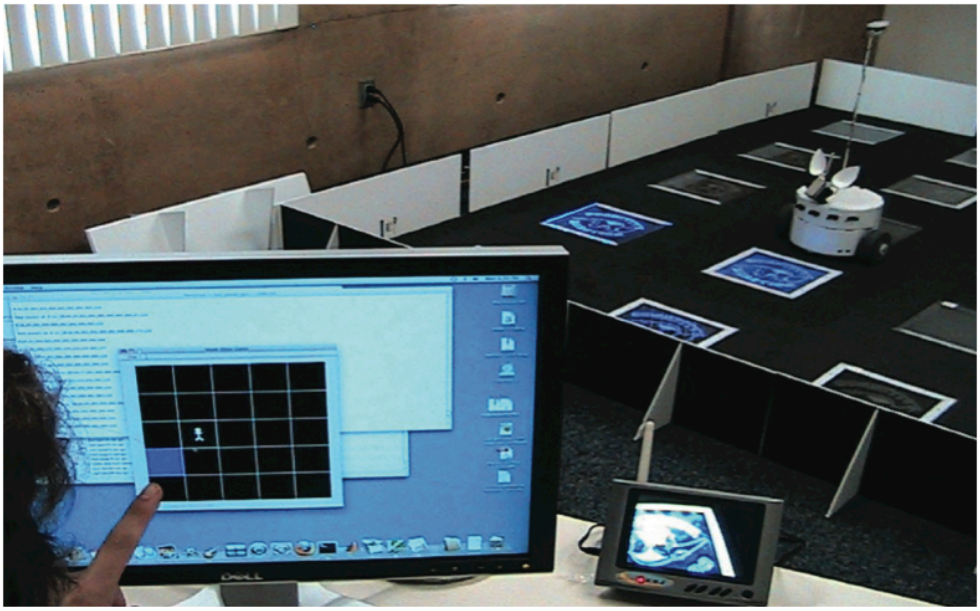

Figure 2.3. Hawk-Dove Apparatus. A subject is playing the Hawk-Dove game with the CARL robot (Cox and Krichmar 2009). The GUI reflects the state of the interactive floor and allows the subject to move their icon and change the TOI state. A *Neural* agent guides the robot's behavior. Note that the TOI on the GUI and CARL's interactive floor are in the same location with the same color.

A simulated variant of Hawk-Dove was also implemented for human subjects to play against using the same interactive screen, but without a physical robot for the *Neural* agent to guide. Instead, the *Neural* agent control an icon on the display that would represent the robot. This simulated setup allowed judgment of whether playing against a robot had an effect on human behavior.

Embodiment Apparatus for Chicken

In the embodied version of Chicken, human subjects and the *Neural* agent controlled race cars from a digital slot car racing set (Figure 2.4). The Carrera Digital 1/24 23602 Classic Legends racing car set (http://us.carrera-toys.com) were

used and modified in this study such that two cars moved in opposite directions toward each other. Slot cars were placed on opposite ends of a 12'6" long straightaway. Controlling both cars was handled through RS-232 serial communication from a computer. The race car controller consisted of a PIC (Peripheral Interface Controller) microcontroller with two digital potentiometers used to control the speed of the cars, and a serial line level converter necessary for serial communication between the software and racing car set. The speed was fixed to insure that both cars reached the *Swerve*/*Straight* decision point at the same time. A graphical user interface was developed to allow the human subject's car to switch lanes with a mouse click. The output of the model for the *Neural* agent dictated whether the other car would *Swerve* or not. If both cars chose *Straight*, they crashed in the middle of the track. Rubber foam bumpers were placed on the race cars to prevent damage from collisions. If both cars chose *Swerve*, they both switched lanes and stopped before hitting each other. In the case where one car chose *Swerve* and the other car chose *Straight*, the car that chose *Straight* traveled down the track, and the car that chose *Swerve* switched to the other lane and stopped.

Similar to Hawk-Dove, human subjects played a pure simulation version of this game. The interactive representation was identical to controlling the race cars. Instead of seeing the cars move on the track, the outcome of the game was shown on the subject's computer screen.

Subjects and Procedures

Eight subjects (three female; average age: 26.6 ± 3.8 years) participated in this study. The Institutional Review Board at University of California, Irvine, approved the experimental protocol and informed consent was obtained from all subjects.

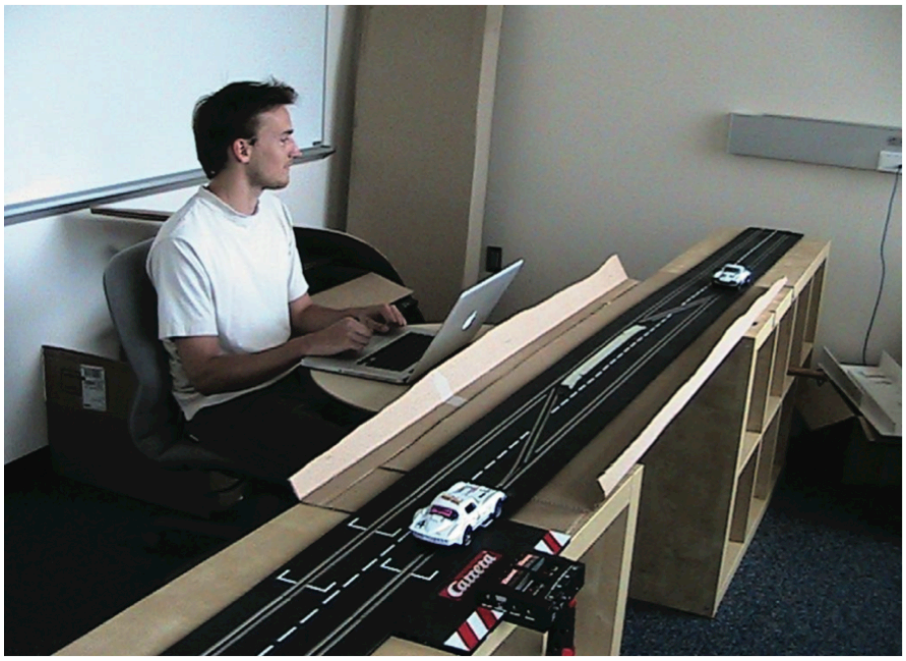

Figure 2.4. Chicken Apparatus. Subjects have control of one racecar, and the agent has control of the other. The subject may choose to *Swerve* by clicking on a button shown on the interactive screen.

Prior to enrollment in the study, all potential participants were screened for psychiatric and neurological disorders using the Structured Clinical Interview for DSM-IV-TR Axis I Disorders (SCID-I Research Version, Biometrics Research; (Williams and Gibbon 1992). Potential participants were excluded for a history of cardiac, hepatic, renal, pulmonary, neurological, psychiatric or gastrointestinal disorders, pregnancy, psychiatric medication, drug use, or a personal or family history of mood disorders. Because serotonin levels can be affected by estrogen

fluctuations, female subjects participated in the study only during the first two weeks of their menstrual cycles (Oldman, Walsh et al. 1995; Ellenbogen, Young et al. 1996; Jans, Riedel et al. 2007).

In this study, which was set up using a double-blind procedure, human subjects were randomly assigned on the first experimental day to receive either the Tryp+ control mixture or the Tryp- mixture. Each subject then returned to participate in the other condition at least seven days later to ensure the return to baseline blood plasma tryptophan levels between experimental days. On the morning of each experimental day, a blood sample was drawn to determine baseline blood plasma tryptophan levels. Following the blood draw, subjects ingested one of the amino acid drinks (either Tryp+ or Tryp-). A second blood sample was drawn approximately five hours after ingestion of the amino acid drink to confirm reduction (Tryp- condition) or maintenance (Tryp+ condition) of blood plasma tryptophan levels. Roughly five and a half hours after consumption of the amino acid drink, human subjects then participated in a series of Hawk–Dove and Chicken games against a *Neural* agent.

To track potential ATD short-term mood effects and ensure no long term effects on subjects' mood, the positive and negative affect scale (PANAS) was administered on two occasions during each experimental day (Watson, Clark et al. 1988), once before the amino acid drink was consumed and once just prior the start of the interactive games. A follow-up PANAS assessment was also performed at least seven days after the experiments and compared with baseline measurements.

Neural Agent's Performance Against Subjects

In both Hawk-Dove and Chicken, the *Neural* agent became more aggressive when its simulated serotonergic system was lesioned by escalating or going straight more often (Figure 2.5). These results from games against subjects were consistent with the behavior of the *Neural* agent against simulated opponents in Chapter 1 (Neural Agent's Performance in Simulations).

In Hawk-Dove, similar to its performance against simulated opponents (Chapter 1, Neural Agent's Performance in Simulations), the *Neural* agent needed an intact neuromodulatory system to appropriately adapt its performance to a human subject's strategy and the environmental conditions. The percentage of times the *Neural* agents chose to *Escalate* in Hawk–Dove were assessed using a four-way repeated-measures analysis of variance (ANOVA; $\alpha = 0.0125$, Bonferroni corrected) that included the factors of Neural State (Control and Raphe), Embodiment (Robot and Simulation), Probability of Serious Injury (0.25 and 0.75), and Experimental Day (Tryp- and Tryp+). The Neural State had a significant effect Neural State ($F(1,7) = 254.085$, $p < 1x10^{-4}$), driven by a higher percentage of choices to *Escalate* for Raphe ($\mu = 66.56\% \pm 2.22\%$ standard error of the mean) than for Control ($\mu = 35.47\% \pm 2.64\%$ standard error of the mean) (Figure 2.5, top). No significant effect for Embodiment ($F(1,7) = 0.050$, $p = 0.829$), Probability of Serious Injury ($F(1,7) = 3.651$, $p = 0.097$), or Experimental Day ($F(1,7) = 0.116$, $p = 0.743$) were found, nor were there any significant interactions ($p > 0.05$).

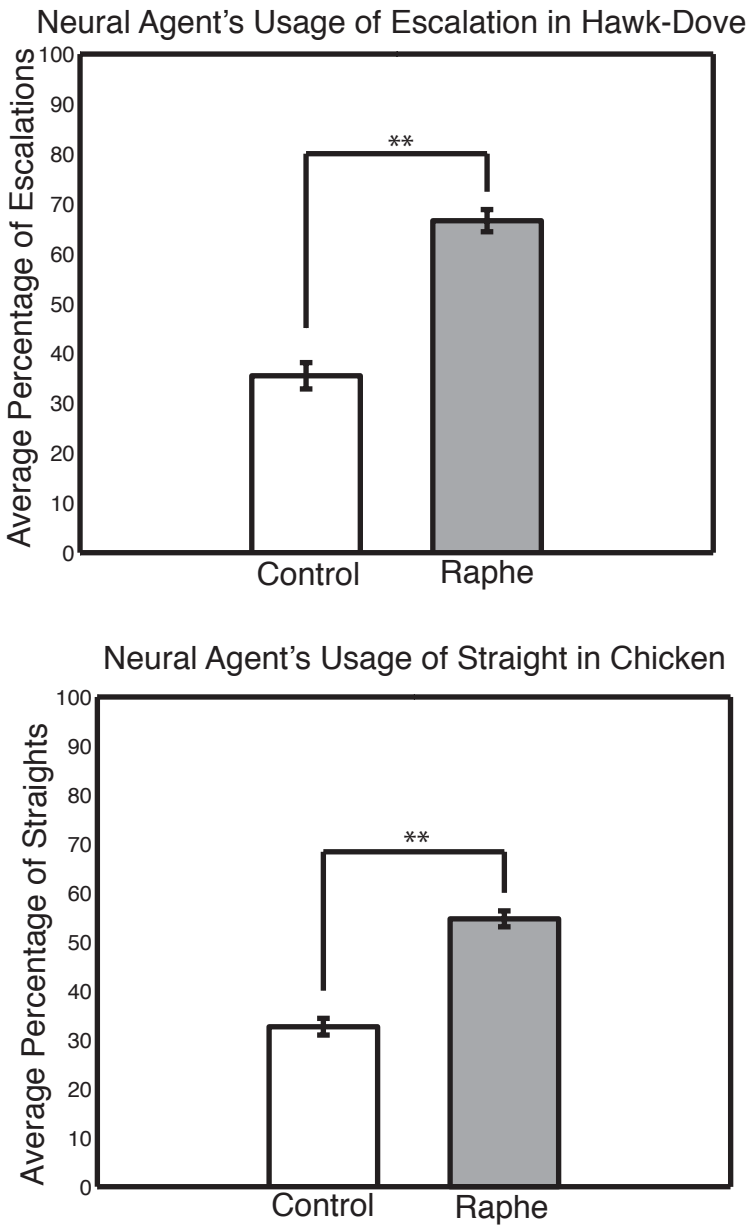

Figure 2.5. Neural Agent's Percentage of Escalation and Straight in Hawk-Dove and Chicken. The bar plots show the mean and SEM for each level (Control and Raphe) within the main factor Neural State for the dependent variable % Escalations and % Straight. The double asterisks indicate significance for an intact *Neural* agent (Control) and for a *Neural* agent with a lesion to its simulated serotonergic system (Raphe). The double asterisks indicate that there was a significant difference at $p < 1x10^{-4}$.

In Chicken, the percentage of times the *Neural* agents chose to drive *Straight* were assessed with a three-way repeated-measures analysis of variance (ANOVA; $\alpha = 0.017$, Bonferroni corrected) that included the Neural State (Control and

Raphe), Embodiment (Robot and Simulation) and Experimental Day (Tryp- and Tryp+) as its factors. The Neural State ($F(1,7) = 116.069$, $p < 1x10\text{-}4$) was significant, driven by a higher percentage of choices to drive *Straight* for Raphe ($\mu = 54.69\% \pm 1.63\%$ SEM) than for Control ($\mu = 32.66\% \pm 1.71\%$ SEM) (Figure 2.5, bottom). There were no significant effect for Embodiment ($F(1,7) = 1.252$, $p = 0.300$) or Experimental Day ($F(1,7) = 0.101$, $p = 0.760$), nor were there any significant interactions ($p > 0.100$).

Subjects' Performance

The ATD procedure effectively altered subjects' blood plasma tryptophan levels. The ratio between total blood plasma tryptophan levels at the two time points (baseline T = 0 hours and experimental T = 5 and 1/2 hours) for each day resulted in a highly significant difference when comparing Tryp- with Tryp+ ($p < 0.0005$, Wilcoxon rank-sum test, Figure 2.6). At baseline, the total blood plasma tryptophan levels for both days ranged from 49 to 69 μmol/L. At five hours after the amino acid drink, tryptophan levels ranged from 5 to 8 μmol/L for the Tryp- condition, and 51 to 182 μmol/L for the Tryp+ condition.

ATD did not have an effect on mood assessment. No significant differences were found through analysis of the human subjects' responses to the PANAS immediately before drink consumption and immediately before human robot interaction for each experimental day. Positive and negative affect with 2 separate two-way repeated-measures analysis of variance (ANOVA; $\alpha = 0.025$, Bonferroni corrected) that included factors Time of Day (Morning and Afternoon) and

Experimental Day (Tryp- and Tryp+) were assessed. There were no significant main effects (positive affect: $p > 0.400$; negative affect: $p > 0.200$) or interactions (positive affect: $p > 0.800$; negative affect: $p > 0.100$) when comparing the two time points within an experimental day or across days, or when comparing negative affect within a day or across days.

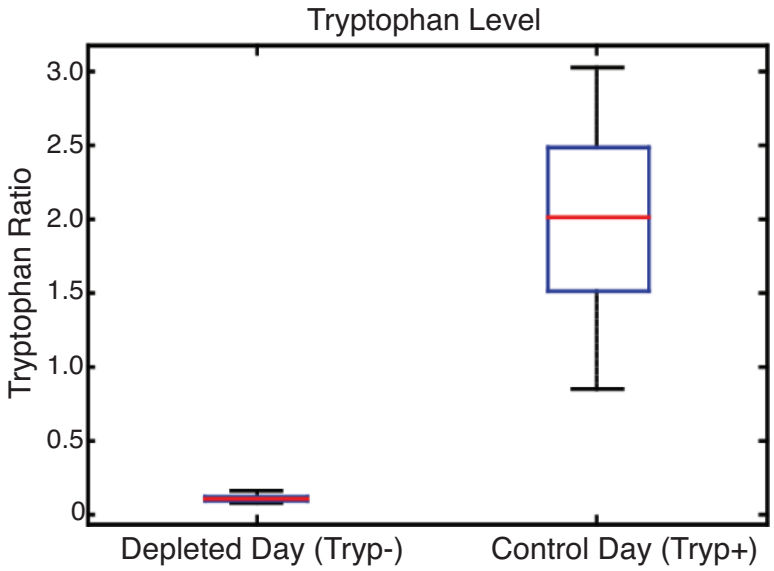

Figure 2.6. Tryptophan Ratios. The y-axis shows the ratio of total blood plasma tryptophan levels at the experimental time point (5 and 1/2 hours) to the baseline time point (before ATD shake consumption). The left column represents the ATD day and the right column represents the control day. The red lines represent the median value for each distribution, and the whiskers are the spread of each distribution. The horizontal bars represent the upper and lower quartile values for each distribution.

In Hawk-Dove, subjects tended to change their strategies depending on which *Neural* agent they were playing against. Specifically, they tended to adopt a WSLS strategy against control neural agents with intact neuromodulatory systems and a TT strategy against simulated *Raphe*-lesioned *Neural* agents (Figure 2.7). Percentages of human subjects' strategy choices (TT or WSLS) and the percentage of choices to *Escalate* were assessed with two separate four-way repeated-measures analysis of variance (ANOVA; $\alpha = 0.0125$, Bonferroni corrected) that included

Neural State (Control and Raphe), Embodiment (Robot and Simulation), Probability of Serious Injury (0.25 and 0.75), and Experimental Day (Tryp- and Tryp+) factors. There was a significant main effect of Neural State ($F(1,7) = 38.949$, $p < 0.001$; Figure 2.7, bottom), driven by a higher percentage of choices to use the TT strategy for Raphe ($\mu = 60.36\% \pm$ of 1.98% SEM) than for Control ($\mu = 40.13\% \pm 2.49\%$ SEM). Additionally, there was a marginally significant main effect of Neural State ($F(1,7) = 5.731$, $p < 0.05$; Figure 2.7, top), driven by a higher percentage of choices to use the WSLS strategy for the Control ($\mu = 64.56\% \pm 1.99\%$ SEM) than for Raphe ($\mu = 51.56\% \pm 1.83\%$ SEM). No significant effects for Embodiment (TT: $F(1,7) = 0.310$, $p = 0.595$; WSLS: $F(1,7) = 0.455$, $p = 0.522$), Probability of Serious Injury (TT: $F(1,7) = 3.309$, $p = 0.112$; WSLS: $F(1,7) = 0.133$, $p = 0.726$), or Experimental Day (TT: $F(1,7) = 1.075$, $p = 0.334$; WSLS: $F(1,7) = 0.319$, $p = 0.590$) were found, nor were there any significant interactions (TT: $p > 0.100$; WSLS: $p > 0.150$). There were also no significant effects when assessing the percentage of choices to *Escalate* for all the factors: Neural State ($F(1,7) = 1.43$, $p = 0.271$), Embodiment ($F(1,7) = 0.704$, $p = 0.429$), Probability of Serious Injury ($F(1,7) = 0.178$, $p = 0.686$), and Experimental Day ($F(1,7) = 0.7103$, $p = 0.427$). There were no significant interactions with the percentage of choices to *Escalate* ($p > 0.213$). This shift from WSLS to TT against a *Neural* agent with a *Raphe* lesion suggested that subjects were retaliating against an aggressive opponent. Subjects tended to respond to cooperation with cooperation and aggression with aggression by adopting a TT strategy.

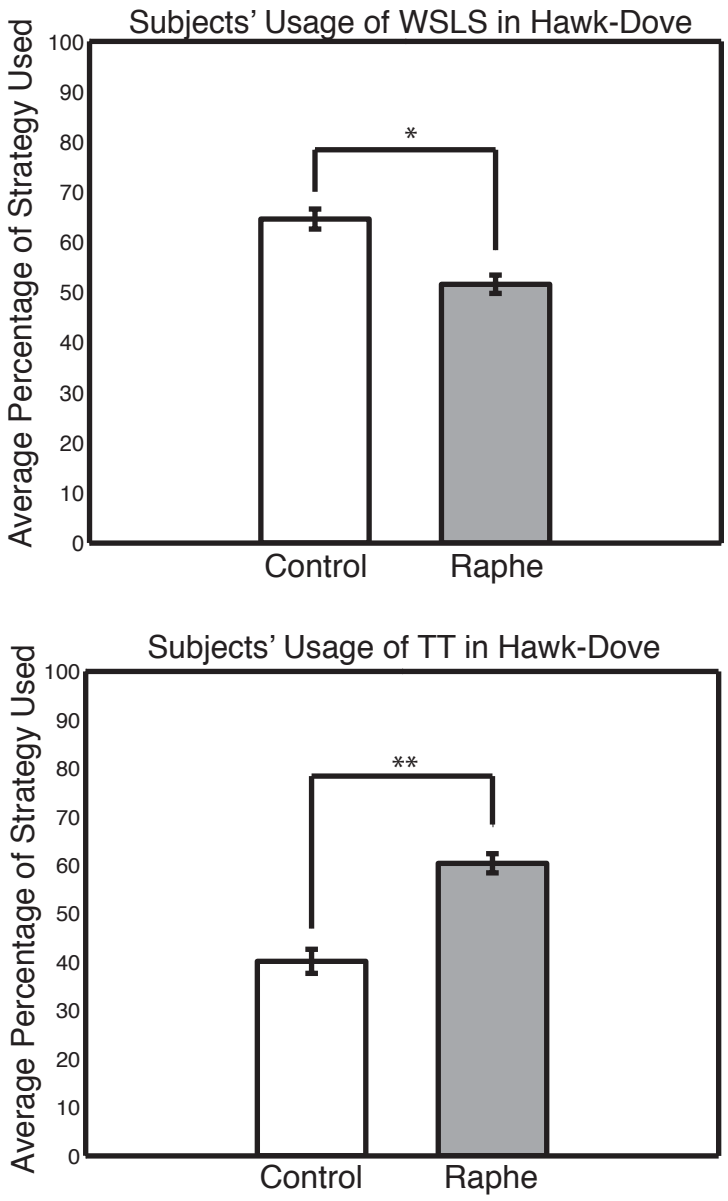

Figure 2.7. Human Subjects' Strategy Adoption in Hawk-Dove. The bar plots show the mean and SEM for each level (Control and Raphe) within the main factor Neural State for the respective dependent variables, %TT and %WSLS. The double asterisks indicate that there was a significant increase in the percentage of choices to use TT against Raphe-lesioned *Neural* agents ($p < 0.001$). The single asterisk indicates that there was a marginally significant decrease in the percentage of choices to use WSLS against Raphe-lesioned *Neural* agents ($p < 0.05$).

In Chicken, consistent with Hawk-Dove results, subjects tended to change their strategies depending on the state of the *Neural* agent they were playing against. That is, they tended to adopt a WSLS strategy against a control *Neural*

agent with an intact neuromodulatory system and tended to adopt the TT strategy against a simulated Raphe-lesioned *Neural* agent (Figure 2.8). Percentages of strategies (TT or WSLS) and percentages of driving *Straight* were assessed with two separate three-way repeated-measures analysis of variance (ANOVA; $\alpha = 0.017$, Bonferroni corrected) that included factors Neural State (Control and Raphe), Embodiment (Robot and Simulations), and Experimental Day (Tryp- and Tryp+). The Neural State main effect was marginally significant for both TT ($F(1,7) = 8.537$, $p < 0.025$; Figure 2.8, bottom) and WSLS ($F(1,7) = 5.240$, $p < 0.06$; Figure 2.8, top), driven by a higher percentage of choices to use the TT strategy for Raphe (μ = 50.17% ± 2.01% SEM) than for Control (μ = 37.67% ± 2.38% SEM) and driven by a higher percentage of choices to use the WSLS strategy for the Control (mean = 55.10% ± 1.97% SEM) than for Raphe (μ = 47.37% ± 1.43% SEM). No significant effects were found for Embodiment (TT: $F(1,7) = 0.492$, $p = 0.506$; WSLS: $F(1,7) = 3.943$, $p = 0.088$) nor Experimental Day (TT: $F(1,7) = 1.584$, $p = 0.249$; WSLS: $F(1,7) = 2.696$, $p = 0.145$). There were no significant interactions (TT: $p > 0.340$; WSLS: $p > 0.170$). There were also no significant effects when assessing the percentage of choices to drive *Straight* for all factors: Neural State ($F(1,7) = 0.069$, $p = 0.801$), Embodiment ($F(1, 7) = 0.003$, $p = 0.957$), and Experimental Day ($F(1,7) = 0.349$, $p = 0.573$). No significant interactions were found between factors for choices to drive *Straight* ($p > 0.4$).

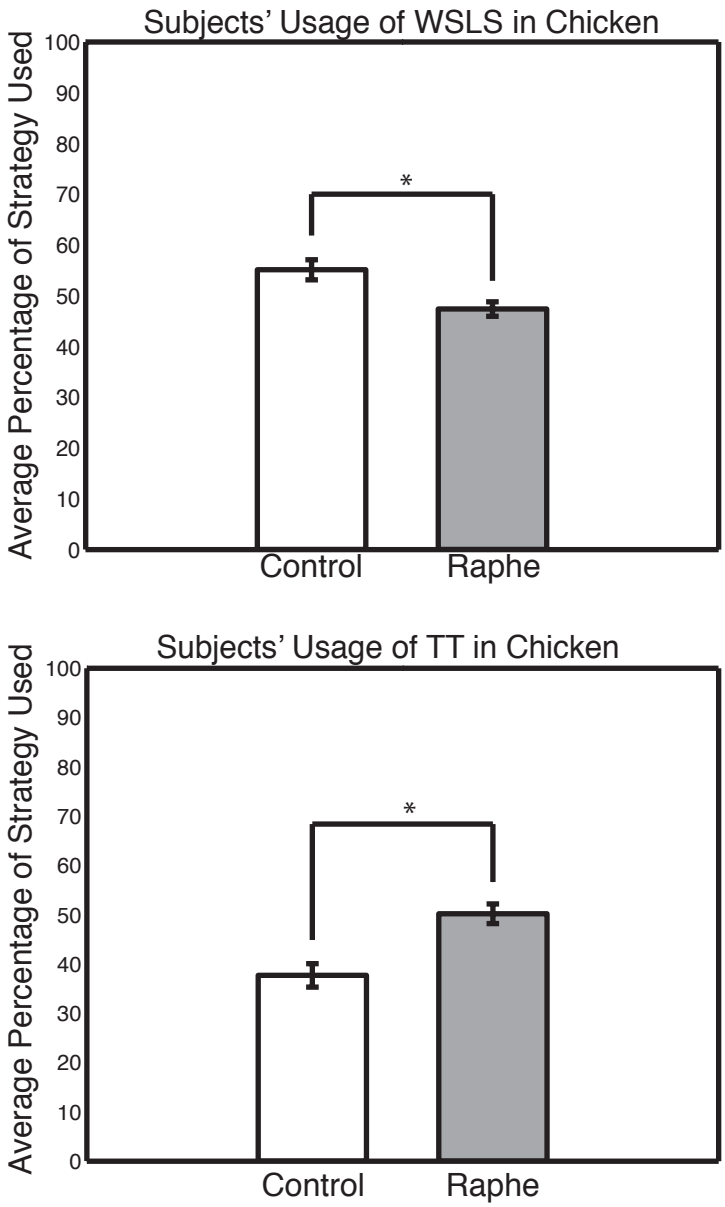

Figure 2.8. Human Subjects' Strategy Adoption in Chicken. .The bar plots show the mean and SEM for each level (Control and Raphe) within the main factor Neural State for the respective dependent variables, %TT and %WSLS. The single asterisk indicates marginal significance at $p < 0.025$ (bottom) and $p < 0.06$ (top).

Discussion

This study made several predictions regarding the mechanisms underlying cognitive behaviors, such as cooperation, competition, social contracts and reciprocity. For one, playing games against opponents that are interactive and

personified evoked strong responses in subjects. Furthermore, an agent with the ability to adapt to contextual changes in the environment or its opponent's behavior was an important factor in evoking these responses. Lastly, subjects tend to reciprocate and retaliate against adaptive agents when they believed being treated unfairly.

The main finding of this study was that human subjects changed their overall strategies in response to changes in the neural agent's state (Control or Raphe). Specifically, subjects switched from a WSLS strategy when playing against a neural agent with an intact simulated nervous system to a TT strategy when playing against a neural agent with a lesion to its serotonergic system (Figure 2.7 and 2.8). This change in strategy was independent of the embodiment of the *Neural* agent and independent of tryptophan levels. A *Neural* agent with a simulated lesion to its serotonergic system tended toward more aggressive behavior, because it lost its ability to assess the cost of an action (Figure 1.3). Subjects playing against such an opponent did not increase their levels of aggression; that is, there were no significant increases in their decisions to choose to *Escalate* or drive *Straight*. Rather, subjects responded to aggressive behavior with aggression and cooperative behavior with cooperation, through the adoption of the TT strategy.

The shift to a TT strategy may be similar to the rejection of unfair offers in the Ultimatum Game (Nowak, Page et al. 2000). In both cases, subjects behaved irrationally by lowering their overall utility through aggressive behavior. That is, aggressive behavior by both cases resulted in lower payoffs. In the Ultimatum

Game, a subject rejects what he or she deems unfair even if he or she is the only one penalized by their rejection, and even if the proposer of the offer is unaware of their actions (Yamagishi, Horita et al. 2009). A TT strategy, which is strategically less advantageous than WSLS, could send a message to another player that the subject believes he is being treated unfairly. The *Neural* agent, which was developed in simulations against fixed-strategy opponents, did not have the capacity to retaliate.

Playing an opponent that is interactive and personified has previously been observed to evoke strong responses in subjects. For example, in the Ultimatum Game, subjects reject more offers made by a human partner than those offers made by a computer, suggesting that participants have a stronger emotional reaction to unfair offers from humans than from a computer (Sanfey, Rilling et al. 2003). In the present study, the physical instantiation of the *Neural* agent in both games did not evoke stronger responses from subjects than did the simulated *Neural* agent. Perhaps both the simulated and embodied versions of the *Neural* agent evoked strong responses in subjects because of the *Neural* agent's adaptive behavior. The *Neural* agent demonstrated a variety of strategies and adjusted its behavior to environmental conditions and its opponent. Moreover, lesions to the *Neural* agent's simulated serotonergic system resulted in additional classes of more aggressive opponents.

References

Asher, D. E., A. Zaldivar, et al. (2010). Effect of Neuromodulation on Performance in Game Playing: A Modeling Study. 2010 IEEE 9th International Conference on Development and Learning, Ann Arbor, Michigan, IEEE Xplore.

Bell, C. J., S. D. Hood, et al. (2005). "Acute tryptophan depletion. Part II: clinical effects and implications." Aust N Z J Psychiatry 39(7): 565-574.

Biggio, G., F. Fadda, et al. (1974). "Rapid depletion of serum tryptophan, brain tryptophan, serotonin and 5-hydroxyindoleacetic acid by a tryptophan-free diet." Life Sci 14(7): 1321-1329.

Cools, R., A. C. Roberts, et al. (2008). "Serotoninergic regulation of emotional and behavioural control processes." Trends Cogn Sci 12(1): 31-40.

Cox, B. R. and J. L. Krichmar (2009). "Neuromodulation as a Robot Controller: A Brain Inspired Design Strategy for Controlling Autonomous Robots." IEEE Robotics & Automation Magazine 16(3): 72-80.

Crockett, M. J., L. Clark, et al. (2012). "Serotonin modulates the effects of Pavlovian aversive predictions on response vigor." Neuropsychopharmacology 37(10): 2244-2252.

Crockett, M. J., L. Clark, et al. (2009). "Reconciling the role of serotonin in behavioral inhibition and aversion: acute tryptophan depletion abolishes punishment-induced inhibition in humans." J Neurosci 29(38): 11993-11999.

Crockett, M. J., L. Clark, et al. (2008). "Serotonin modulates behavioral reactions to unfairness." Science 320(5884): 1739.

Ellenbogen, M. A., S. N. Young, et al. (1996). "Mood response to acute tryptophan depletion in healthy volunteers: sex differences and temporal stability." Neuropsychopharmacology 15(5): 465-474.

Gessa, G. L., G. Biggio, et al. (1974). "Effect of the oral administration of tryptophan-free amino acid mixtures on serum tryptophan, brain tryptophan and serotonin metabolism." J Neurochem 22(5): 869-870.

Hood, S. D., C. J. Bell, et al. (2005). "Acute tryptophan depletion. Part I: rationale and methodology." Aust N Z J Psychiatry 39(7): 558-564.

Jans, L. A., W. J. Riedel, et al. (2007). "Serotonergic vulnerability and depression: assumptions, experimental evidence and implications." Mol Psychiatry 12(6): 522-543.

Nowak, M. A., K. M. Page, et al. (2000). "Fairness versus reason in the ultimatum game." Science 289(5485): 1773-1775.

Oldman, A., A. Walsh, et al. (1995). "Biochemical and behavioural effects of acute tryptophan depletion in abstinent bulimic subjects: a pilot study." Psychol Med 25(5): 995-1001.

Rapoport, A. and A. M. Chammah (1966). "The game of chicken." American Behavioral Scientist 10(3): 10-28.

Sanfey, A. G., J. K. Rilling, et al. (2003). "The neural basis of economic decision-making in the Ultimatum Game." Science 300(5626): 1755-1758.

Seymour, B., N. D. Daw, et al. (2012). "Serotonin selectively modulates reward value in human decision-making." J Neurosci 32(17): 5833-5842.

Tanaka, S. C., K. Shishida, et al. (2009). "Serotonin affects association of aversive outcomes to past actions." J Neurosci 29(50): 15669-15674.

Watson, D., L. A. Clark, et al. (1988). "Development and validation of brief measures of positive and negative affect: The PANAS scales." Journal of personality and social psychology 54(6): 1063.

Williams, J. B. W. and M. Gibbon (1992). "The structured clinical interview for DSM-III-R (SCID) II. Multisite test-retest reliability." Archives of General Psychiatry 49(8): 630.

Wood, R. M., J. K. Rilling, et al. (2006). "Effects of tryptophan depletion on the performance of an iterated Prisoner's Dilemma game in healthy adults." Neuropsychopharmacology 31(5): 1075-1084.

Yamagishi, T., Y. Horita, et al. (2009). "The private rejection of unfair offers and emotional commitment." Proc Natl Acad Sci U S A 106(28): 11520-11523.

Young, S. N., S. E. Smith, et al. (1985). "Tryptophan depletion causes a rapid lowering of mood in normal males." Psychopharmacology (Berl) 87(2): 173-177.

Zaldivar, A., D. E. Asher, et al. (2010). "Simulation of How Neuromodulation Influences Cooperative Behavior." Simulation of Adaptive Behavior: From Animals to Animats. S. Doncieux, J.-A. Meyer, A. Guillot and J. Hallam. Berlin Heidelberg, Springer-Verlag Lecture Notes on Artificial Intelligence (LNAI 6226): 649-660.

CHAPTER 3: Exploratory Survey of Neuromodulatory Systems and the Amygdala Using the Allen Brain Atlas

Combining game theory and computational modeling from Chapter 1 with embodiment and pharmacological manipulations from Chapter 2 helped reveal how humans interact with agents utilizing adaptive behavior in conflicting situations. The computational model used in Chapter 1 and 2, though built on the assumptions that all neuromodulators have the same effect on downstream targets and that specific neuromodulator levels are driven by environmental stimuli (Krichmar 2008), is in itself not enough to fully explore the interactions between neuromodulatory systems (Introduction). A computational model of how the brain works may integrate experimental facts from different levels of investigation, which may come from neuroanatomy, neurophysiology, and psychology (Trappenberg 2010). Otherwise, the computational model may not be considered biologically plausible; thereby, its predictions may not be taken seriously.

One way to obtain experimental facts for modeling is by analyzing publicly available data sets containing brain connectivity, neural activity, and gene expression. The survey presented in this chapter explores one such data set, the Allen Mouse Brain Atlas (ABA), a project that features an interactive, comprehensive, genome-wide image database of expression data for over 20,000 genes (Lein, Hawrylycz et al. 2007; Ng, Pathak et al. 2007). Using the ABA could assist in analyzing and understanding the organization of brain circuitry involved with neuromodulators. Specifically, the methodology presented in this chapter

makes predictions about the connectivity of neuromodulator systems with other brain regions based on receptor localization.

Allen Brain Atlas

The ABA is a standardized atlas of gene expression data from 56-day-old male C57BL/6J mice strains visualized by in situ hybridization (ISH). The ISH was performed using a non-radioactive, digoxigenin-labeled anti-sense riboprobes. This survey utilized an early version of the ABA's Application Programming Interface (API) to access gene expression energy in different anatomical regions of the mouse brain atlas (http://community.brain-map.org/confluence/display/DataAPI/Home). The API featured several method calls that allow users to obtain data including high-resolution images, expression data from an experiment's image series and 3D coordinates for atlas-annotated structures in 200 μm resolution.

To investigate expression energy volumes in the brain regions of interest, a Java application to access the ABA via calls to API methods was implemented. Data was retrieved on February 28th, 2012. In particular, two ABA API methods were utilized for the survey: Gene API and Expression Energy Volumes API. The Gene API method was first used to obtain a listing of image series identification (ID) numbers given a list of genes (Table 3.1). The Expression Energy Volumes API returned gene expression energy data per voxel of the mouse brain for a given ID. The volume space returned by this method was divided into individual 200 μm 3D cubic sagittally arranged voxels on an (x,y,z) coordinate plane. Expression energy value, as defined in the ABA, represents the density of expression within a 200 μm

voxel from grid data taken per image series ID (sum of expressing pixels ÷ sum of all pixels in division) divided by the pixel intensity of expression in that voxel (sum of expressing pixel intensity ÷ sum of expressing pixels). To account for different sized brain regions, expression energy values for a brain region were normalized by dividing the voxels in a brain region that contained expression energy by the maximum voxels for that given brain area. No attempts were made in normalizing based on neuron size. Instead, normalization was applied at the level of the receptor gene expression per anatomical region.

Table 3.1 List of Neuromodulatory Receptor Genes. ImageSeriesID is an identification number for the experiment used to analyze gene expression.

Symbol	Name	ImageSeriesID	Receptor Subtype
Adra1a	adrenergic receptor, alpha 1a	74277700	G_q-protein coupled
Adra1d	adrenergic receptor, alpha 1d	69236807	G_q-protein coupled
Adra2a	adrenergic receptor, alpha 2a	70723343	G_i-protein coupled
Adra2c	adrenergic receptor, alpha 2c	70723357	G_i-protein coupled
Adrb1	adrenergic receptor, beta 1	77340494	G_s/G_i-protein coupled
Adrb2	adrenergic receptor, beta 2	68744522	G_s/G_i-protein coupled
Chrm1	cholinergic receptor, muscarinic 1	73907497	G_q/G_s/G_i-protein coupled
Chrm2	cholinergic receptor, muscarinic 2	70560343	G_i-protein coupled
Chrm3	cholinergic receptor, muscarinic 3	2095	G_q-protein coupled
Chrm4	cholinergic receptor, muscarinic 4	261	G_i-protein coupled
Chrm5	cholinergic receptor, muscarinic 5	74821591	G_q-protein coupled
Chrna1	cholinergic receptor, nicotinic, alpha polypeptide 1	75551465	Ligand-gated Na^+/K^+ cation channel

Chrna2	cholinergic receptor, nicotinic, alpha polypeptide 2	75551460	Ligand-gated Na^+/K^+ cation channel
Chrna3	cholinergic receptor, nicotinic, alpha polypeptide 3	69734723	Ligand-gated Na^+/K^+ cation channel
Chrna4	cholinergic receptor, nicotinic, alpha polypeptide 4	1173	Ligand-gated Na^+/K^+ cation channel
Chrna5	cholinergic receptor, nicotinic, alpha polypeptide 5	74821601	Ligand-gated Na^+/K^+ cation channel
Chrna6	cholinergic receptor, nicotinic, alpha polypeptide 6	75551461	Ligand-gated Na^+/K^+ cation channel
Chrna7	cholinergic receptor, nicotinic, alpha polypeptide 7	69237107	Ligand-gated $Na^+/K^+/Ca^{2+}$ cation channel
Chrna9	cholinergic receptor, nicotinic, alpha polypeptide 9	74821602	Ligand-gated Na^+/K^+ cation channel
Chrnb1	cholinergic receptor, nicotinic, beta polypeptide 1	75831174	Ligand-gated Na^+/K^+ cation channel
Chrnb2	cholinergic receptor, nicotinic, beta polypeptide 2	2097	Ligand-gated Na^+/K^+ cation channel
Chrnb3	cholinergic receptor, nicotinic, beta polypeptide 3	79760470	Ligand-gated Na^+/K^+ cation channel
Drd1a	dopamine receptor D1A	352	G_s-protein coupled
Drd2	dopamine receptor 2	357	G_i/G_o-protein coupled
Drd3	dopamine receptor 3	69859867	$G_i/G_o/G_s$-protein coupled
Htr1a	5-hydroxytryptamine (serotonin) receptor 1A	79394355	G_i/G_o-protein coupled
Htr1b	5-hydroxytryptamine (serotonin) receptor 1B	583	G_i/G_o-protein coupled
Htr1d	5-hydroxytryptamine (serotonin) receptor 1D	71393418	G_i/G_o-protein coupled
Htr1f	5-hydroxytryptamine (serotonin) receptor 1F	69859867	G_i/G_o-protein coupled
Htr2b	5-hydroxytryptamine (serotonin) receptor 2B	71664130	G_q/G_{11}-protein coupled

Htr2c	5-hydroxytryptamine (serotonin) receptor 2C	71393424	G_q/G_{11}-protein coupled
Htr3a	5-hydroxytryptamine (serotonin) receptor 3A	74724760	Ligand-gated Na^+/K^+ cation channel
Htr3b	5-hydroxytryptamine (serotonin) receptor 3B	68745408	Ligand-gated Na^+/K^+ cation channel
Htr4	5-hydroxytryptamine (serotonin) receptor 4	69257849	G_s-protein coupled
Htr5a	5-hydroxytryptamine (serotonin) receptor 5A	71393430	G_i/G_o-protein coupled
Htr5b	5-hydroxytryptamine (serotonin) receptor 5B	69257975	G_i/G_o-protein coupled
Htr6	5-hydroxytryptamine (serotonin) receptor 6	69257981	G_s-protein coupled
Htr7	5-hydroxytryptamine (serotonin) receptor 7	71393436	G_s-protein coupled

The (x,y,z) coordinates associated with an expression energy were mapped to brain structures using the annotated atlas provided with the ABA API main site (AtlasAnnotation200.sva). The annotated atlas provided an identifier for a brain structure at a given coordinate. This identifier was then compared with a separate dataset file (brainstructures.csv) to obtain the name of the brain region associated with the identifier. For instance, suppose an expression energy value was found at coordinate (40,26,26) for the dopamine receptor, Drd1a. The annotated atlas would reveal that those coordinates corresponded to the informatics ID number 139. The brainstructures.csv file would then indicate that the informatics ID number 139 represented the ventral tegmental area (VTA).

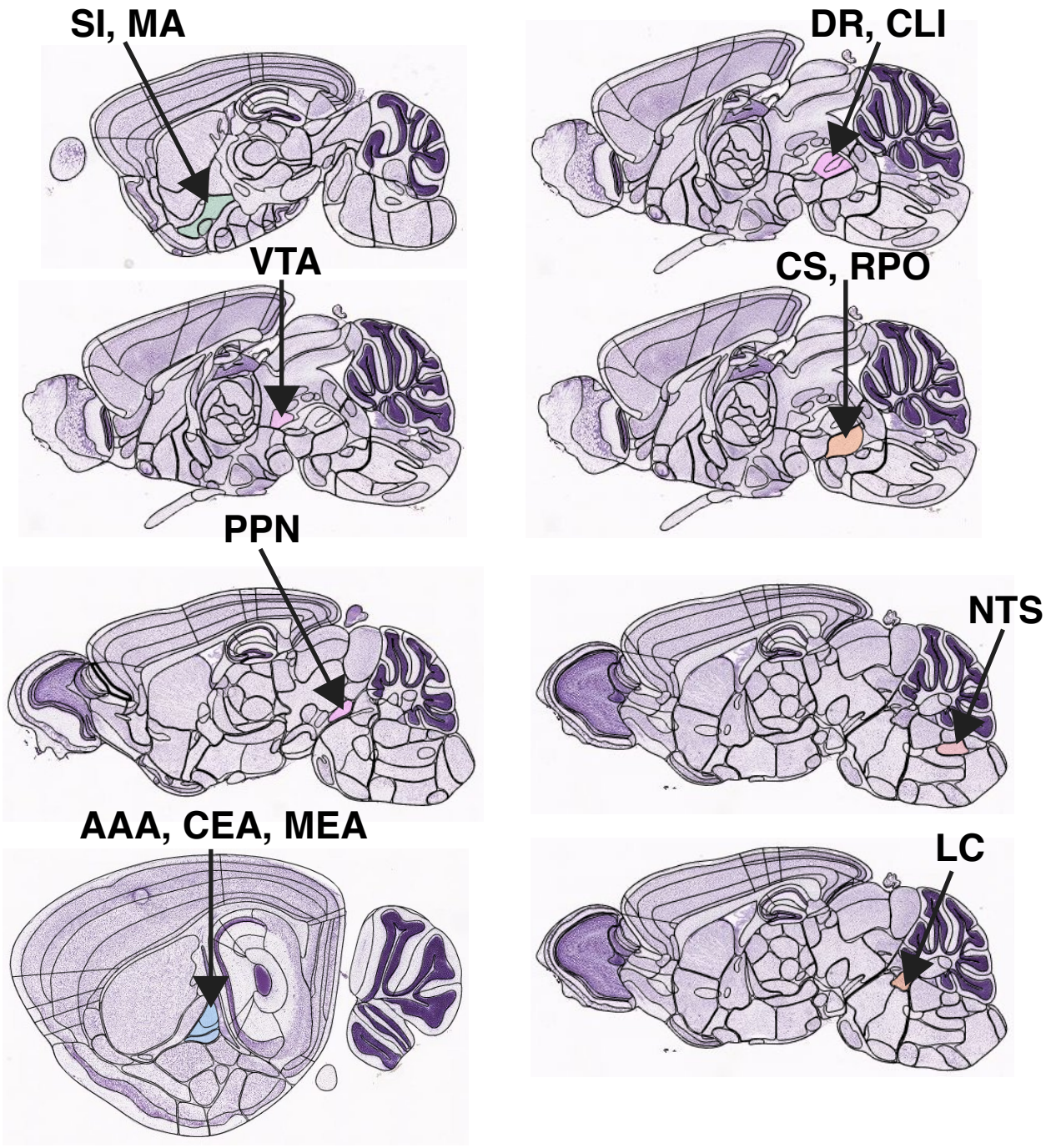

Figure 3.1 Allen Reference Atlas Images of Brain Regions. Brain regions studied include: dorsal raphe nucleus (DR), superior central nucleus raphe (CS), central linear nucleus raphe (CLI), nucleus raphe pontis (RPO), ventral tegmental area (VTA), locus coeruleus (LC), nucleus of the solitary tract (NTS), substantia innominata (SI), magnocellular nucleus (MA), pedunculopontine nucleus (PPN), anterior amygdalar area (AAA), central amygdalar nucleus (CEA) and medial amygdala nucleus (MEA). Image originally from the Allen Mouse Brain Reference Atlaas (http://mouse.brain-map.org/static/atlas).

Brain Regions

Expression data from the ABA were extracted from 13 different brain regions (Figure 3.1). Ten of those regions are considered sources of neuromodulatory systems: noradrenergic (locus coeruleus, LC; nucleus of the solitary tract, NTS), cholinergic (substantia innominata, SI; magnocellular nucleus, MA; pedunculopontine nucleus, PPN), dopaminergic (ventral tegmental area, VTA), and serotonergic (dorsal raphe nucleus, DR; superior central nucleus raphe, CS; central linear nucleus raphe, CLI; nucleus raphe pontis, RPO) (Mesulam, Mufson et al. 1983; Bhatia, Saha et al. 1997; Hornung 2003; Sodhi and Sanders-Bush 2004). The remaining three brain regions are in the amygdala (i.e., anterior amygdalar area, AAA; central amygdalar nucleus, CEA; medial amygdalar nucleus, MEA), which were chosen because of their strong bidirectional interaction with neuromodulatory systems (Woolf and Butcher 1982; Han, Holland et al. 1999; Bouret, Duvel et al. 2003; McGaugh 2004; Lee, Wheeler et al. 2011). Note that substantia nigra pars compacta, which is also a source of dopamine neurons, was not included because it is thought to project primarily to the basal ganglia, an area not included in this survey.

Neuromodulatory Receptor Genes

Using the Gene API, a search was performed for all known neuromodulatory receptor genes, which included 5 dopaminergic, 16 serotonergic, 19 cholinergic and 9 adrenergic receptors for a total of 49 different receptor types (Nicholas, Hokfelt et al. 1996; Hoyer, Hannon et al. 2002; Ishii and Kurachi 2006; Lan, DuRand et al.

2006; Dani and Bertrand 2007). Of these 49, only 38 receptors were available for evaluation (Table 3.1). Drd4 and Drd5 were not available in the ABA, and thus, were not included in this survey. Although ABA data extends from mouse brain tissue, all genes listed in Table 3.1 are orthologous to rat and human genes according to the Mouse Genome Informatics database, which can be accessed at: http://www.informatics.jax.org.

While the detection sensitivity for probes vary across mRNA species, the ABA has performed validation experiments to ensure consistent data quality and internal reproducibility (Lein, Hawrylycz et al. 2007; Lee, Sunkin et al. 2008). In every ISH run, a positive control slide was incubated with a Drd1a riboprobe and a negative control was incubated in hybridization buffer without that riboprobe (Lein, Hawrylycz et al. 2007). These slides were then used to determine whether data from the run would advance into their data analysis pipeline by qualitatively scoring the run as 'Pass' or 'Fail'. In addition, an experiment was performed to replicate data across a series of days, using riboprobes generated in parallel through in vitro translation, which include Calb1, Calb2, Cst3, Dkk3, Gad1, Man1a, Plp1, Pvalb and Nov (Lee, Sunkin et al. 2008). For each gene, an independently synthesized probe was hybridized on consecutive serial sections from the same brains over the span of four days, which maximizes comparability over time while minimizing other biological variability, including differential hapten incorporation in riboprobes, and batch reagent preparation variability. The results reported in Lee et al. 2008 demonstrate consistency of the ABA ISH platform.

In cases where multiple experiments (image series IDs) for a particular gene were found, the experiment that contained the highest expression energy data within brain regions of interest were used and the remaining experiments were discarded.

GABA and Glutamate Genes

Within the SI and LC, the expression energy of GABA and glutamate receptors was also surveyed. The same procedures for retrieving gene expression data on neuromodulatory receptors were applied for GABA and glutamate receptors in SI and LC. All known GABA and glutamate receptors were queried and found in the ABA via Gene API, which includes 17 $GABA_A$, 2 $GABA_B$, 4 AMPA, 5 kainate, 7 NMDA, and 7 mGluR receptors for a total of 42 different receptors. All GABA and glutamate genes are orthologous to rat and human genes according to the Mouse Genome Informatics database (http://www.informatics.jax.org).

Total Expression and Individual Receptor Subtypes

In the examined brain regions, expression energy of cholinergic receptors was much higher and expression energy of adrenergic receptors was much lower than that for dopaminergic and serotonergic receptors. Figure 3.2 represents the total expression energy for available adrenergic, cholinergic, dopaminergic and serotonergic receptors from the ABA across the 13 brain regions examined (note the different scale on the x-axes of Figure 3.2). Each bar in Figure 3.2 represents gene expression energy when combining all receptor subtypes per region. Brain regions

were ranked and arranged based on total expression in Figure 3.2, with the brain region having the highest expression energy at the top bar of each plot.

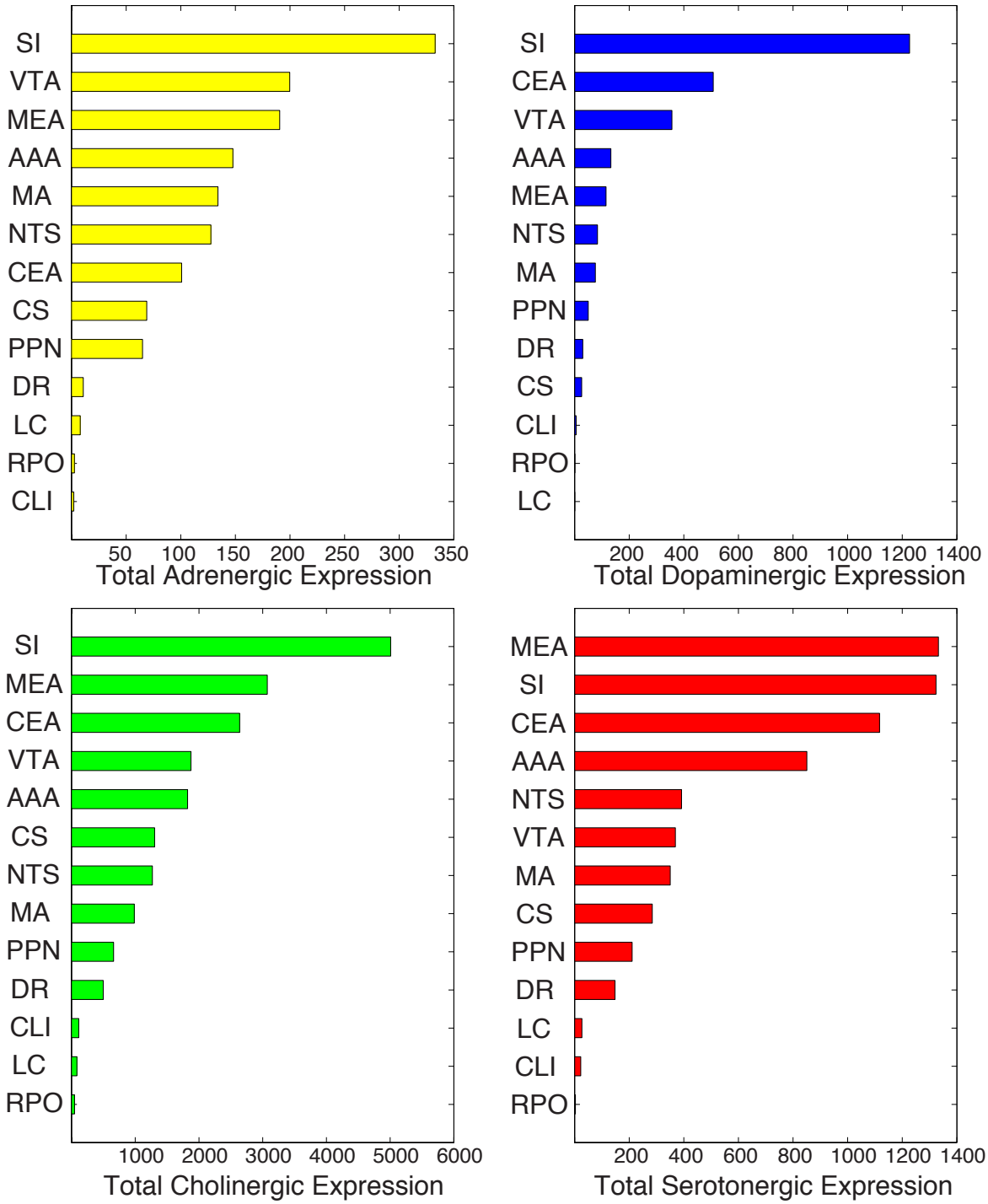

Figure 3.2. Total Gene Expression Energy of Neuromodulatory Receptors. Gene expression values for each subtype were collapsed into their respective neuromodulatory systems and separated by brain region. Brain regions were arranged from most (top) to least (bottom) amount of total expression.

The substantia innominata (SI) of the basal forebrain, amygdala (AAA, CEA, and MEA), and the ventral tegmental area (VTA) had relatively high levels of receptor expression energy. The SI had the highest receptor expression energy of all neuromodulatory regions tested, implying that this region of the basal forebrain is strongly innervated by all neuromodulatory systems (Figure 3.2). The amygdala closely followed SI in terms of overall neuromodulatory receptor expression energy, but expression energy in the amygdala differed based on neuromodulatory receptor type and amygdala subregions. For example, MEA had the highest adrenergic, cholinergic and serotonergic receptor expression energy among the amygdala regions. However, the CEA had the most dopaminergic receptor expression energy. Similar to the SI, the VTA, which contains dopaminergic neurons, displayed high expression energy for all neuromodulatory receptors.

LC and raphe nuclei (DR, CS, CLI, and RPO), which are sources of norepinephrine and serotonin respectively, did not have high expression energy of neuromodulatory receptors relative to the other regions examined (Figure 3.2). Note that the small sizes of these brain regions may not influence expression energy reporting because of the normalization procedures described above.

Different brain areas had distinct patterns of receptor subtype expression. Expression energy for individual receptor subtypes across all neuromodulatory systems are displayed in Figure 3.3. Subtypes were sorted by expression per neuromodulatory system with the top charts having the highest expression. Within each neuromodulatory system, the arrangement of brain regions from left to right

on each chart was based on their overall expression as in Figure 3.2. It is apparent that the distribution of gene expression per subtype from one brain region to another was not uniform (Figure 3.3). However, examining individual expression energy helps identify receptor subtypes that contribute to the total expression of a particular brain region being described in Figure 3.2.

The expression profile of SI, which has the highest receptor expression energy among all for neuromodulatory regions (Figure 3.2), is influencing select subtypes within neuromodulatory systems. Within the adrenergic receptors, Adra1d and Adrb2 made up a large proportion of the expression energy found in SI, while the remaining four adrenergic receptors did not contribute nearly as much (Figure 3.3). The cholinergic system, which had the most receptor subtypes, was dominated by expression of the muscarinic subtypes Chrm1, Chrm2 and Chrm4, and the nicotinic Chrna1 (Figure 3.3). Even the dopaminergic system, having the fewest receptor subtypes, had differing receptor expression, with Drd1a and Drd2 having much higher expression value in SI than Drd3 (Figure 3.3). Lastly, serotonergic receptors Htr2c, Htr1f, Htr1a, and Htr1b described most of the total expression energy in SI with comparatively lower contribution from the other subtypes (Figure 3.3).

VTA also displayed higher overall receptor expression energy compared to other regions. In general, many of the subtypes that have noticeably high expression energy in the SI also have high energy in the VTA (Figure 3.3). The main difference observed was that muscarinic receptor (Chrm2), the nicotinic

(Chrna4, Chrna6, Chrnb3), and the dopaminergic Drd2 receptor expression were higher in VTA than in SI.

Different regions of the amygdala have distinct patterns of neuromodulatory receptor expression energy. The neuromodulatory receptor expression energy found in the amygdala, which was among the highest of the brain regions studied in this survey, differed based on the neuromodulatory system (Figure 3.2), amygdalar subregion, and by receptor subtypes (Figure 3.3). For ease of visualization, pie charts were used to illustrate how receptor subtypes were distributed within the different amygdala areas (Figure 3.4). Figure 3.4 revealed a similar distribution set of prominent gene expression across the amygdala areas with similar proportions. In the noradrenergic system, Adra1a was highly expressed in the CEA and AAA, but lower in the MEA. In contrast, Adrb2 had higher expression energy in MEA than AAA or CAE (Figure 3.4, first row). The nicotinic receptor Chrna1 and the muscarinic receptor Chrm1 were more highly expressed across all the amygdala areas in comparison to other nicotinic and muscarinic receptors, though it is interesting to note that Chrm2 had relatively higher expression in the AAA, compared to CEA and MEA (Figure 3.4, second row). Dopamine and serotonin receptors were also different in receptor expression energy across the amygdala. Drd2 and Htr1f contributed most strongly to the expression found in the CEA, whereas Drd1a and Htr2c contributed most strongly to the expression found in the AAA and MEA regions (Figure 3.4, third and fourth row).

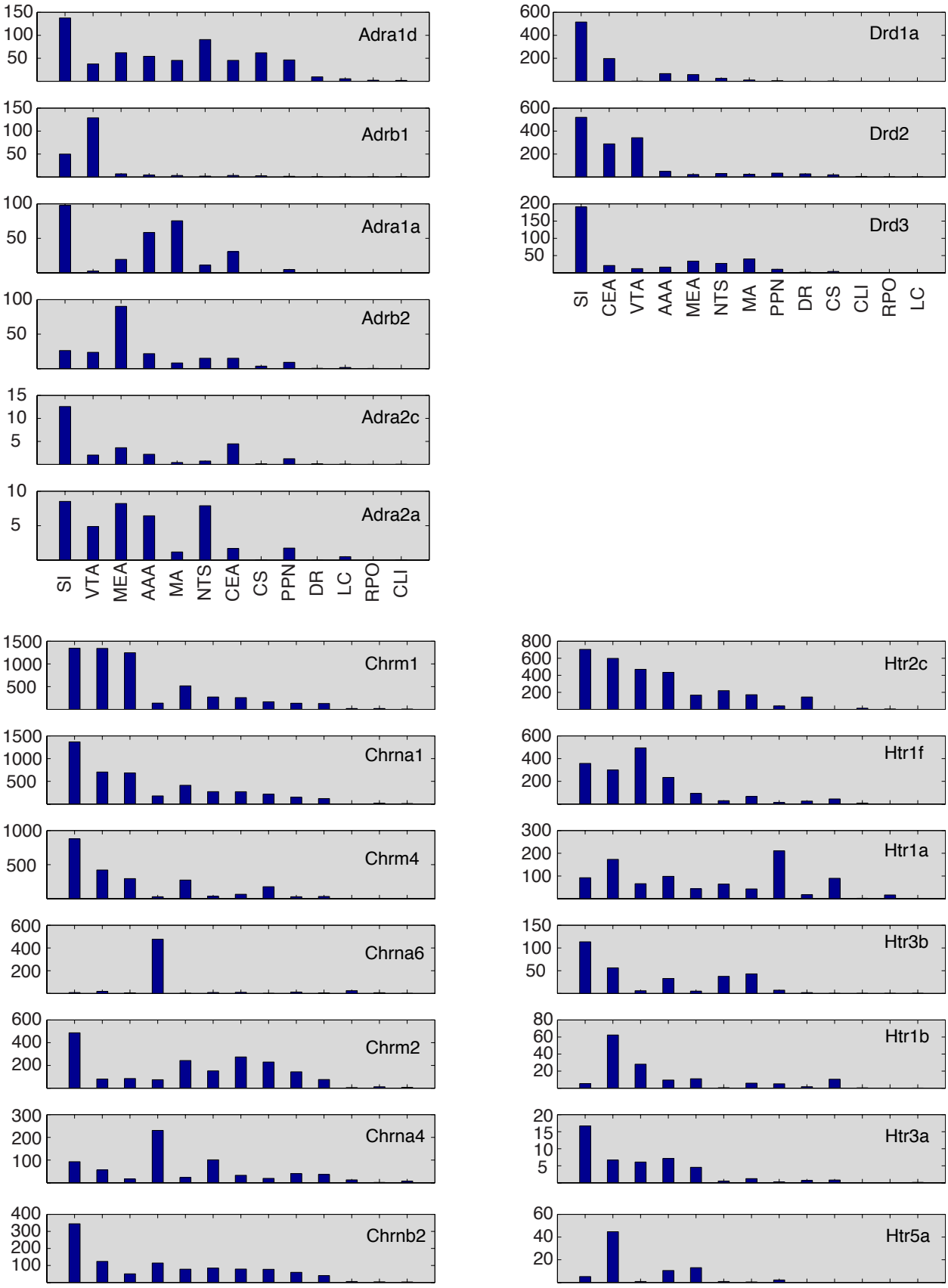
Adra1d
Adrb1
Adra1a
Adrb2
Adra2c
Adra2a
SI VTA MEA AAA MA NTS CEA CS PPN DR LC RPO CLI
Drd1a
Drd2
Drd3
SI CEA VTA AAA MEA NTS MA PPN DR CS CLI RPO LC
Chrm1
Chrna1
Chrm4
Chrna6
Chrm2
Chrna4
Chrnb2
Htr2c
Htr1f
Htr1a
Htr3b
Htr1b
Htr3a
Htr5a

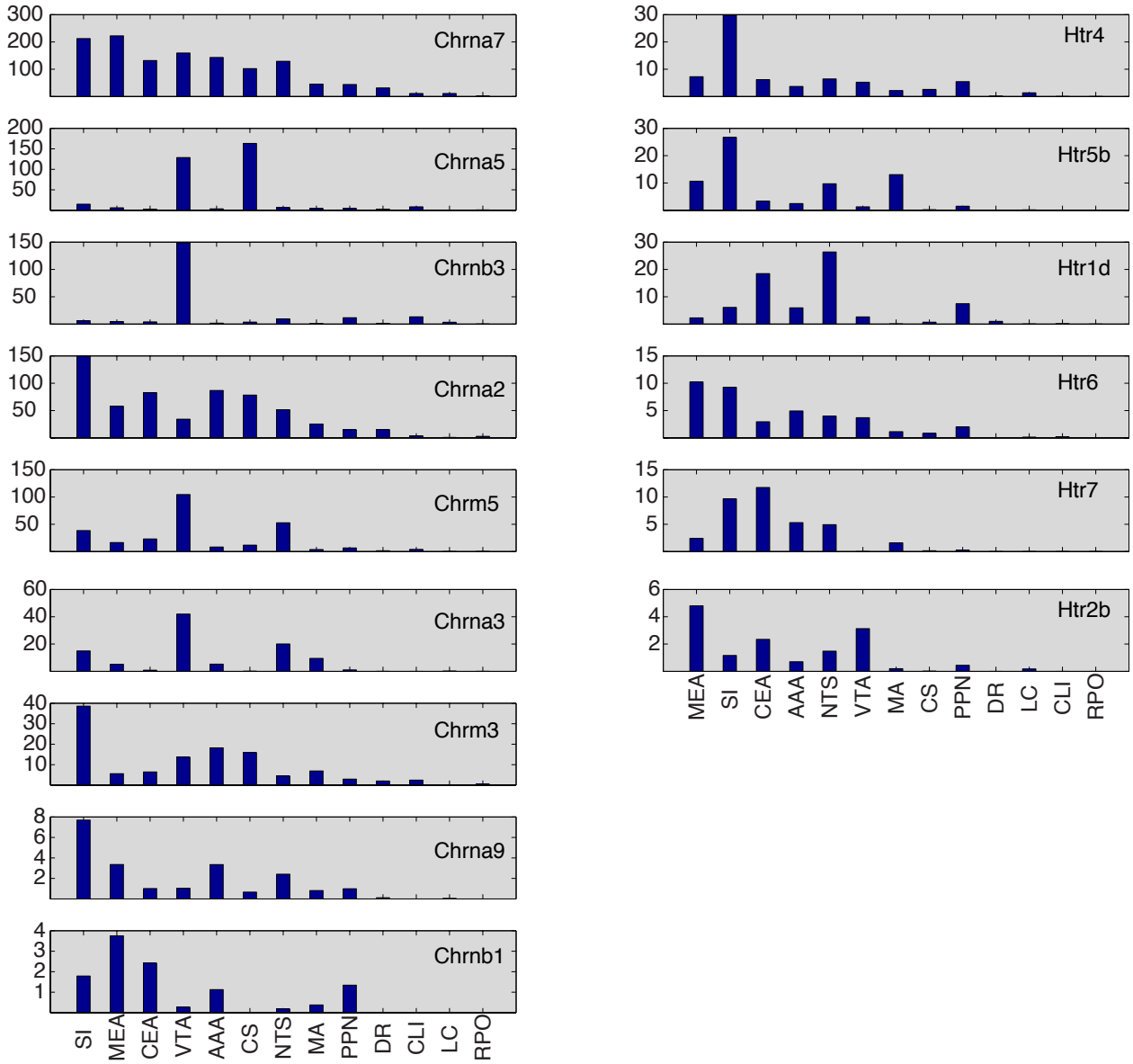

Figure 3.3. Individual Gene Expression Energy of Neuromodulatory Receptors. Charts were grouped by neuromodulatory systems. In each receptor subtype, amount of expression along the x-axis were arranged from most (left) to least (right). Brain regions were ordered from most (top) to least (bottom) amount of total expression energy for each neuromodulatory system. The y-axis represents expression energy. Note the y-axis scale varies per receptor subtype.

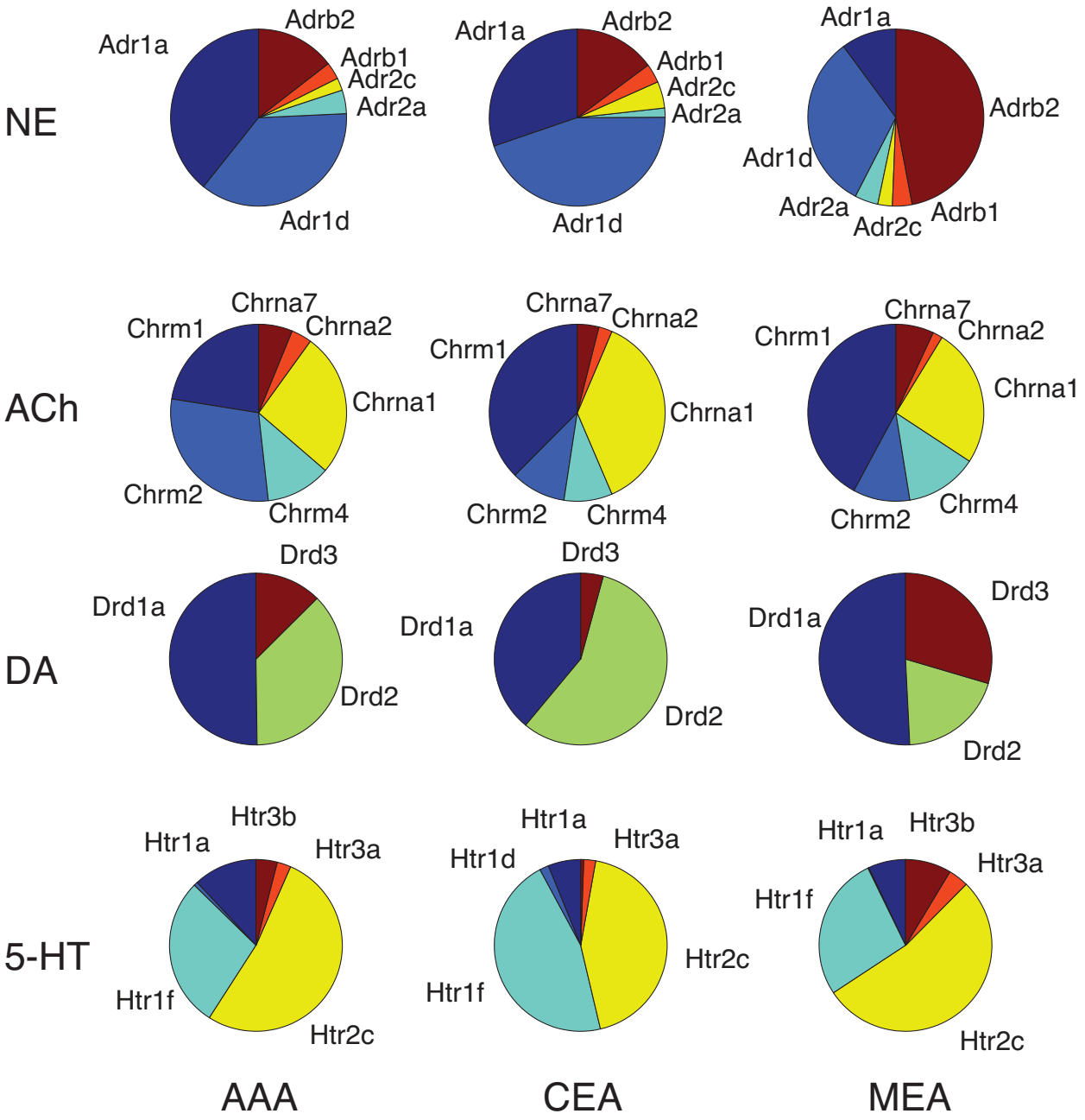

Figure 3.4 Distribution of Gene Expression Energy Within Amygdala Areas. Each column represents a different amygdala region (AAA, Anterior Amygdalar Area; CEA, Central Amygdalar Area; MEA, Medial Amygdalar Area). Each row represents the distribution of expression energy for a particular neuromodulatory system. The amount of expression energy is relative to the size of each slice in each chart.

Hierarchical Clustering Analysis

To illustrate the relationship between neuromodulatory receptor expression energy and brain region, hierarchical cluster analyses were performed for

expression energy and anatomical location (Figure 3.5). A hierarchical clustering analysis is a commonly used exploratory technique to handle a large set of data whose interrelationships are elusive and not fully understood. The cluster analysis assigned subsets of gene expression data into groups based on the similarity in their expression patterns (Figure 3.5, top), and based on the location of the brain regions examined (Figure 3.5, bottom). A hierarchy of groupings can emerge using this methodology, and such analyses have previously revealed relationships between biological function and anatomical location (Gerstein and Jansen 2000).

To perform the receptor expression energy cluster analysis, a vector of the total expression across the 38 genes was constructed for each of the 13 brain regions. The pairwise distance between these vectors were calculated using Euclidean distance. To create the dendrogram in Figure 3.5 (top), an Unweighted Pair Group Method with Arithmetic Mean (UPGMA) was calculated based on the Euclidean distance metric. Threshold values in Figure 3.5 (top) represented the computed distance and linkage between brain regions. The cutoff for determining clusters was set to a threshold of 0.19 to yield three separate clusters, denoted by their different coloring scheme in Figure 3.5 (top).

To examine the relationship between gene expression and anatomical location, a separate hierarchical cluster analysis was conducted using the centroid location for all of the 13 brain regions (Figure 3.5, bottom). The procedure was identical to the hierarchical cluster in Figure 3.5 (top), except a vector of the (x,y,z) coordinates from the reference atlas file (AtlasAnnotation200.sva) was used for

clustering instead of gene expression data. The threshold for determining clusters was set to 0.02 to yield four clusters, as in Figure 3.5 (bottom).

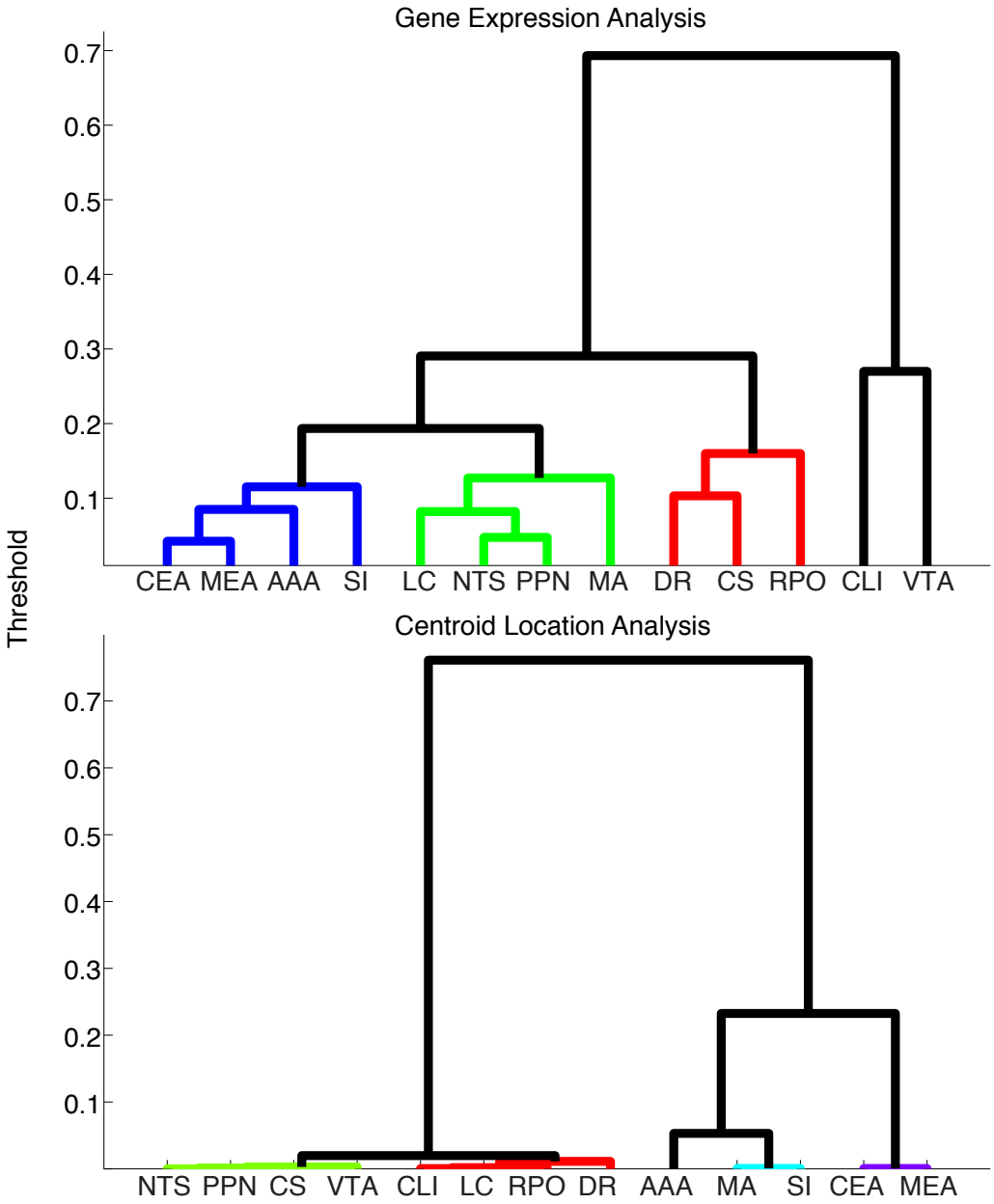

Figure 3.5. Hierarchical Cluster of Gene Expression Energy and Brain Area. The top dendrogram was derived from the expression of selected genes. The bottom dendrogram was derived from the x,y,z coordinates of brain area centroid given in the reference atlas. These dendrograms were generated using a Euclidean distance metric. The cutoff for generating the different clusters was set to 0.19 (top) and 0.02 (bottom), which broke the hierarchical cluster into four separate constitutes, denoted by their different coloring scheme.

The clusters in Figure 3.5 suggest several relationships between neuromodulatory receptor expression and anatomical location. The amygdala (AAA, MEA, CEA) and the SI formed a tight cluster (Figure 3.5, top, blue) in gene expression, as well as anatomically (Figure 3.5, bottom, cyan and purple). The SI and basal forebrain are located near the amygdala (Figure 3.1) and like the amygdala contain high overall neuromodulatory receptor expression energy (Figure 3.2 and 3.3). LC and NTS, which contain noradrenergic neurons (McGaugh 2004; Samuels and Szabadi 2008), formed a tight cluster both in terms of gene expression and to a slightly lesser extent anatomically (Figure 3.5, top, green; Figure 3.5, bottom, green and red). There was also tight clustering among the raphe nuclei, the source of serotonin in the CNS (Figure 3.5, top, red; Figure 3.5, bottom, red and green).

There were a few receptor expression energy clusters that did not match their anatomical cluster counterpart or did not form a strong cluster based on expression. The cholinergic sources SI and MA (Nicholas, Hokfelt et al. 1996; Ishii and Kurachi 2006; Dani and Bertrand 2007) did not cluster together based on expression energy, though their distance apart from each other is still relatively small (Figure 3.5, top, blue and green). However, they are found in neighboring regions of the brain (Figure 3.1) and thus clustered together based their centroid location (Figure 3.5, bottom, cyan). The SI and MA may not cluster together because their proportionally higher expression energy across all four neuromodulatory systems in the SI compared to MA (Figure 3.2 and 3.3). The dopaminergic region (VTA) and the CLI

of the raphe nucleus brain region did not fall within a cluster below the threshold when analyzing gene expression (Figure 3.5). However, in the anatomical cluster analysis, the VTA clustered together with all the raphe regions, PPN, and NTS (Figure 3.5, green and red), as they are located beside each other (Figure 3.1).

GABA and Glutamate Receptor Distribution Across SI and LC

One main finding was that the SI of the basal forebrain had high receptor expression energy for all four neuromodulatory systems (Figure 3.2). In contrast, the LC had the lowest overall expression energy across the receptors examined (Figure 3.2).

To see if high expression energy in SI and low expression energy in LC exist beyond neuromodulators receptors, the expression energy of GABA and glutamate receptors in the SI and LC (Chapter 3, GABA and Glutamate Genes) was analyzed. The same analysis used as before (Chapter 3, Total Expression and Individual Receptor Subtypes) was applied here for profiling the distribution of GABA and glutamate receptors in SI and LC.

Similar to neuromodulatory receptors expression profiles, SI had very high expression energy of GABA and glutamate receptors, while LC was low (Figure 3.6). For directed comparison, the total expression energy of adrenergic, cholinergic, dopaminergic, and serotonergic receptors from Figure 3.2 were included in Figure 3.6. The values in each bar in Figure 3.6 represent the accumulated amount of expression energy when combining all subtypes per region. Note that there is a much higher order of magnitude in expression found in the SI compared to LC.

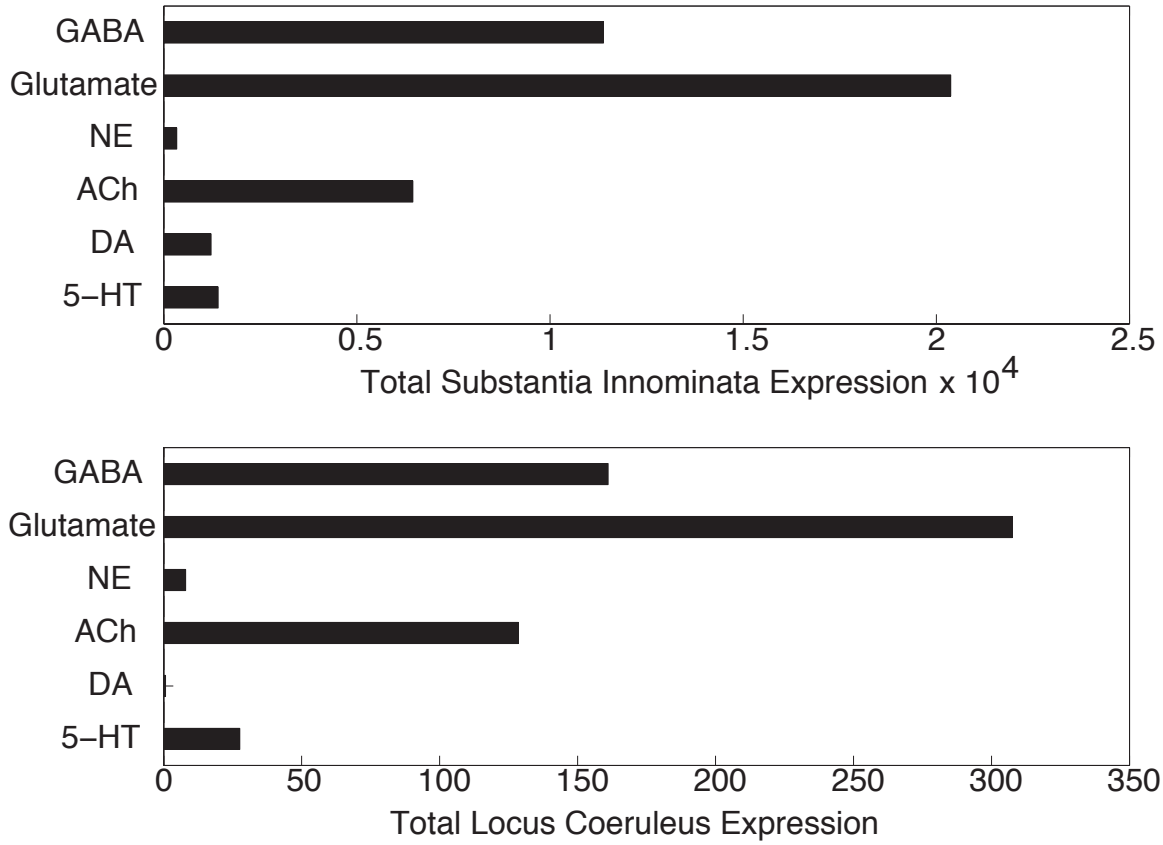

Figure 3.6. Total Gene Expression Energy for GABA, Glutamate, and Neuromodulatory Receptors in SI and LC. Expression energy from neuromodulatory receptors came from Figure 3.2.

There is a proportional relationship between the receptor expression found in SI and LC. Though receptor expression in SI was much higher than in LC, the relative distribution of expression between GABA, glutamate, adrenergic, cholinergic, dopaminergic, and serotonergic receptors had similar profiles to LC, with glutamate receptors displaying the highest amount of expression, followed by GABA, acetylcholine and serotonin (Figure 3.6). This implies that LC region has proportionally lower receptor expression energy when compared to SI, and other brain regions in this survey. Since the receptor expression energy was normalized

over region size, this lower overall receptor expression energy level reflects a unique property of the LC region.

Contrast Between ABA Expression Data and Prior ISH mRNA Literature

Neuroinformatics resources such as the Gene Expression Nervous System Atlas (GENSAT) and the Neuroscience Information Framework (NIF) provide an accessible way to obtain gene expression data from various experiments (Heintz 2004; Gardner, Akil et al. 2008; Müller, Rangarajan et al. 2008). To gauge the impact of ABA, data retrieved from the ABA were compared to results from studies retrieved from these resources.

Table 3.2 is the relative expression level in the brain regions of interest per receptor subtype. This was accomplished by first querying NIF using all genes listed in Table 3.1. NIF returned results from GENSAT that contained gene expression information from the mouse brain based on bacterial artificial chromosomes (BACs) experiments. However, because BAC experiments measure the relative rates of transcription for each gene, it is thereby not a direct measurement of mRNA accumulation. As such, in addition to the BAC expression data, GENSAT provides background literature, primarily from rat experiments, that measure localized mRNA using ISH, which GENSAT uses to correlate with their results. This feature was utilized to collect prior literature on gene receptor expression localization and intensities.

Altogether, twenty-six papers were retrieved from GENSAT to compare gene receptor expression with the ABA in Table 3.2. With the exception of two receptors

(Htr3a and Htr3b) coming from mouse literature, and six not having any prior literature found in GENSAT (Chrna1, Chrna7, Chrna9, Chrnb1, Chrnb3, Htr2b), all remaining receptors from Table 3.2 were available in GENSAT and featured rat brain in their experiment. It is worth noting that Table 3.2 is an indirect comparison of species to species receptor expression. However, all experiments retrieved from GENSAT document localization of mRNA using ISH.

Once literature was acquired, classification of expression level in prior studies was taken directly from the referenced wording. For example, some studies stated relative values (high, moderate, low), while others created tables using symbols (-, +, ++, +++) to denote the density of expression from ISH analysis. Classification of expression level in the present ABA study was based on the relative expression energy within a brain category. Expression energy less than the 33rd percentile was classified as low expression, moderate expression was between the 33rd and 66th percentiles, and above the 66th percentile was considered highly expressed. The 13 brain regions were condensed into 5 categories: Amygdala (AAA, MEA, CEA), Dopaminergic (VTA), Serotonergic (DR, RPO, CLI, CS), Cholinergic (SI, MA, PPN), and Adrenergic (LC, NTS) regions. To determine the energy of expression, the average expression across these categorized brain regions was computed, and then percentiles were calculated across each gene in each category. If the expression of a gene (row) in a brain category (column) from the ABA coincided with previous work, then the comparison was considered in agreement (Table 3.2, green cells). The table cell was colored in red if the expression in the

ABA was classified higher than in prior studies. Blue cells denoted lower expression in the ABA than in prior studies. Gray cells in the table represent expression data not found in previous studies, while yellow cells represent experiments not conducted in the literature. In cases where there was no expression found, but experiments were conducted in both the literature and ABA, table cells were colored orange. Black cells represent a case where, for a given gene, no data was found in the ABA and no experiment was found through literature.

Table 3.2. Comparison Between Gene Expression Levels Found in ABA and Previous Literature. Data from previous studies taken from: 1. (Bouthenet, Souil et al. 1991), 2. (Bruinvels, Landwehrmeyer et al. 1994), 3. (Buckley, Bonner et al. 1988), 4. (Day, Campeau et al. 1997), 5. (Diaz, Levesque et al. 1995), 6. (Fremeau, Duncan et al. 1991), 7. (Kinsey, Wainwright et al. 2001), 8. (McCune, Voigt et al. 1993), 9. (Mengod, Martinez-Mir et al. 1989), 10. (Narang 1995), 11. (Nicholas, Pieribone et al. 1993), 12. (Nicholas, Hokfelt et al. 1996), 13. (Novere, Zoli et al. 1996), 14. (Pompeiano, Palacios et al. 1992), 15. (Pompeiano, Palacios et al. 1994), 16. (Scheinin, Lomasney et al. 1994), 17. (Sugaya, Clamp et al. 1997), 18. (Tecott, Maricq et al. 1993), 19. (Vilaró, Cortés et al. 1990), 20. (Vilaro, Cortes et al. 2005), 21. (Wada, Wada et al. 1989), 22. (Wada, McKinnon et al. 1990).

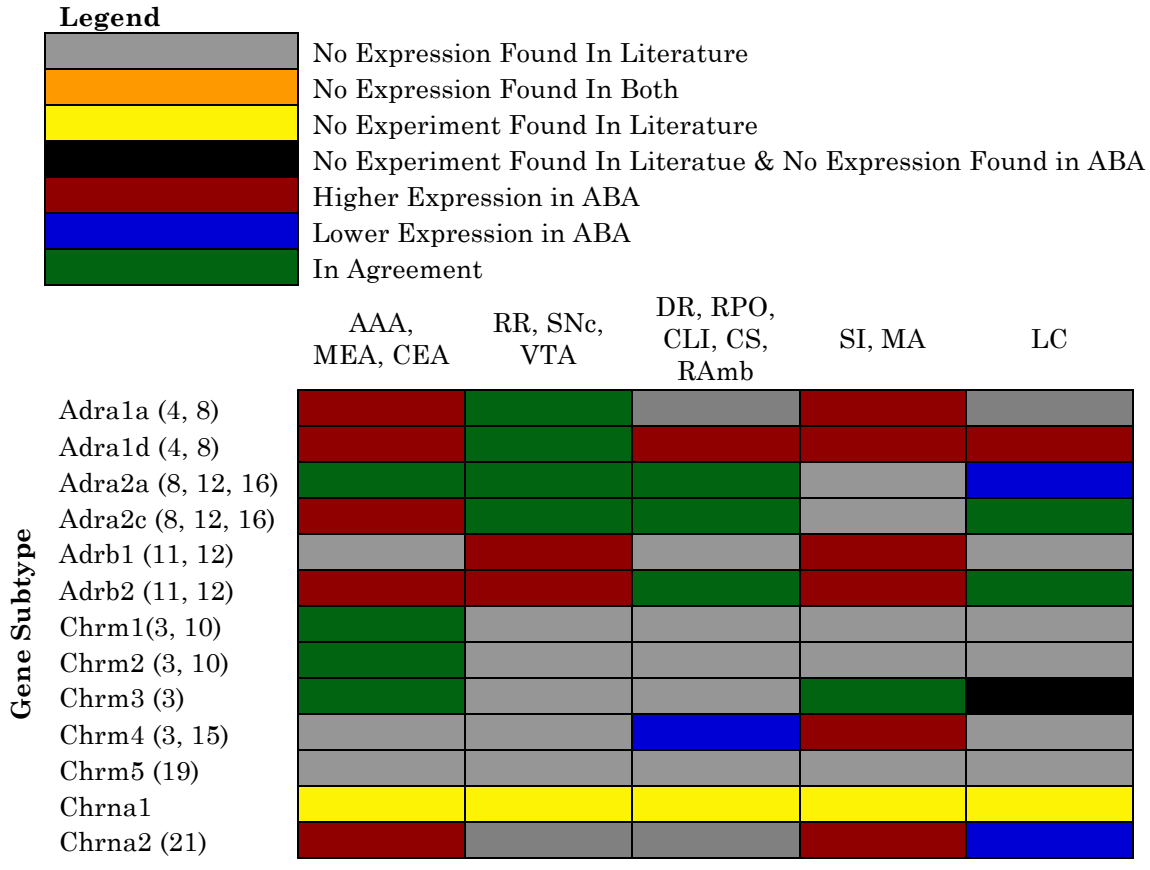

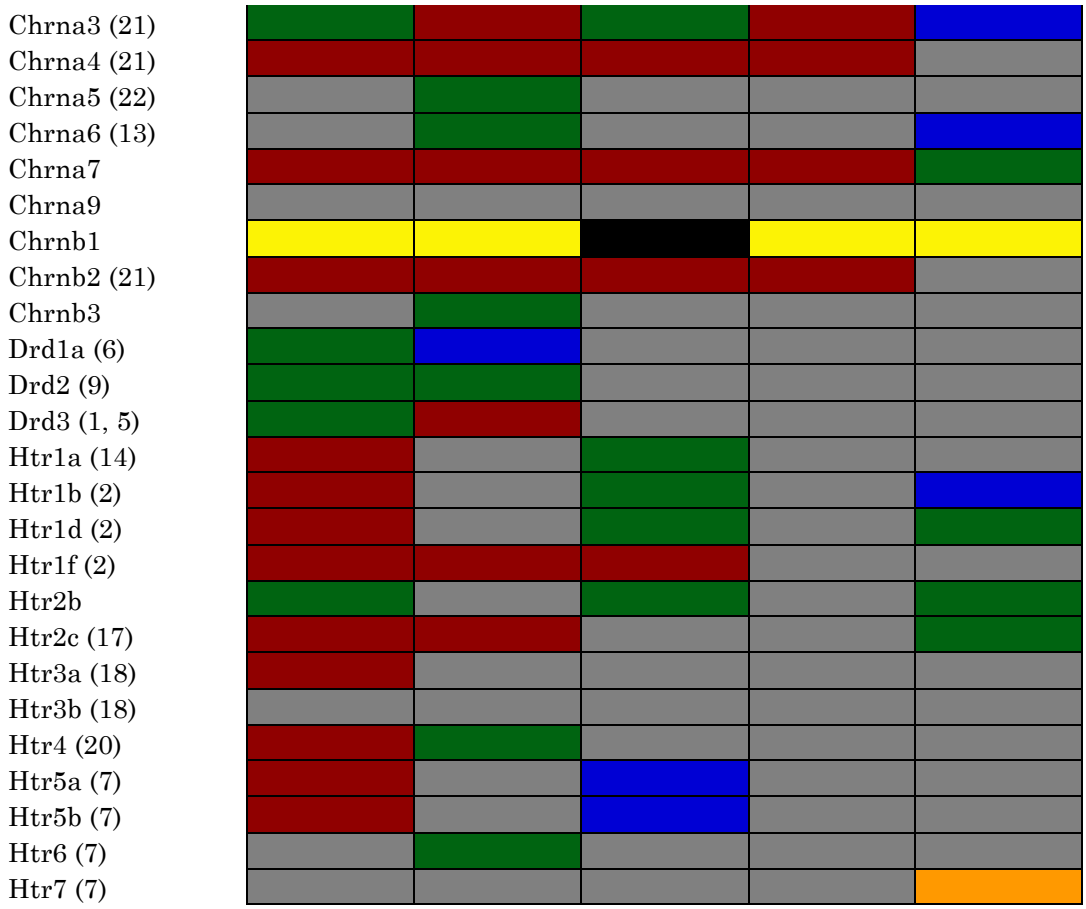

In general, the comprehensiveness of the ABA revealed information that was previously unreported (Table 3.2, gray and yellow cells), and reported higher receptor expression in the amygdala and basal forebrain across all neuromodulatory systems than previously reported studies (Table 3.2, red cells).

Network Visualization and Connectivity

To analyze neuromodulatory interaction, Pajek, a software package designed for examining large networks (Batagelj and Mrvar), was used to visualize potential connectivity relationships between brain regions based on expression data from the ABA (Figure 3.7 – 3.11). Given a neuromodulatory source, such as VTA, one can

infer the strength of a projection to a target area from that source based on the receptor expression energy.

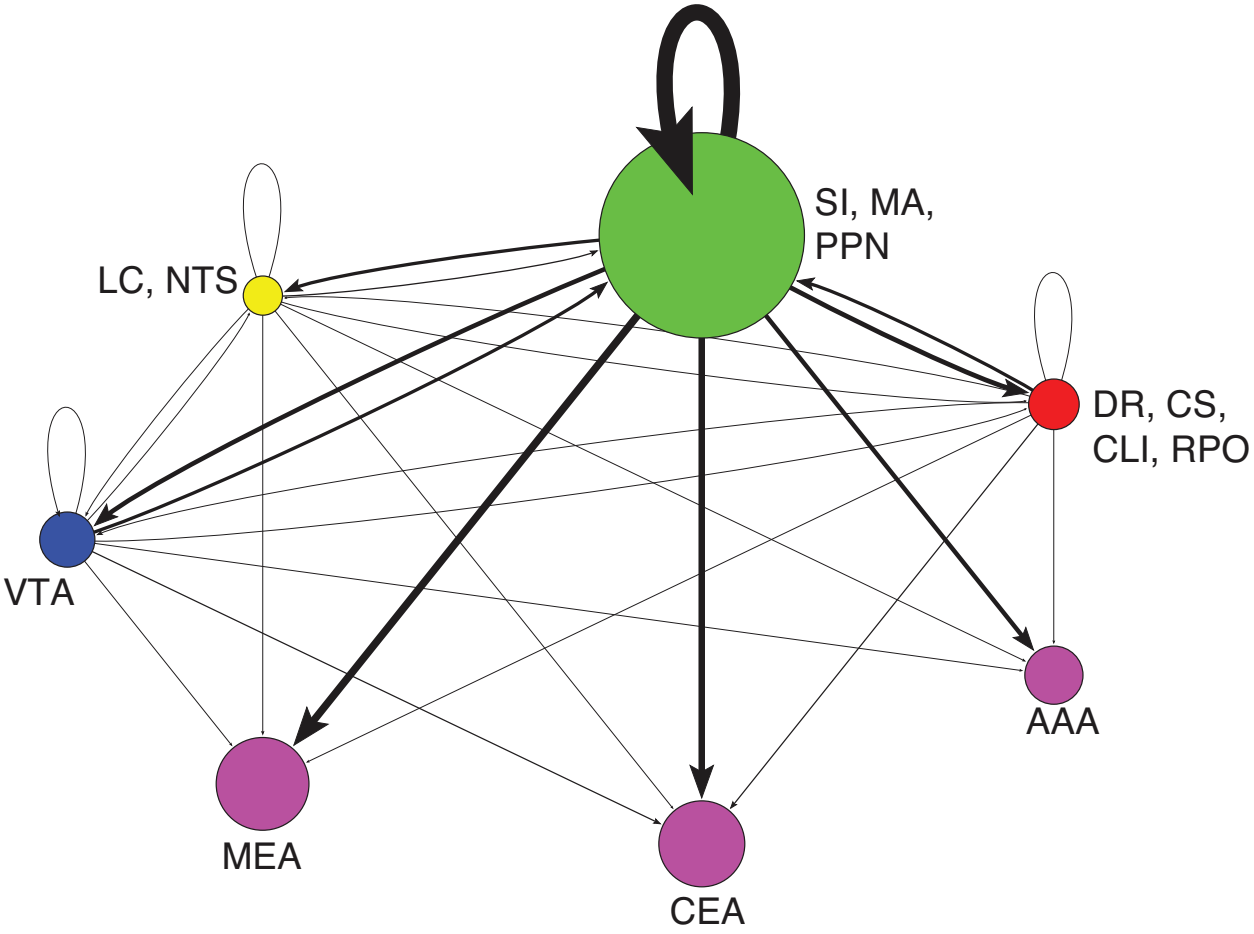

Figure 3.7. Network Graph of Neuromodulatory Receptors. Vertices represent brain regions that are either standalone or are combined regions. Directed arcs represent projections going to and from a source. The pointed-arrow indicates the target location and the non-arrow end of the arc indicates the origin. The thickness of each arc, as well as the size of vertices, is proportional to the amount of expression found in the target location. Colors were used for visualization purposes, similar to Figure 3.2 and 3.3.

Figure 3.7 depicts the overall relationship among the neuromodulatory systems and its interactions with the amygdala. Nodes corresponded to either a class of neurotransmitter source (e.g., ACh from SI, MA, and PPN) or different regions of the amygdala. Arcs represented inferred projections from a neuromodulatory system to a target brain area. Thickness of each arc is

proportional to the amount of receptor expression energy found target region. Diameter of each node represented the total amount of receptor expression energy in brain region. For ease of visualization, receptor expression energy was scaled down by 10^{-2}.

Expression energy emanating from the cholinergic system is overwhelmingly the highest, followed by serotonergic, dopaminergic, and adrenergic (Figure 3.7). All neuromodulatory systems project strongest to the cholinergic system (Figure 3.7, green node). The rest of the projections remained relatively low, though serotonin projects more heavily to AAA compared to other amygdala areas (Figure 3.7).

In addition examining at the overall neuromodulatory connectivity network, the influence of receptor subtypes on the different brain regions were examined. Families of receptors were categorized in the following way: α (Adra1a, Adra1b, Adra2a, Adra2c) versus β (Adrb1, Adrb2) adrenergic receptors; muscarinic (Chrm1, Chrm2, Chrm3, Chrm4, Chrm5) versus nicotinic (Chrna1, Chrna2, Chrna3, Chrna4, Chrna5, Chrna6, Chrna7, Chrna9, Chrnb1, Chrnb2, Chrnb3) cholinergic receptors; D1 (Drd1a) versus D2 (Drd2, Drd3) dopaminergic receptors; and serotonin receptors that produce an inhibitory response (Htr1a, Htr1b, Htr1d, Htr1f, Htr5a, Htr5b) versus serotonin receptors that produce an excitatory response (Htr2b, Htr2c, Htr3a, Htr3b, Htr4, Htr6, Htr7).

Different families of receptors were distributed differently across brain regions (Figure 3.8 – 3.11). For comparison purposes, the layout, arc thickness, and node diameter proportions were scaled down, dividing the amount of receptor

energy expression by 1,000. Expression energy from α-adrenergic receptors (Figure 3.8, top) was more prevalent in cholinergic regions, as well as in the anterior amygdalar area (AAA), and within itself compared to β-adrenergic receptors (Figure 3.8, bottom), which had a stronger influence on dopaminergic areas. Both D1 and D2 dopamine families had a strong influence on regions associated with acetylcholine and the CEA (Figure 3.9, top). However, the D2 family of receptors expressed more in dopaminergic sources compared to D1 (Figure 3.9, bottom). Muscarinic (Figure 3.10, top) was higher expressed than nicotinic acetylcholine receptors in the amygdala (MEA, CEA), while nicotinic receptors (Figure 3.10, bottom) were more strongly expressed in the dopaminergic areas. As for serotonergic receptors, expression was roughly the same for inhibitory and excitatory families (Figure 3.11).

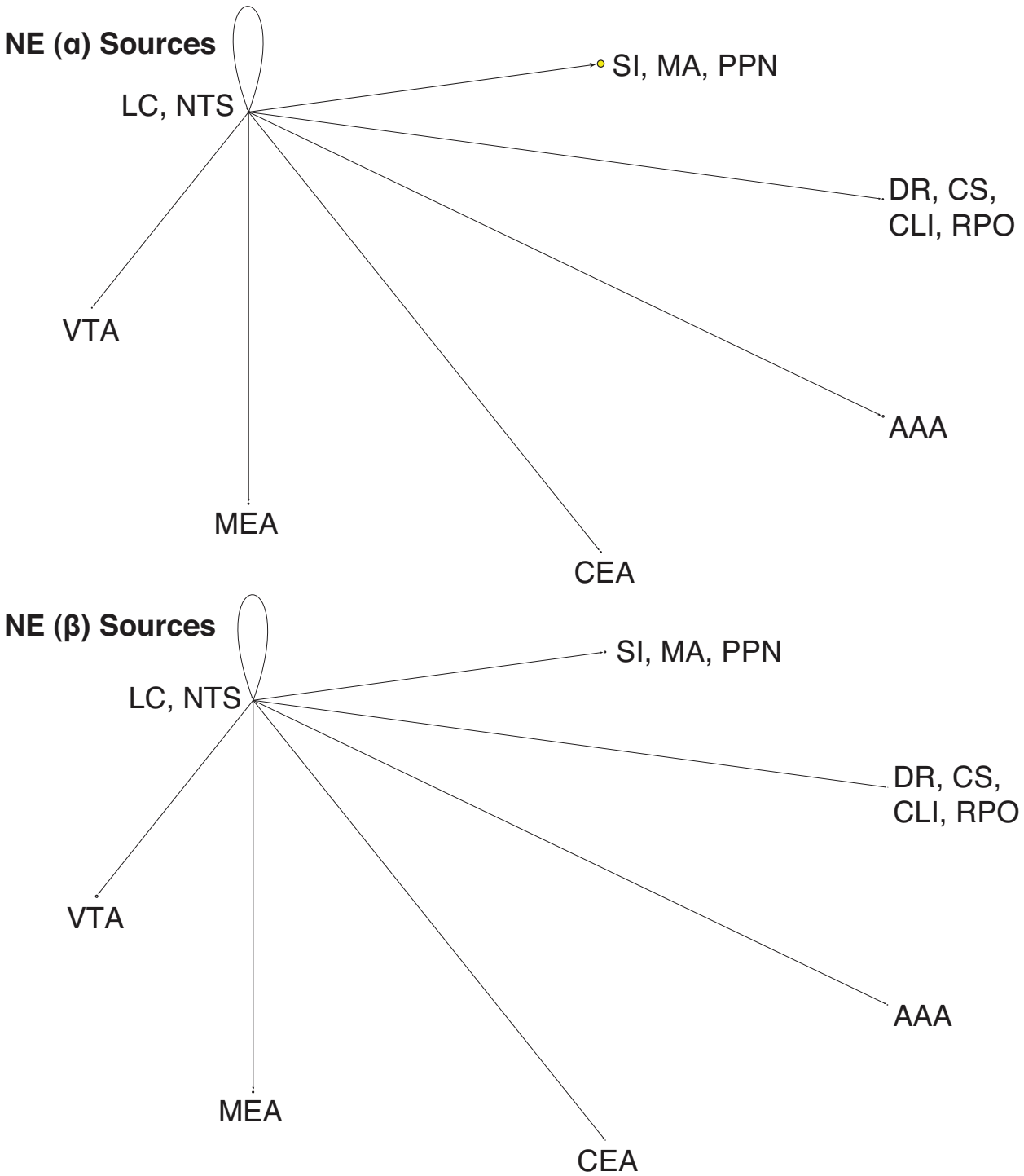

Figure 3.8. Network Graph of α and β Adrenergic Receptors.

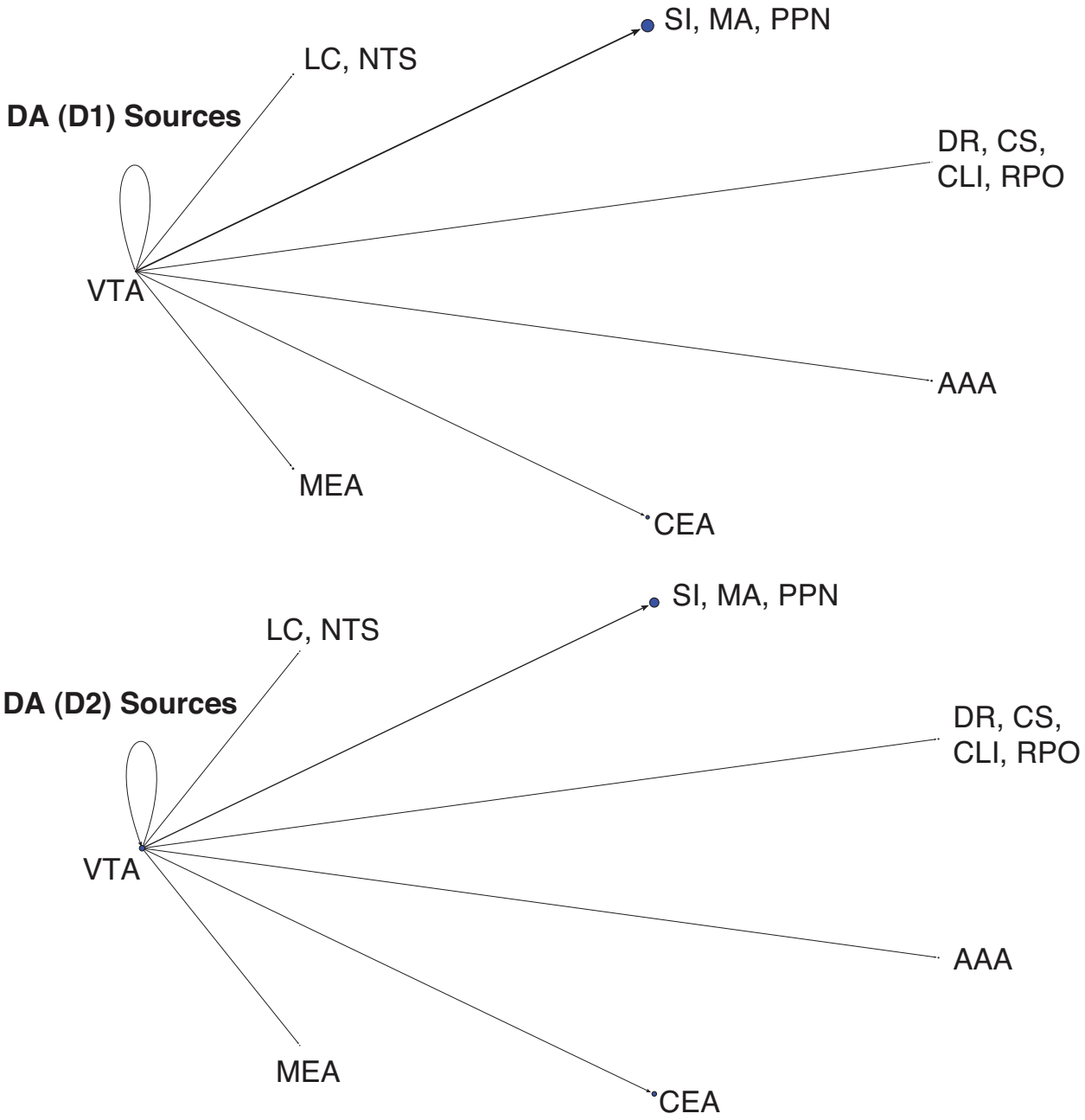

Figure 3.9. Network Graph of Muscarinic and Nicotinic Cholinergic Receptors.

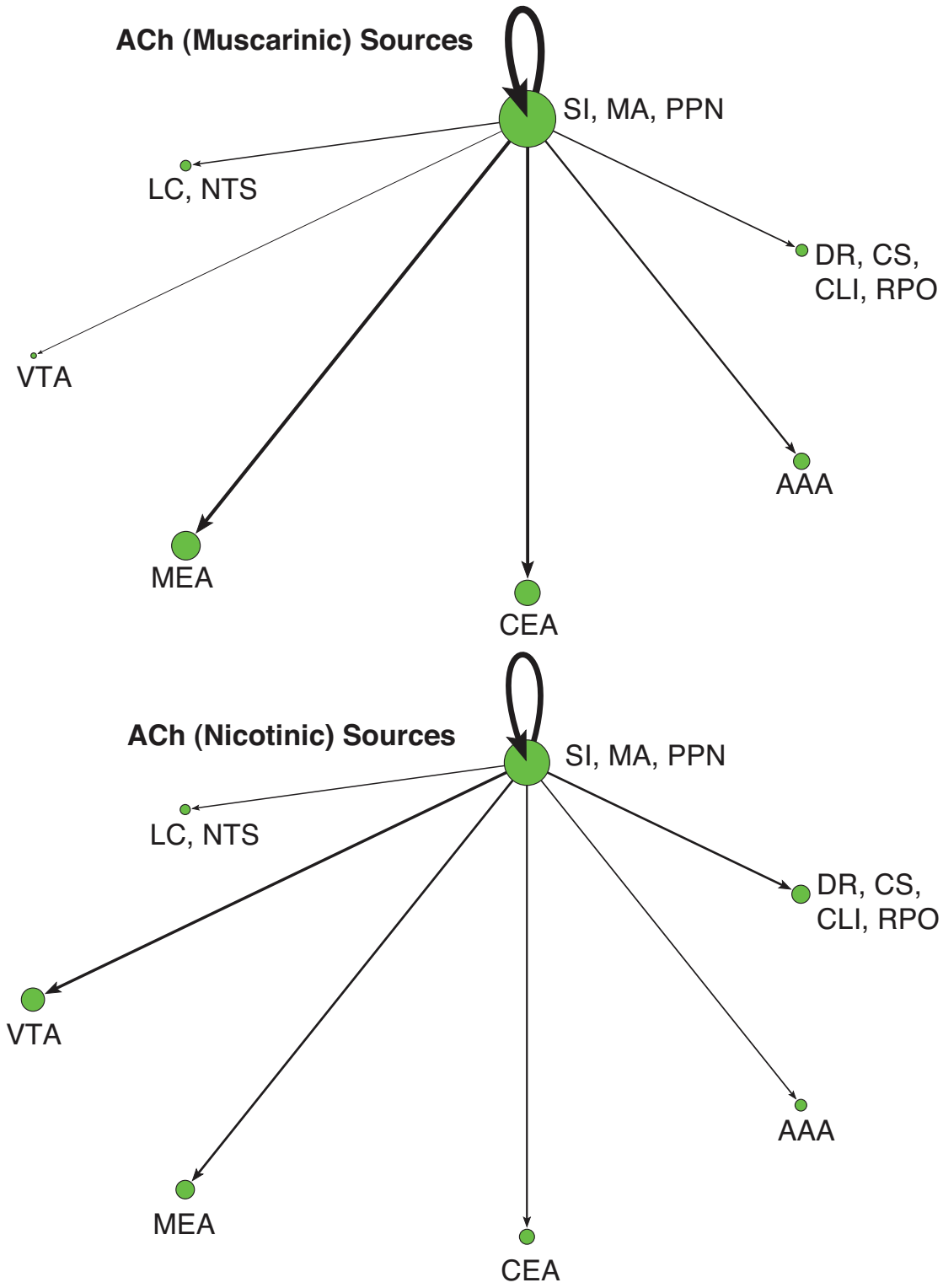

Figure 3.10. Network Graph of D1 and D2 Family Dopamine Receptors

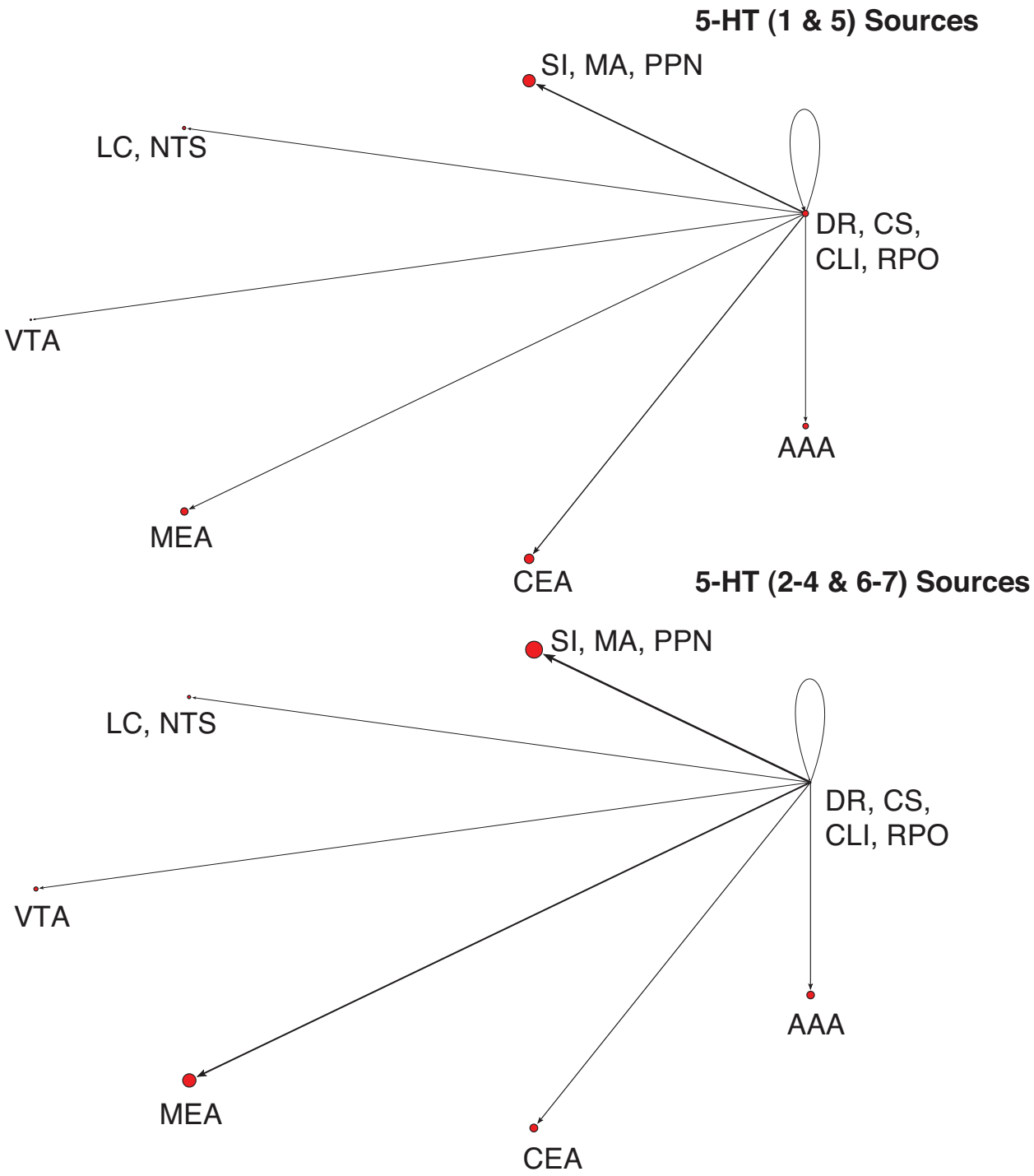

Figure 3.11. Network Graph of Inhibitory (Htr1 and Htr5) and Excitatory (Htr2, Htr3, Htr4, Htr6 and Htr7) Serotonergic Receptors.

Discussion

An exploratory ABA survey of receptor expression energy was conducted using data from the classical neuromodulatory systems (cholinergic, dopaminergic, noradrenergic, serotonergic) within anatomical origins of these systems and in the amygdala. This survey was based on the assumption that sources of these systems are localized in small subcortical nuclei, and that the amygdala is thought to be a major target of neuromodulation (Gallagher and Chiba 1996; McGaugh ; McGaugh 2006). Based on these assumptions, the targets of these neuromodulatory systems using receptor gene expression data were inferable from the ABA.

Several findings emerged from this survey that could have functional implications: 1) Cholinergic receptors have overwhelmingly higher expression in the neuromodulatory nuclei than the other classic neuromodulatory systems. The expression of cholinergic receptors is an order of magnitude higher than serotonin and norepinephrine, and much higher than dopamine. 2) The level of adrenergic receptor expression was small in all the brain areas tested. Moreover, the amount of neuromodulatory expression within the locus coeruleus was low compared to other regions. NTS, which is another source of noradrenergic neurons, displayed comparatively moderate expression energy of all neuromodulatory receptors. 3) SI and VTA appear to be hubs, or 'rich clubs' of neuromodulation (van den Heuvel and Sporns 2011). In particular, SI had the highest expression of all four neuromodulatory receptors compared to other examined brain regions. 4) The amygdala and its anatomical neighbor SI are another hub of neuromodulation, with

high receptor expression energy from all 4 neuromodulatory classes. 5) The comprehensive ABA allowed the present survey to fill in many gaps in our knowledge of receptor expression using ISH. Many of the inferred connections and receptor expressions found in this survey have not been reported previously in the rodent brain.

The completeness of the ABA revealed interesting patterns of neurotransmitter receptor expression energy, which supplement current anatomical knowledge on neuromodulatory systems. Many of these expression patterns had not been previously reported (Table 3.2, gray and yellow cells). The amygdala (AAA, CEA, MEA), SI, and VTA were the highest receptor expression energy of the regions examined (Figure 3.2). The pattern of expression was similar within neuromodulator classes and among anatomical regions (Figure 3.5). Within an anatomical region, such as the amygdala, distinct patterns of receptor expression were observed across subregions (Figure 3.4).

Bearing in mind that literature retrieved from GENSAT to compare and contrast receptor expression energies with the ABA in Table 3.2 originate from rat studies (with the exception of Htr3a and Htr3b), this survey suggests that the amygdala may express more neuromodulatory receptors than previously reported (Haber, Ryoo et al. 1995; Han, Holland et al. 1999; McGaugh 2004; Meneses and Perez-Garcia 2007).

Among prominent expression in the amygdala (Figure 3.4), Chrm1, Chrm2, and the dopaminergic receptors were in agreement with literature findings

(Buckley, Bonner et al. 1988; Narang 1995) (Table 3.2). The rest, which includes Adra1d, Adrb2, Htr1f, Htr2c, and Htr3a has higher expression energy in the ABA than what was previously reported (Goldman, Simmons et al. 1986; Bruinvels, Landwehrmeyer et al. 1994; Pompeiano, Palacios et al. 1994; Nicholas, Hokfelt et al. 1996; Day, Campeau et al. 1997). Though there were a few genes, Adra2a and Chrna3, that did not have abundant expression yet were in agreement with literature data, the remaining genes were either considered more expressed than has been known, or no data was available for comparison (Table 3.2).

Our reporting of neuromodulatory receptor expression energy in the midbrain area, where dopaminergic neurons are found, were comparable to prior work in many cases (Table 3.2). In particular, all of the α-adrenoreceptors, Chrna6, Chrnb3, Drd2, Htr4, and Htr6 were in agreement with studies that also have expression data from these receptors in the midbrain region (Deneris, Boulter et al. 1989; Novere, Zoli et al. 1996; Day, Campeau et al. 1997; Kinsey, Wainwright et al. 2001; Vilaró, Cortés et al. 2005).

Raphe nuclei, a source for serotonergic neurons, had fairly low expression energy overall (Figure 3.2). This expression profile was in agreement with several other studies (Table 3.2). Adra2a, Adra2c, Adrb2, Chrna3, Htr1a, Htr1b, and Htr1d, had low-to-moderate expression energy in the ABA and other studies (McCune, Voigt et al. 1993; Scheinin, Lomasney et al. 1994; Nicholas, Hokfelt et al. 1996). Adra1d, Chrna4, Chrnb2, and Htr1f have higher expression in the ABA than previously reported. Chrm4, Chrna5, Htr5a, and Htr5b, on the other hand,

displayed lower expression in the ABA than stated in prior literature. Still, no literature data was found in many genes, with one gene in particular (Chrnb1) not found in both the literature and ABA data set (Table 3.2).

Basal forebrain, a source of cholinergic neurons, which displayed the highest amount of expression out of all the brain regions in this survey (Figure 3.2), was a surprising finding when compared with literature data (Table 3.2). It has been reported that there are efferent projections of the adrenergic and serotonergic systems into the basal forebrain (Hornung 2003; Samuels and Szabadi 2008; Holmstrand and Sesack 2011). However, this survey suggests a larger neuromodulatory innervation of the basal forebrain compared to other neuromodulatory regions. Adrenergic (Adra1a, Adra1d, Adrb1, Adrb2) and cholinergic (Chrm4, Chrna2, Chrna3, Chrna4, Chrnb2) receptors were classified as having higher expression in the ABA than in previous studies. However, no information in literature data was found for the remaining receptors (Table 3.2).

LC and the NTS, which are major sources of noradrenergic neurons, had several genes that were classified as having lower expression energy in the ABA than in other studies (Figure 3.2 and Table 3.2). Adra2a, Chrna2, Chrna3, Chrna6, and Htr1b all reported to have moderate-to-high expression in the locus coeruleus (McCune, Voigt et al. 1993; Scheinin, Lomasney et al. 1994; Nicholas, Hokfelt et al. 1996), yet the data in the ABA suggests lower expression. Furthermore, Htr7 was the only gene that had no data in both the ABA and literature. In terms of agreement, only Adra2c, Adrb2, Htr1d, and Htr2c receptors, which had low-to-

moderate energy of expression, match former findings (Goldman, Simmons et al. 1986; Wada, Wada et al. 1989; McCune, Voigt et al. 1993; Bruinvels, Landwehrmeyer et al. 1994; del Toro, Juiz et al. 1994; Pompeiano, Palacios et al. 1994; Scheinin, Lomasney et al. 1994; Nicholas, Hokfelt et al. 1996; Mengod, Vilaró et al. 2006). All other receptor genes in this survey were not found in any literature that covers LC and the NTS.

The ABA ISH mouse brain project is a rich resource that made this neuroinformatics survey possible (Lein, Hawrylycz et al. 2007; Jones, Overly et al. 2009). This survey, which took advantage of the unique structure of the neuromodulatory systems, was able to create a connectivity map from the sources of neuromodulation to their receptor targets in the amygdala and other neuromodulatory nuclei (Figure 3.7 – 3.11). This survey revealed connectivity relations and receptor localization that had not been reported previously. The pattern of expression varied across region, not just in the level of expression, but also by receptor subtypes. These variations may have important functional implications.

References

Batagelj, V. and A. Mrvar (1998). "Pajek-program for large network analysis." Connections 21(2): 47-57.

Bhatia, S. C., S. Saha, et al. (1997). "Role of midbrain ventro-lateral tegmental area (VTA) adrenergic mechanisms in facilitation of hypothalamically-induced predatory attack behaviour." Indian J Exp Biol 35(4): 332-337.

Bouret, S., A. Duvel, et al. (2003). "Phasic activation of locus ceruleus neurons by the central nucleus of the amygdala." J Neurosci 23(8): 3491-3497.

Bouthenet, M. L., E. Souil, et al. (1991). "Localization of dopamine D3 receptor mRNA in the rat brain using in situ hybridization histochemistry: comparison with dopamine D2 receptor mRNA." Brain Research 564(2): 203-219.

Bruinvels, A. T., B. Landwehrmeyer, et al. (1994). "Localization of 5-HT1B, 5-HT1D alpha, 5-HT1E and 5-HT1F receptor messenger RNA in rodent and primate brain." Neuropharmacology 33(3-4): 367-386.

Buckley, N. J., T. I. Bonner, et al. (1988). "Localization of a family of muscarinic receptor mRNAs in rat brain." J Neurosci 8(12): 4646-4652.

Dani, J. A. and D. Bertrand (2007). "Nicotinic acetylcholine receptors and nicotinic cholinergic mechanisms of the central nervous system." Pharmacology and Toxicology 47(1): 699.

Day, H. E., S. Campeau, et al. (1997). "Distribution of α1a-, α1b- and α1d-adrenergic receptor mRNA in the rat brain and spinal cord." J Chem Neuroanat 13(2): 115-139.

del Toro, E. D., J. M. Juiz, et al. (1994). "Immunocytochemical localization of the 7 subunit of the nicotinic acetylcholine receptor in the rat central nervous system." The Journal of comparative neurology 349(3): 325-342.

Deneris, E., J. Boulter, et al. (1989). "β3: a new member of nicotinic acetylcholine receptor gene family is expressed in brain." Journal of Biological Chemistry 264(11): 6268.

Diaz, J., D. Levesque, et al. (1995). "Phenotypical characterization of neurons expressing the dopamine D3 receptor in the rat brain." Neuroscience 65(3): 731-745.

Fremeau, R. T., Jr., G. E. Duncan, et al. (1991). "Localization of D1 dopamine receptor mRNA in brain supports a role in cognitive, affective, and neuroendocrine aspects of dopaminergic neurotransmission." Proc Natl Acad Sci U S A 88(9): 3772-3776.

Gallagher, M. and A. A. Chiba (1996). "The amygdala and emotion." Curr Opin Neurobiol 6(2): 221-227.

Gardner, D., H. Akil, et al. (2008). "The neuroscience information framework: a data and knowledge environment for neuroscience." Neuroinformatics 6(3): 149-160.

Gerstein, M. and R. Jansen (2000). "The current excitement in bioinformatics-analysis of whole-genome expression data: how does it relate to protein structure and function?" Curr Opin Struct Biol 10(5): 574-584.

Goldman, D., D. Simmons, et al. (1986). "Mapping of brain areas expressing RNA homologous to two different acetylcholine receptor alpha-subunit cDNAs." Proceedings of the National Academy of Sciences of the United States of America 83(11): 4076.

Haber, S., H. Ryoo, et al. (1995). "Subsets of midbrain dopaminergic neurons in monkeys are distinguished by different levels of mRNA for the dopamine transporter: comparison with the mRNA for the D2 receptor, tyrosine hydroxylase and calbindin immunoreactivity." The Journal of comparative neurology 362(3): 400-410.

Han, J. S., P. C. Holland, et al. (1999). "Disconnection of the amygdala central nucleus and substantia innominata/nucleus basalis disrupts increments in conditioned stimulus processing in rats." Behav Neurosci 113(1): 143-151.

Heintz, N. (2004). "Gene expression nervous system atlas (GENSAT)." Nat Neurosci 7(5): 483.

Holmstrand, E. C. and S. R. Sesack (2011). "Projections from the rat pedunculopontine and laterodorsal tegmental nuclei to the anterior thalamus and ventral tegmental area arise from largely separate populations of neurons." Brain Structure & Function 216(4): 331-345.

Hornung, J. P. (2003). "The human raphe nuclei and the serotonergic system." J Chem Neuroanat 26(4): 331-343.

Hoyer, D., J. P. Hannon, et al. (2002). "Molecular, pharmacological and functional diversity of 5-HT receptors." Pharmacol Biochem Behav 71(4): 533-554.

Ishii, M. and Y. Kurachi (2006). "Muscarinic acetylcholine receptors." Curr Pharm Des 12(28): 3573-3581.

Jones, A. R., C. C. Overly, et al. (2009). "The Allen Brain Atlas: 5 years and beyond." Nat Rev Neurosci 10(11): 821-828.

Kinsey, A., A. Wainwright, et al. (2001). "Distribution of 5-HT5A, 5-HT5B, 5-HT6 and 5-HT7 receptor mRNAs in the rat brain." Molecular brain research 88(1-2): 194-198.

Krichmar, J. L. (2008). "The Neuromodulatory System – A Framework for Survival and Adaptive Behavior in a Challenging World." Adaptive Behavior 16: 385-399.

Lan, H., C. J. DuRand, et al. (2006). "Structural determinants of pharmacological specificity between D1 and D2 dopamine receptors." Molecular pharmacology 69(1): 185.

Lee, C. K., S. M. Sunkin, et al. (2008). "Quantitative methods for genome-scale analysis of in situ hybridization and correlation with microarray data." Genome Biol 9(1): R23.

Lee, H. J., D. S. Wheeler, et al. (2011). "Interactions between amygdala central nucleus and the ventral tegmental area in the acquisition of conditioned cue-

directed behavior in rats." European Journal of neuroscience 33(10): 1876-1884.

Lein, E. S., M. J. Hawrylycz, et al. (2007). "Genome-wide atlas of gene expression in the adult mouse brain." Nature 445(7124): 168-176.

McCune, S. K., M. M. Voigt, et al. (1993). "Expression of multiple alpha adrenergic receptor subtype messenger RNAs in the adult rat brain." Neuroscience 57(1): 143-151.

McGaugh, J. L. (2004). "The amygdala modulates the consolidation of memories of emotionally arousing experiences." Annu Rev Neurosci 27: 1-28.

McGaugh, J. L. (2006). "Make mild moments memorable: add a little arousal." Trends Cogn Sci 10(8): 345-347.

Meneses, A. and G. Perez-Garcia (2007). "5-HT(1A) receptors and memory." Neurosci Biobehav Rev 31(5): 705-727.

Mengod, G., M. I. Martinez-Mir, et al. (1989). "Localization of the mRNA for the dopamine D2 receptor in the rat brain by in situ hybridization histochemistry." Proc Natl Acad Sci U S A 86(21): 8560-8564.

Mengod, G., M. T. Vilaró, et al. (2006). Chemical Neuroanatomy of 5-HT Receptor Subtypes in the Mammalian Brain

The Serotonin Receptors. B. L. Roth, Humana Press: 319-364.

Mesulam, M. M., E. J. Mufson, et al. (1983). "Cholinergic innervation of cortex by the basal forebrain: cytochemistry and cortical connections of the septal area, diagonal band nuclei, nucleus basalis (substantia innominata), and

hypothalamus in the rhesus monkey." Journal of Comparative Neurology 214(2): 170-197.

Müller, H. M., A. Rangarajan, et al. (2008). "Textpresso for neuroscience: searching the full text of thousands of neuroscience research papers." Neuroinformatics 6(3): 195-204.

Narang, N. (1995). "In situ determination of M1 and M2 muscarinic receptor binding sites and mRNAs in young and old rat brains." Mech Ageing Dev 78(3): 221-239.

Ng, L., S. D. Pathak, et al. (2007). "Neuroinformatics for genome-wide 3-d gene expression mapping in the mouse brain." Computational Biology and Bioinformatics, IEEE/ACM Transactions on 4(3): 382-393.

Nicholas, A. P., T. Hokfelt, et al. (1996). "The distribution and significance of CNS adrenoceptors examined with in situ hybridization." Trends Pharmacol Sci 17(7): 245-255.

Nicholas, A. P., V. A. Pieribone, et al. (1993). "Cellular localization of messenger RNA for β1 and β2 adrenergic receptors in rat brain: an in situ hybridization study." Neuroscience 56(4): 1023-1039.

Novere, N., M. Zoli, et al. (1996). "Neuronal nicotinic receptor α6 subunit mRNA is selectively concentrated in catecholaminergic nuclei of the rat brain." European Journal of neuroscience 8(11): 2428-2439.

Pompeiano, M., J. M. Palacios, et al. (1992). "Distribution and cellular localization of mRNA coding for 5-HT1A receptor in the rat brain: correlation with receptor binding." Journal of Neuroscience 12(2): 440-453.

Pompeiano, M., J. M. Palacios, et al. (1994). "Distribution of the serotonin 5-HT2 receptor family mRNAs: comparison between 5-HT2A and 5-HT2C receptors." Brain Res Mol Brain Res 23(1-2): 163-178.

Samuels, E. R. and E. Szabadi (2008). "Functional neuroanatomy of the noradrenergic locus coeruleus: its roles in the regulation of arousal and autonomic function part II: physiological and pharmacological manipulations and pathological alterations of locus coeruleus activity in humans." Curr Neuropharmacol 6(3): 254-285.

Scheinin, M., J. W. Lomasney, et al. (1994). "Distribution of α2-adrenergic receptor subtype gene expression in rat brain." Molecular brain research 21(1-2): 133-149.

Sodhi, M. S. and E. Sanders-Bush (2004). "Serotonin and brain development." Int Rev Neurobiol 59: 111-174.

Sugaya, K., C. Clamp, et al. (1997). "mRNA for the M4 muscarinic receptor subtype is expressed in adult rat brain cholinergic neurons." Molecular brain research 50(1-2): 305-313.

Tecott, L., A. Maricq, et al. (1993). "Nervous system distribution of the serotonin 5-HT3 receptor mRNA." Proceedings of the National Academy of Sciences of the United States of America 90(4): 1430.

Trappenberg, T. P. (2010). "Fundamentals of computational neuroscience." New York, Oxford University Press.

van den Heuvel, M. P. and O. Sporns (2011). "Rich-club organization of the human connectome." The Journal of Neuroscience 31(44): 15775-15786.

Vilaró, M., R. Cortés, et al. (1990). "Localization of M5 muscarinic receptor mRNA in rat brain examined by in situ hybridization histochemistry." Neuroscience letters 114(2): 154-159.

Vilaró, M., R. Cortés, et al. (2005). "Serotonin 5-HT4 receptors and their mRNAs in rat and guinea pig brain: Distribution and effects of neurotoxic lesions." The Journal of comparative neurology 484(4): 418-439.

Wada, E., D. McKinnon, et al. (1990). "The distribution of mRNA encoded by a new member of the neuronal nicotinic acetylcholine receptor gene family ([alpha] 5) in the rat central nervous system." Brain research 526(1): 45-53.

Wada, E., K. Wada, et al. (1989). "Distribution of α2, α3, α4, and β2 neuronal nicotinic receptor subunit mRNAs in the central nervous system: a hybridization histochemical study in the rat." J Comp Neurol 284(2): 314-335.

Woolf, N. J. and L. L. Butcher (1982). "Cholinergic projections to the basolateral amygdala: a combined Evans Blue and acetylcholinesterase analysis." Brain Research Bulletin 8(6): 751-763.

CHAPTER 4: Allen Brain Atlas-Driven Visualization

The survey in Chapter 3 unveiled novel relationships between the neuromodulatory systems and the amygdala. While the comprehensive mouse atlas the ABA provided helped form a more complete picture of these neuromodulatory interactions, the ABA tools limit the amount of genes and brain structures researchers can view at once. The Allen Brain Atlas-Driven Visualization (ABADV) was created to provide an easy way for other researchers to survey expression data. ABADV is a web application that generates multiple pie charts, bar charts and heat maps of expression energy values for any given set of genes and brain structures. By creating this web application, researchers can immediately obtain and survey numerous amounts of expression energy data from the ABA, which they can then use to supplement their work or perform meta-analysis.

Other Resources

The ABA and its vast array of resources enable researchers to develop new methods for investigating brain data. For instance, Liscovitch (Liscovitch, Shalit et al. 2013) created FuncISH, a method to learn functional representations of any neural in situ hybridization (ISH) images by applying Gene Ontology categories with the genomic set of mouse neural ISH images available in the ABA. Another group also systematically explored high resolution ISH images contained in the ABA by using a data mining tool they developed called Hippo-ATESC (Automatic Texture Extraction from the Hippocampal region using Soft Computing). Hippo-ATESC helps detect neuropil-encoded genes in the hippocampus that are known for

their involvement in synaptic structure and plasticity (Ugolotti, Mesejo et al. 2013). Ji et al. integrated resources from both the ABA and the recent Allen Mouse Brain Connectivity Atlas to systematically study the relationship between gene expression and structure-level brain connectivity (Ji, Fakhry et al. 2014). This was accomplished by employing ensemble models for predicting brain connectivity. Altogether, the richness of the ABA resources helps researchers conduct scientific data analysis and discover new knowledge in neuroscience, accelerating the understanding of how the brain works.

These resources and applications, though offering sophisticated ways of navigating across ABA and their large database, come with a steep learning curve. Many ABA tools limit the amount of genes and brain areas researchers can view at once. Furthermore, while the ABA provides documentation and tutorials on how to use their resources, some users may not want to devote their time in reading and understanding their overwhelming amount of features for retrieving a small amount of data.

ABA provides programmatic access to their published data set for any user to perform any data retrieval and analysis beyond interfacing with their existing software. Some groups that have built software on top of the ABA through this programmatic service are typically motivated by a specific hypothesis-driven analysis (Ugolotti, Mesejo et al. 2013; Ji, Fakhry et al. 2014). Though beneficial, hypothesis-driven software may prevent other users from using their software in the first place, as those users instead may prefer software that enables explorative

analysis. Inspired by lack of exploratory software, ABADV was designed to increase the exploration and usability of ABA.

Data-Driven Documents

ABADV visualized data by using D3, a Javascript library that uses digital data to drive the creation and control of dynamic and interactive web-based visualizations (Bostock, Ogievetsky et al. 2011). D3 works by binding input data to arbitrary document elements through the document object model (DOM) API. The DOM API enables collaboration of web technologies such as HyperText Markup Language (HTML) for page creation, Cascading Style Sheets (CSS) for aesthetics, JavaScript for web interaction, and Scalable Vector Graphics (SVG) for vector graphics (Bostock, Ogievetsky et al. 2011).

Implementation

ABADV was implemented to selectively display expression energy across many genes and brain structures at once. The flowchart in Figure 4.1 depicts the program flow from user input to visualization.

Upon accessing the web application (Figure 4.2), the user is provided with several options to filter and visualize results (Figure 4.3 – 4.5). For filter options, the user can set which probe (antisense, sense or both) and section (coronal, sagittal or both) to retrieve. These choices are provided to the user because various probe features and brain sections may influence a gene's expression profile. For visualization options, the user can either select multiple pie charts, grouped bar charts, a heatmap, or all three. By default, ABADV is set to visualize all three

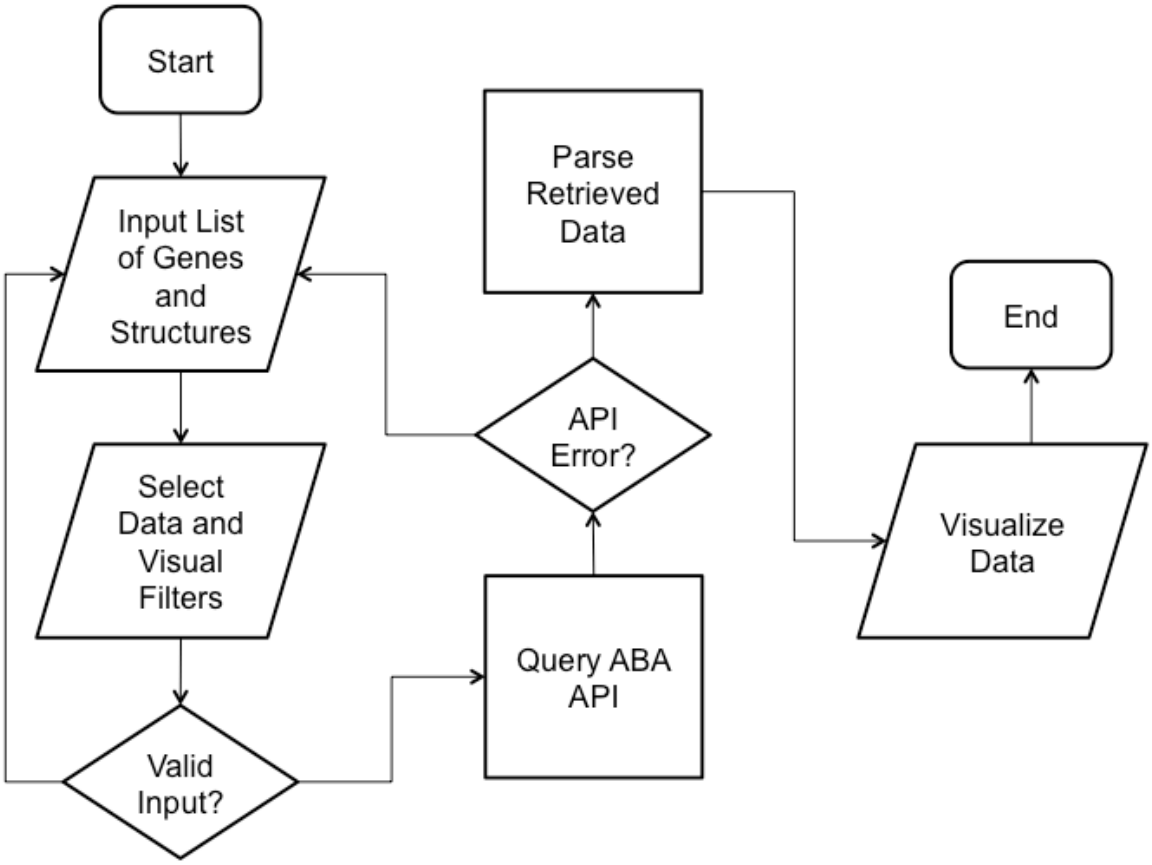

Figure 4.1 ABADV Flowchart. Depicts how each process in ABADV works, as well as the flow of these processes. The user sets filters (probe and section), visualization type (pie, bar, heatmap, or all three) and inserts a list of genes and brain structures of interest. Upon validating the input, ABADV queries the ABA API for expression data. If the query successfully returns data, ABADV will utilize D3 to display the results.

options. After selecting these filters and visualizations, the user can insert a list of genes and brain structures. ABADV accepts gene symbols and brain structure acronyms. Symbols used to query genes in the Allen Mouse Brain Atlas follow the same guidelines the International Committee on Standardized Genetic Nomenclature for Mice (Eppig, Blake et al. 2012) established. A list of gene symbols can be downloaded at http://www.informatics.jax.org/genes.shtml (Eppig, Blake et al. 2012). Acronyms used to query brain structures in the Allen Mouse Brain Atlas come from the Allen Reference Atlas. These brain structure acronyms can be found

at http://atlas.brain-map.org. ABADV also provides a full list of these structures, located in a hyperlink below the text field where users insert brain structures (Figure 4.3 – 4.5).

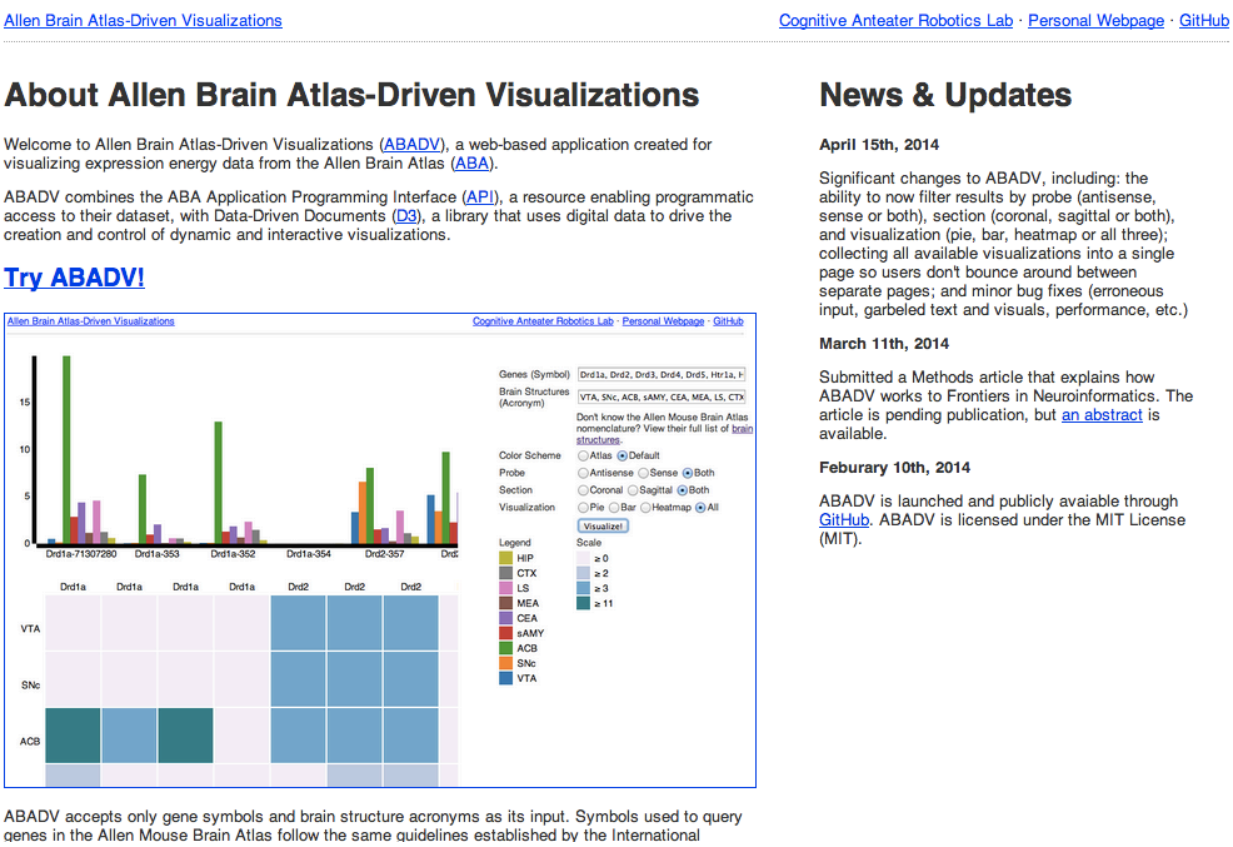

Figure 4.2 ABADV Main Page Screenshot.

After the user enters their genes and brain structures of interest, they are ready to click the "Visualize!" button, which triggers the application to query the ABA API. ABADV first ensures valid inputs before generating API URLs. Once the process goes through, ABADV obtains a set of SectionDataSetId values. A SectionDataSetId is a value associated with the collection of images and metadata for a gene expression experiment. Some genes may return multiple SectionDataSetId values, while other genes may return null. These

SectionDataSetId values are necessary to access expression energy values. Once a list of SectionDataSetId values has been obtained, the application completes its query, using each SectionDataSetId and brain structure to acquire expression energy values. Expression energy values are retrieved in JSON, which is compatible with D3, making JSON an ideal format for data interchange. During this process, ABADV will inform the user if any error arises from attempting to access the API.

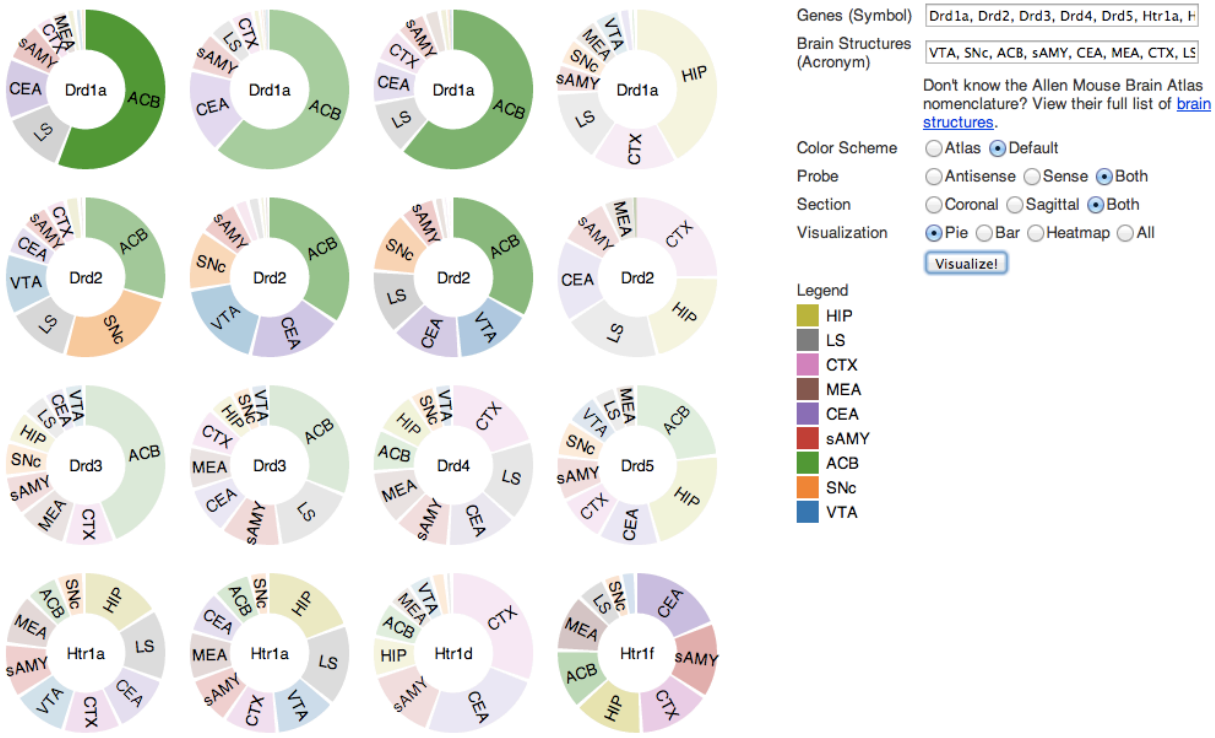

Figure 4.3. ABADV Pie Charts Results Page Screenshot.

With data retrieved from the API and stored in the user's web browser, ABADV can now visualize this information to the user. Data is further parsed and formatted depending on the visualization the user selects.

If multiple pie charts were selected, ABADV will generate one pie chart for each gene of interest with a pie slice within a chart representing a brain structure

of interest (Figure 4.3). Multiple pie charts are useful for demonstrating relative proportions. To quickly identify prevalent genes from their query, ABADV augments the color intensity of the pie charts. Genes with lower expression energy relative to other genes from the query will appear more transparent, while genes with higher expression energy will appear more opaque. The width of a pie slice represents the total amount of expression energy of a given gene in a brain structure relative to other brain structures within the same gene.

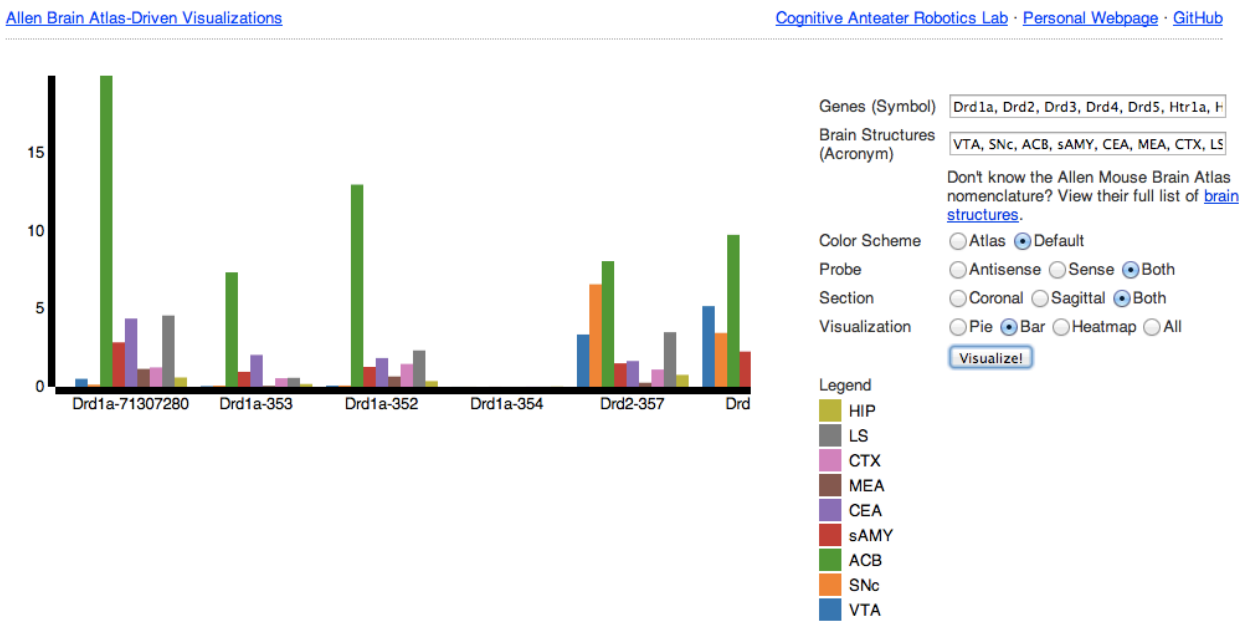

Figure 4.4. ABADV Bar Charts Results Page Screenshot.

If grouped bar charts were selected, ABADV will appropriately create various bar charts of expression energy (Figure 4.4). Grouped bar charts provide a way to show information about various sub-groups (brain structures) of the main categories (genes). Each bar within a group, categorized by gene of interest, represents the amount of expression energy found in a brain structure of interest and are colored differently to distinguish between them. The height of the bar is proportional to the

amount of expression energy. As such, there is no need to augment the color intensity of each bar, as its height identifies predominant genes.

Lastly, if heatmap was selected, ABADV will substitute each individual gene expression value into a 2D data matrix of colors (Figure 4.5). Heatmaps are useful for finding high and low values, as well as patterns. Each row in this data matrix represents a brain structure and each column represents a gene of interest. Various shades of colors per cell represent the actual expression energy value of a gene per structure, with a darker shade denoting high expression energy and a lighter shade denoting low expression energy.

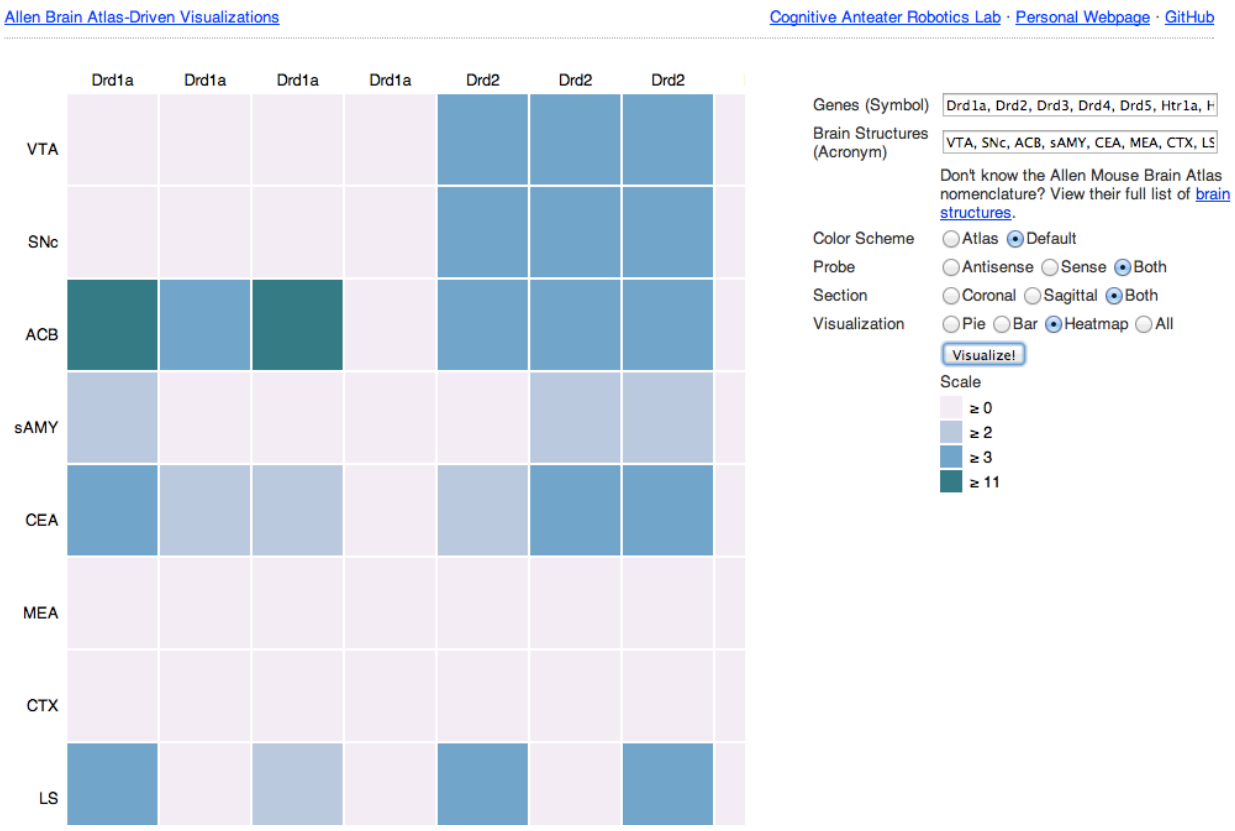

Figure 4.5. ABADV Heatmap Results Page Screenshot.

ABADV can link back to the ABA experiment page, so users may view a summary of its experimental detail, by clicking on any portion of the pie chart, bar

chart, or cell in heatmap. The ABA experimental detail includes an interactive 3-D representation of gene expression, a histogram of expression energy across major brain structures, probe and gene metadata, and an interactive image viewer that displays ISH images from the experiment. In addition, various color schemes are provided for pie and bar charts. Users can either select a color scheme from RGB values assigned to each brain structure according to the anatomic ontology derived from the Allen Reference Atlas (Dong 2008), or a default categorical color set generated by D3.

Web-Application Demonstration

Using the Allen Mouse Brain Atlas API with D3, ABADV was designed to aid users in visualizing expression energy data across many genes and brain structures. This section presents an output example of ABADV. These examples were performed using the ABADV web application available at: http://www.socsci.uci.edu/~jkrichma/ABADV/.

To demonstrate ABADV's capabilities, a sample query was performed consisting of dopamine receptors (Drd1a, Drd2, Drd3, Drd4, Drd5), serotonin receptors (Htr1a, Htr1b, Htr2a, Htr2b, Htr2c), and various brain structures involved in reward, which include: prelimbic area (PL), infralimbic area (ILA), hypothalamus (HY), hippocampal formation (HPF), striatum-like amygdalar nuclei (sAMY), nucleus accumbens (ACB), ventral tegmental area (VTA), and dorsal raphe nucleus (DR). These receptors and brain structures form a significant part of the reward circuit, a network responsible for processing various aspects of positive

emotional stimulus (Nakamura ; Russo and Nestler). This reward circuit is key for incentive-based drives and goal-directed behaviors (Berridge and Robinson). Recent findings suggest that, in particular, the dopaminergic neurons in the VTA projecting to the ACB are principally involved in guiding attention toward rewards and consuming rewards (Koob and Le Moal). It has also been argued that serotonin neurons in the DR have possible functions in reward processing as it interacts with dopamine (Nakamura). A full overview of reward circuits in the brain is beyond the scope of this demonstration and discussed later in Chapter 5. However, these genes and brain structures associated with the reward circuit help demonstrate the capabilities of ABADV.

Of the entire query, 22 unique experiments were found. 12 experiments came from dopamine receptor genes and 10 from serotonin receptor genes. Their SectionDataSetId number denotes each experiment, which was truncated to their first three digits for visualization purposes (Figure 4.6).

Out of all the dopamine receptor genes queried, Drd1a SectionDataSetId #713 contained the highest amount expression energy, denoted by both the opacity of its slices and height of its bars (Figure 4.6). Within Drd1a SectionDataSetId #713, ACB was highest in expression energy at approximately 20, while expression energy in other brain structures ranged from moderate to nearly quiescent. The heatmap in Figure 4.7 further illustrates this difference in expression, both across brain areas and gene expression experiments. Across other dopamine receptor genes, expression energy in ACB remained dominant, again as denoted by dark blue

shaded cells in Figure 4.7. However, the total amount of expression found within each gene compared to Drd1a SectionDataSetId #713 was lower, as was also by its low bar height in Figure 4.7.

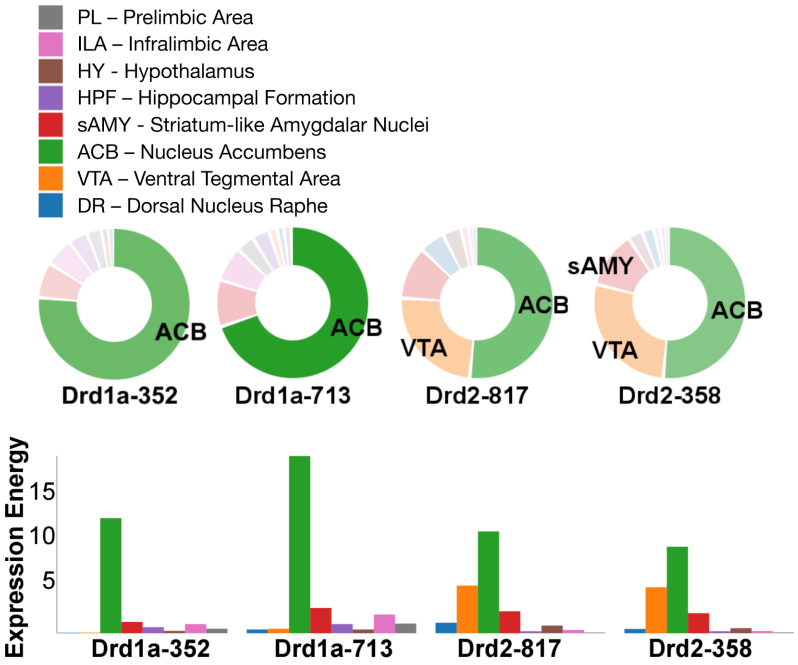

Figure 4.6. ABADV Pie and Bar Chart of Dopamine Receptor Genes in Brain Structures Associated with Reward Processing. (Top) Each pie represents a different gene, while the slices within a pie represents a different brain structure. Opacity of each pie slice denotes the amount of expression energy relative to other gene expression experiments. Size of pie slice denotes the amount of expression energy relative to other brain structure within the same gene. Color scheme derived from both the Allen Reference Atlas or generated by default in D3. (Bottom) Each group of bars represents a different gene expression experiment, while each bar within a group represents a different brain structure. Height of bar denotes the amount of expression energy. Default color generated D3 was used in this plot.

For serotonin receptors, two particular experiments stood out the most: Htr1a SectionDataSetId #793 and Htr2c SectionDataSetId #713. These two genes were highest in expression energy values compared to the rest, though where that expression was located at differed between the two (Figure 4.8 and 4.9). Within Htr1a SectionDataSetId #793, expression energy was found highest in DR, denoted by its tall blue bar and large blue pie slice in Figure 4.8. However, within Htr2c

SectionDataSetId #713, expression energy was found highest in sAMY, followed by ACB and DR. The remaining serotonin receptor expressions were lower, which the amount of light shades cells versus dark shaded cells in Figure 4.9 depicts.

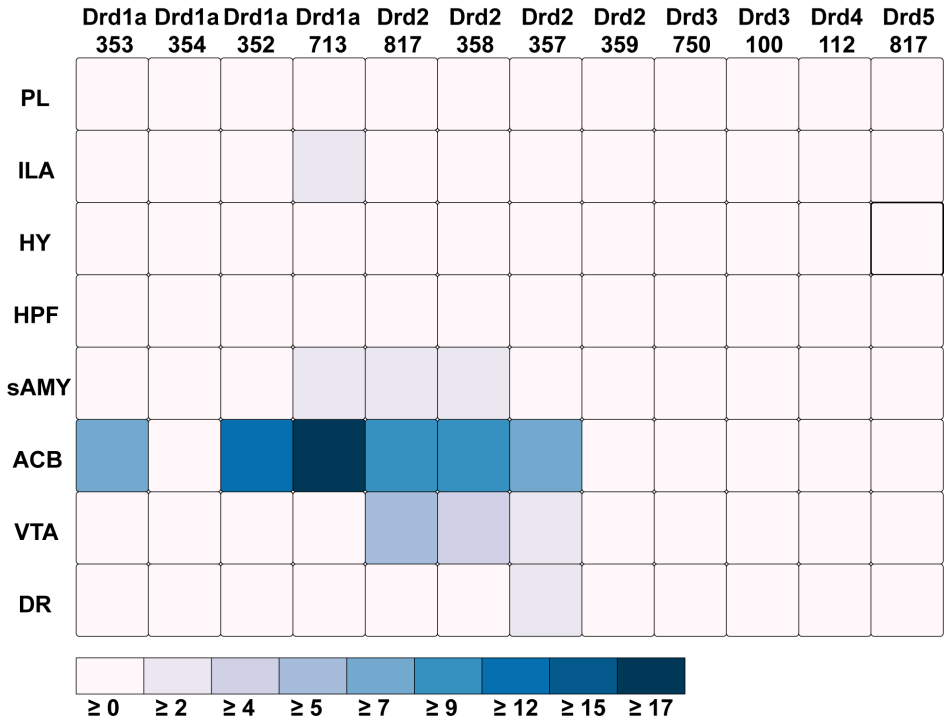

Figure 4.7. ABADV Heatmap of Dopamine Receptor Genes in Brain Structures Associated with Reward Processing. Each cell in the matrix represents an expression energy value for a particular experiment (column) and brain structure (row). The shade of the color denotes how much expression was found in that cell, where the darker the color, the higher the expression, and the lighter the color, the lower the expression.

Drd1a SectionDataSetId #354 and Drd2 SectionDataSetId #359 displayed peculiarly low amounts of expression energy across all brain structures (Figure 4.6 and 4.7). Upon inspection of their respective experimental page in the ABA (via clicking on the pie or chart of these SectionDataSetIds), those two experiments utilized labeled sense RNA probes, while other experiments used labeled antisense RNA probes. A sense probe is a strand of RNA that has the same sequence as its target mRNA, while an antisense probe is an RNA strand that is complementary to

the sequence of its target mRNA. As such, a sense probe gives a measure of non-specific probe binding because of the chemical properties of the probe, as opposed to an antisense probe which measures its target mRNA. Given that, these sense probes are used to gauge protocol efficacy. A low-to-no expression energy found in sense probes, as results from Drd1a SectionDataSetId #354 and Drd2 SectionDataSetId #359, assures that any signal detected by its antisense probe is because of the sequence-specific binding to mRNA and not with other targets within the cell. The ability to retrieve experimental details directly from the Allen Mouse Brain Atlas unveiled this information that might otherwise cause confusion when interpreting data.

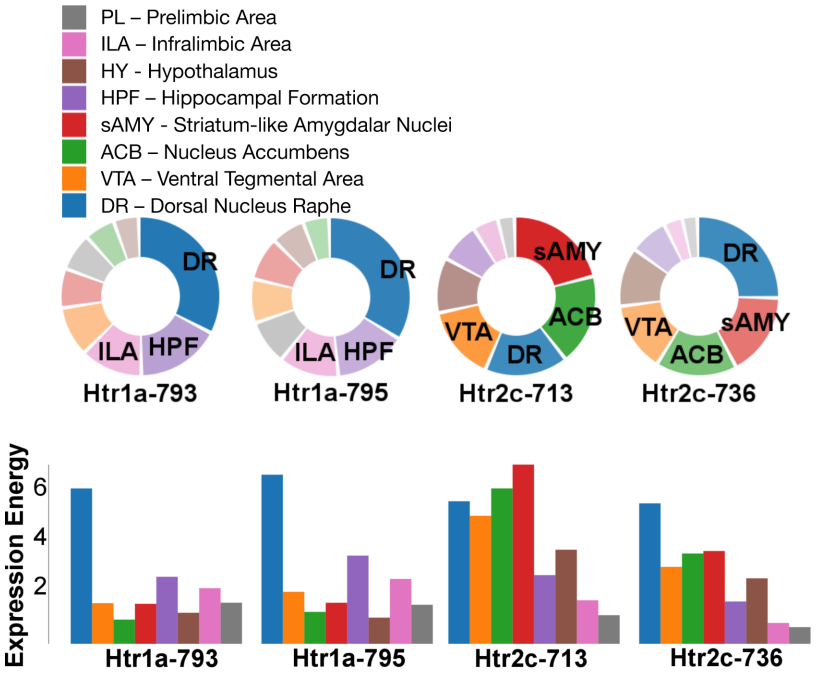

Figure 4.8. ABADV Pie and Bar Chart of Serotonin Receptor Genes in Brain Structures Associated with Reward Processing. (Top) Each pie represents a different gene expression experiment, while the slices within a pie represents a different brain structure. Opacity of each pie slice denotes the amount of expression energy relative to other genes. Size of pie slice denotes the amount of expression energy relative to other brain structure within the same gene. (Bottom) Each group of bars represents a different gene expression experiment, while each bar within a group represents a different brain structure. Height of bar denotes the amount of expression energy. Default color generated D3 was used in this plot.

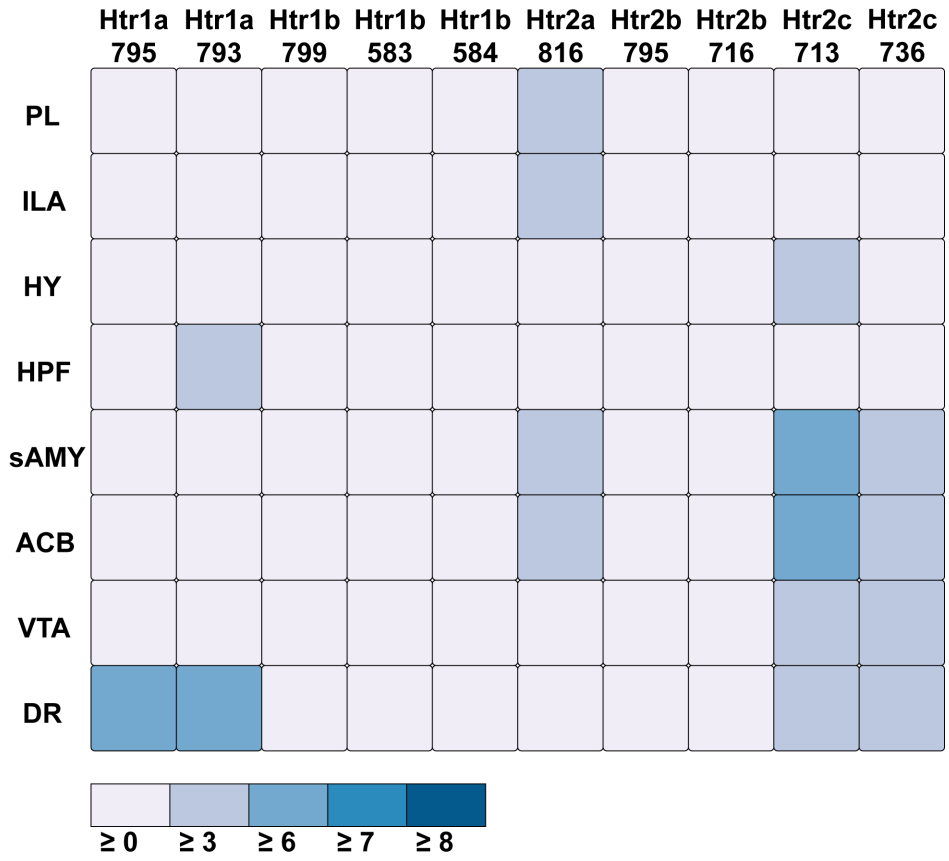

Figure 4.9. ABADV Heatmap of Serotonin Receptor Genes in Brain Structures Associated with Reward Processing. Each cell in the matrix represents an expression energy value for a particular experiment (column) and brain structure (row). The shade of the color denotes how much expression was found in that cell, where the darker the color, the higher the expression, and the lighter the color, the lower the expression.

Brain Explorer Comparison

Brain Explorer is a free-to-download desktop application for viewing brain anatomy and gene expression data in 3D (Lau, Ng et al. 2008). It is integrated with the ABA, enabling users to view spatially registered gene expression data in 3D at a 200-µm3 resolution. With Brain Explorer, users have the ability to display ISH expression data from multiple genes superimposed on each other in 3D, as well as fully interact with the Allen Reference Atlas. To obtain gene expression data for display in Brain Explorer, users can either perform a search on their website at

http://mouse.brain-map.org/, select gene(s) of interest, then click on the 'View in 3D' link in the search results list or search within Brain Explorer itself.

To compare ABADV with Brain Explorer, the same query from above was performed in Brain Explorer. Genes of interest were first searched through their website. After downloading each gene into Brain Explorer, 3D polygonal brain structures associated with the reward circuit was turned on while all other brain structures was turned off. Figure 4.10 is a screenshot of Brain Explorer's main window application displaying all 12 dopamine receptor genes and 8 brain structures from the query. Figure 4.11 is a screenshot of Brain Explorer's main window application displaying all 10 serotonin receptor genes and 8 brain structures from the query. Colored spheres indicate the amount of expression energy in a given brain structure, where blue-green is low, yellow is medium, and red is high. Spheres are used to represent each 200-μm3 voxel, with the size of the spheres directly proportional to the intensity and density of each voxel.

While results from Brain Explorer are identical to ABADV, because the data is the same, there are complementary differences. As with dopamine receptor gene query using ABADV (Figure 4.6 and 4.7), Brain Explorer results revealed ACB containing the highest amount of expression energy compared to other brain structures, as denoted by dense, bright-colored voxels located on the rostral end of the visualized mouse brain in Figure 4.10. Likewise, compared to serotonin receptor genes expression in ABADV (Figure 4.8 and 4.9), Brain Explorer results also revealed both DR and sAMY were highest amongst all other brain structures in

expression energy values (Figure 4.11), which is demonstrated by large, localized voxels in the posterior and lateral end of the visualized mouse brain.

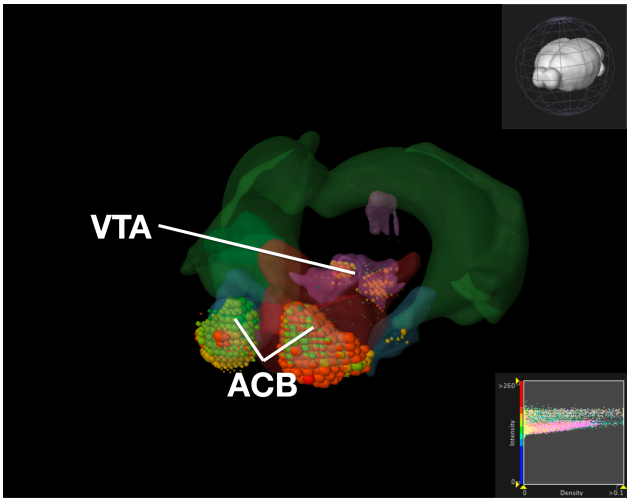

Figure 4.10. Brain Explorer 2 Expression of Dopamine Receptor Genes in Brain Structures Associated with Reward Processing. Colored spheres represent the amount of expression in a given brain structure, where blue-green is low, yellow is medium, and red is high. Spheres also represent each 200-μm^3 voxel, with the size of the spheres directly proportional to the intensity and density of each voxel.

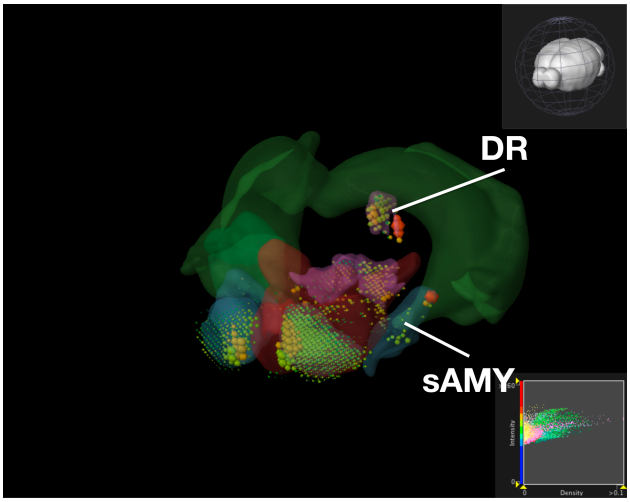

Figure 4.11. Brain Explorer 2 Expression of Serotonin Receptor Genes in Brain Structures Associated with Reward Processing. Colored spheres represent the amount of expression in a given brain structure, where blue-green is low, yellow is medium, and red is high. Spheres also represent each 200-μm^3 voxel, with the size of the spheres directly proportional to the intensity and density of each voxel.

Superimposing multiple genes using Brain Explorer made it difficult to identify which dopamine or serotonin SectionDataSetId were expressing the most.

To know which SectionDataSetId expressed the most in Figure 4.10 and 4.11, in Brain Explorer can either: reveal metadata by clicking on individual voxels, or selectively turn off the display of other SectionDataSetIds and view each experiment separately. Expression visibility is also controllable by setting thresholds on expression values (Figure 4.10 and 4.11, bottom right corner). In ABADV, however, comparisons between genes are easier to portray because a pie chart, bar chart, or heatmap cell is generated for each gene, which does not get in the way of one another.

Another key difference between Brain Explorer and ABADV is the presentation of gene expression. In Brain Explorer, clicking on colored spheres reveals the expression density and intensity of that voxel, whereas ABADV displays expression energy across the entire brain structure. While the Brain Explorer offers detailed expression data at the voxel level, ABADV allows quantitative analysis of expression energy across the entire brain structure.

Aside from these key advantages of ABADV, Brain Explorer does offer features not available in ABADV. In particular, Brain Explorer enables 3D representation of gene expression with the original full resolution 2D tissue sections is a rich feature that may make data exploration convenient, easily mapping the localization of expression. By selecting a colored voxel, Brain Explorer can display the name of the structure and its location in its atlas ontological hierarchy while simultaneously displaying its original image data that was used to generate these quantitative results.

Discussion

ABADV, which is available at: http://www.socsci.uci.edu/~jkrichma/ABADV/, has been developed to extend the ABA by providing users with a quick and intuitive way to survey large amounts of expression energy data across multiple brain regions of interest. ABADV combines the ABA API with D3 to obtain and visualize expression energy data from various genes and brain structures using pie charts, bar charts, and heatmaps to display these quantified measurements. The demonstration of querying the ABA for available dopamine and serotonin receptor genes in this chapter showed that ABADV could help identify prevalent genes and brain structures that may otherwise be obscured in other visualizations (i.e., Brain Explorer). Using ABADV revealed heavily expressed brain regions such as the nucleus accumbens and dorsal raphe across dopamine and serotonin receptor genes, respectively (Figure 4.6 – 4.9). This quantified, exploratory analysis makes it easier for users to obtain such results without having to delve deep into the intricacies of the ABA. ABADV serves as a complement to the resources the ABA provides and can be used in conjunction with other data sets and techniques for complete analysis.

References

Berridge, K. C. and T. E. Robinson (1998). "What is the role of dopamine in reward: hedonic impact, reward learning, or incentive salience?" Brain Res Brain Res Rev 28(3): 309-369.

Bostock, M., V. Ogievetsky, et al. (2011). "D^3 Data-Driven Documents." Visualization and Computer Graphics, IEEE Transactions on 17(12): 2301-2309.

Dong, H. W. (2008). The Allen reference atlas: A digital color brain atlas of the C57Bl/6J male mouse, John Wiley & Sons Inc.

Eppig, J. T., J. A. Blake, et al. (2012). "The Mouse Genome Database (MGD): comprehensive resource for genetics and genomics of the laboratory mouse." Nucleic Acids Res 40(D1): D881-D886.

Ji, S., A. Fakhry, et al. (2014). "Integrative analysis of the connectivity and gene expression atlases in the mouse brain." Neuroimage 84: 245-253.

Koob, G. F. and M. Le Moal (2008). "Addiction and the brain antireward system." Annu Rev Psychol 59: 29-53.

Lau, C., L. Ng, et al. (2008). "Exploration and visualization of gene expression with neuroanatomy in the adult mouse brain." BMC Bioinformatics 9: 153.

Liscovitch, N., U. Shalit, et al. (2013). "FuncISH: learning a functional representation of neural ISH images." Bioinformatics 29(13): i36-43.

Nakamura, K. (2013). "The role of the dorsal raphe nucleus in reward-seeking behavior." Front Integr Neurosci 7: 60.

Russo, S. J. and E. J. Nestler (2013). "The brain reward circuitry in mood disorders." Nat Rev Neurosci 14(9): 609-625.

Ugolotti, R., P. Mesejo, et al. (2013). "Visual Search of Neuropil-Enriched RNAs from Brain In Situ Hybridization Data through the Image Analysis Pipeline Hippo-ATESC." PLoS One 8(9): e74481.

CHAPTER 5: Exploratory Survey of the Reward Circuit Using the Allen Brain Atlas

Chapters 3 and 4 utilized the Allen Mouse Brain Atlas (ABA) in situ hybridization (ISH) expression data to survey receptor gene expression associated with neuromodulatory systems. This chapter further explores the interaction between neuromodulatory systems by focusing on the role of dopamine and serotonin in the mammalian reward circuit.

The reward circuit is a network of brain areas that moderate various aspects of reward processing (Haber and Knutson 2010). These reward processes refer to three features: the 'liking' or the actual pleasure component of a reward, the 'wanting' or motivation for a reward, and the 'learning' or the associations about future rewards based on experience (Berridge and Kringelbach 2008). For mammals, coordinated neural circuits facilitate information from external environmental stimuli and internal physiological cues in order to develop an appropriate behavioral response. The reward circuit governs these neural circuits to produce adaptive, goal-directed decisions (Haber and Knutson 2010; O'Connell and Hofmann 2011). From a clinical perspective, impairments in the reward circuit, perhaps reflecting altered reward evaluation or other distortions in behavior, may amount to models of dysfunctional action selection in psychiatric disorders, including depression, anhedonia, schizophrenia and dementia (Kapur and Remington 1996; Proitsi, Lupton et al. 2012; Tye, Mirzabekov et al. 2013). Thus,

revealing the neural mechanisms involved in this reward circuit is a major goal in neuroscience (O'Connell and Hofmann 2011).

Dopamine has long been implicated in regulating reward-related behaviors (Baik 2013), and yet this hypothesis remains subject to debate (Salamone, Correa et al. 2005). In psychopharmacological animal studies, interfering with dopamine transmission, particularly in the nucleus accumbens, does not reduce primary motivation for natural rewards such as food, which goes against the hypothesis (Kelley 2004). Yet, in conflicting studies, disrupting dopamine transmission hinders the propensity for these animals to engage in obtaining natural rewards (Salamone, Correa et al. 2005). This opens up the possibility that dopamine is selectively involved in reward processing, and that other neural mechanisms in certain circumstances may be more principally involved in reward processing than dopamine.

Serotonin also has functional importance in the reward circuit, though the mechanisms by which serotonin affect behaviors that stem from activity in reward processing regions remains unclear (Cools, Nakamura et al. 2011; Nakamura 2013). In pharmacological research, the role of serotonin is challenged by its ability to bind to various receptor subtypes (14 in total), each having a different or unknown effect on reward-related behavior (Higgins and Fletcher 2003). Under some conditions, reduced serotonin facilitates reward-related behavior (Soubrie 1986). This effect, however, is not observed in all experiments, and inconsistencies between

experiments may come from methodological factors such as the reinforcer stimuli itself or the extent of serotonin depletion (Higgins and Fletcher 2003).

Using the ABA as a fundamental tool to explore serotonin and dopamine receptor gene expression data may shed new light on the structure and function of the reward circuit. Despite dopamine being considered the principal neuromodulator in reward processing, it would be reasonable to predict that serotonin receptors would not be highly expressed throughout the reward circuit, more so than dopamine receptors in certain brain regions. In addition, because the serotonergic system has multifunctional roles outside of reward processing, one would not expect every receptor subtype to be prevalent in the reward circuit. However, the data presented in this chapter suggests otherwise.

While the ABA in of itself cannot reveal behavioral information, corroborating results in literature with ABA results can quantify which receptor subtypes are most prominent in the reward circuit. This is important because the abundance of a particular receptor subtype is suggestive of a brain structure's underlying functionality. Since expression profiles of these neuromodulators have not been curated and remain sparse throughout literature, data mining the ABA for these receptors may be informative for researchers studying the reward circuit. Performing this exploratory analysis could inspire a researcher to, for instance, select a particular pharmacological drug or receptor gene knockout for future reward-based behavioral studies. This in turn can assist in disambiguating the role of dopamine and serotonin in the reward circuit.

Allen Brain Atlas

Similar to how Chapters 3 and 4 approached their respective studies, expression energy volumes of dopamine and serotonin receptors in brain structures associated with reward processing were retrieved from the ABA using their API to investigate the reward circuit. Data from the ABA represents quantified gene expression energy values derived from high-resolution ISH images of specific mRNA species at a resolution of 200-μm3. For each gene, the ABA informatics data analysis pipeline processes expressing pixels, which are then summed to collect pixel-based statistics such as the expression density (sum of expressing pixels divided by sum of all pixels in division) and expression intensity (sum of expression pixel intensity divided by sum of expression pixels). From these statistics, the ABA then calculates the expression energy of a voxel, defined as the sum of expression pixel intensity divided by the sum of all pixels in division. Each voxel located within a brain structure is then unionized to formulate the overall expression energy of the given brain structure.

Brain Structures Associated with the Reward Circuit

Expression data from the ABA were gathered from 15 different brain structures associated with reward processing (Figure 5.1), including ventral tegmental area (VTA), substantia nigra compact part (SNc), substantia nigra reticular part (SNr), prelimibc area (PL), infralimbic area (ILA), nucleus accumbens (ACB), basolateral amygdalar nucleus (BLA), laterodorsal tegmental nucleus (LDT), lateral habenula (LH), dorsal nucleus raphe (DR), lateral septal nucleus (LS),

central amygdalar nucleus (CEA), medial amygdalar nucleus (MEA), hypothalamus (HY) and hippocampal region (HIP). There is much evidence suggesting strong anatomical connections between these forementioned brain structures (Camara, Rodriguez-Fornells et al. 2009; Ikemoto 2010). This section will describe in more detail each brain structure and their reward processing involvement.

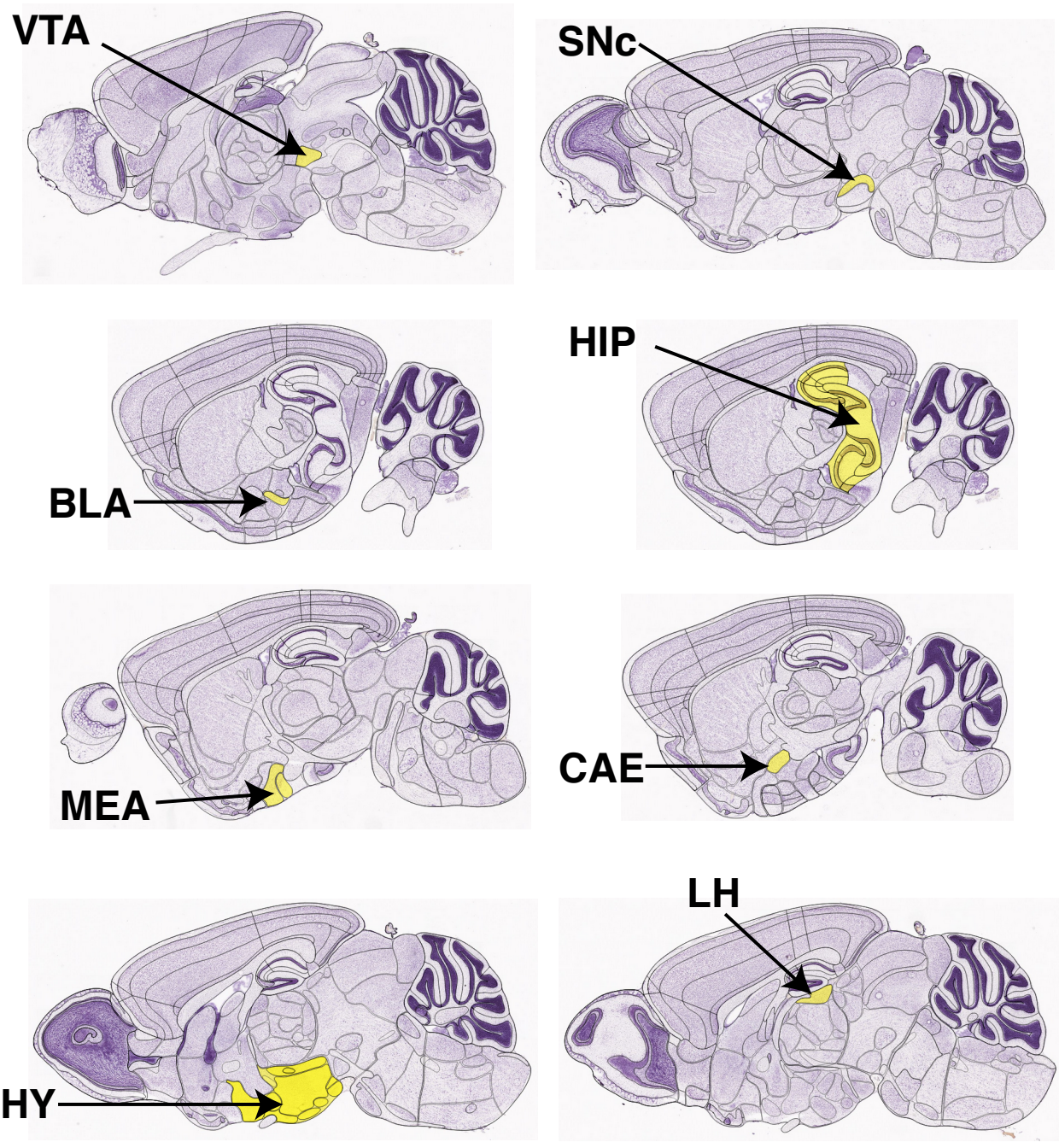

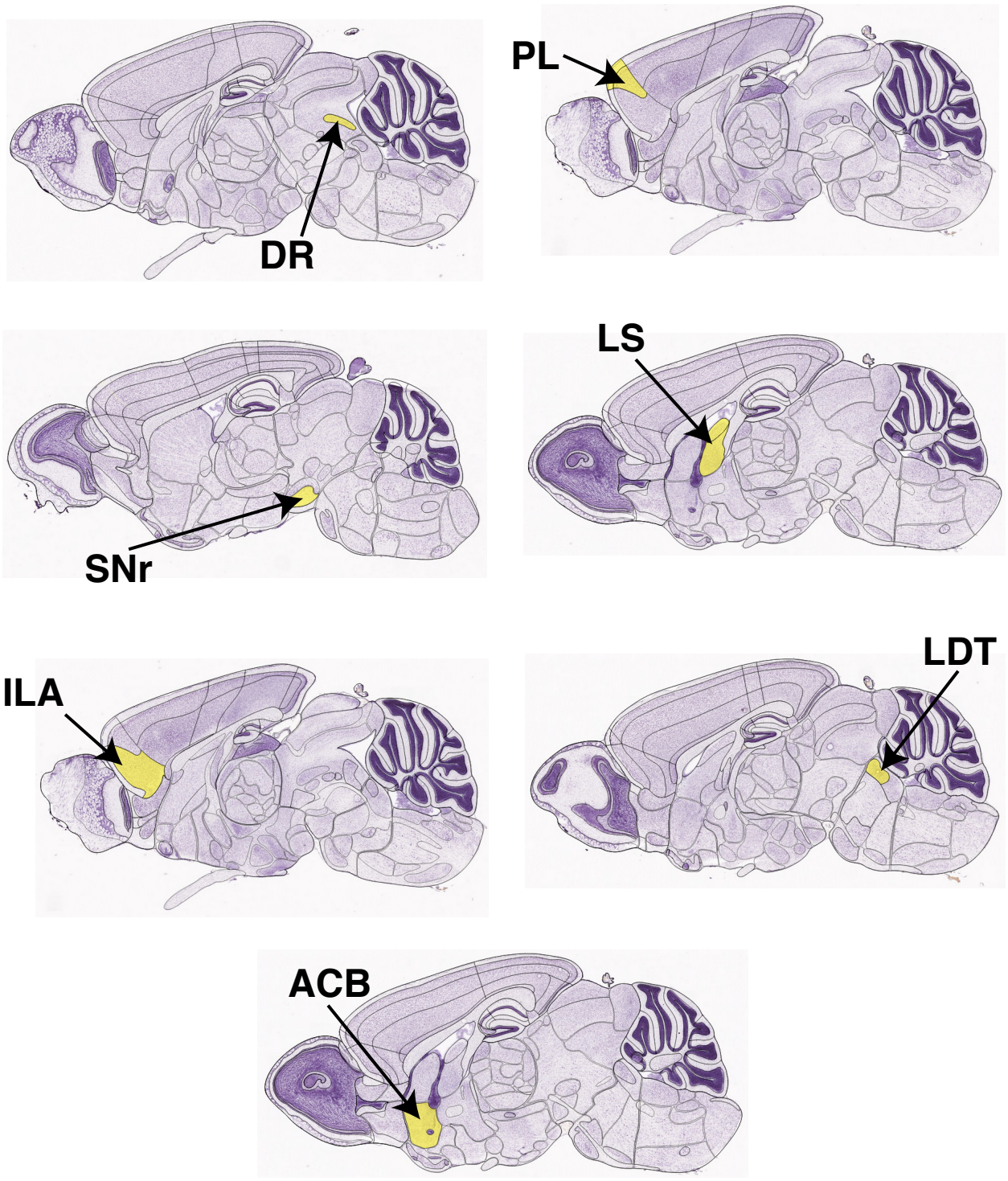

Figure 5.1. Allen Reference Atlas Images of Brain Structures Associated with the Reward Circuit.

Dopamine is a catecholamine neurotransmitter in the brain and is synthesized by neurons primarily in the VTA, and to a lesser extent in SNc.

Dopamine neurons originating in these brain structures project to the striatum, cortex, limbic system and hypothalamus (Bentivoglio and Morelli 2005). Through these pathways, dopamine affects many physiological functions, such as motivated and emotional behaviors, but also hormone secretion and controlling movements (Beaulieu and Gainetdinov 2011; Tritsch and Sabatini 2012). VTA is a heterogeneous brain structure that serves a central role in reward processing (Russo and Nestler 2013; Schultz 2013). Classically known for encoding reward prediction errors through phasic activation, recent evidence suggests dopamine neurons in VTA also respond to aversive, stressful and salient events (Lammel, Lim et al. 2013; Schultz 2013). SNc is another major source of dopamine, with recent reporting suggesting that dopamine neurons in the SNc exhibit functional heterogeneity that may contribute to diverse roles in behavior related to reward, addiction and movement (Kitahama, Nagatsu et al. 2000; Di Giovanni, Esposito et al. 2010; Ungless and Grace 2012). Both VTA and SNc also project to DR, which may facilitate serotonin neurons and in turn mediate motivational behavior (Ferre and Artigas 1993).

Serotonin is a monoamine neurotransmitter in the brain and originates in DR. Similar to VTA, DR is a heterogeneous brain structure that projects extensively to brain areas related to reward processing (Peyron, Petit et al. 1998). DR has been shown have a strong impact on value-based decision-making (Nakamura 2013). Although evidence suggests that serotonin may oppose dopamine's rewarding activities (Crockett, Clark et al. 2009), DR neural recordings found increased firing

activity during reward tasks and that this activation can alter neuronal activity patterns in efferent regions, such as in the cortex (Liu, Zhou et al. 2014).

ACB, referred to as the "hedonic hotspot", is crucial for the recognition of reward in the environment and initiating food consumption (Peyron, Petit et al. 1998; Pecina, Smith et al. 2006; Koob and Le Moal 2008). ACB receives input from both dopaminergic VTA and serotoninergic DR regions (Peyron, Petit et al. 1998; Bentivoglio and Morelli 2005). Much of the research has focused ACB and its role in reward-related functions has received come from dopamine's rewarding effects of drugs of abuse (Rodd-Henricks, McKinzie et al. 2002; Pierce and Kumaresan 2006). It is also known that serotonergic neurons from the DR innervate the mesolimbic dopaminergic system, which ACB is a part of this system (De Deurwaerdere, Stinus et al. 1998; Fletcher and Korth 1999).

Both VTA and DR project to the prefrontal cortex (Peyron, Petit et al. 1998; Bentivoglio and Morelli 2005). Though the prefrontal cortex is not defined in the ABA, PL and ILA are considered homologues of human and primate anterior cingulate cortex and is a subdivision of the medial prefrontal cortex (Groenewegen and Uylings 2000). PL and ILA are responsible for mediating different behavioral responses to specific rewarding, environmental stimuli (Bromberg-Martin, Matsumoto et al. 2010; Pentkowski, Duke et al. 2010; Russo and Nestler 2013).

As discussed in Chapter 3, the amygdala has strong bidirectional interaction with the dopaminergic and serotonergic systems (Steinbusch 1981; Lee, Wheeler et al. 2011). The amygdala participates in responding to aversive events as well as

encoding predictive cues of reward (LeDoux 2003; Belova, Paton et al. 2007). Three regions from the amygdala were explored in this survey: BLA, CEA and MEA. BLA is reported to play a crucial role in many emotional and cognitive functions of the brain (Bjorklund and Dunnett 2007; Lammel, Hetzel et al. 2008; Russo and Nestler 2013), while both CEA and MEA encode positive and negative motivational values (Lee, Eum et al. 2007; Belova, Paton et al. 2008).

The remaining subcortical structures, SNr, LDT, LH, HY, LS and HIP, play a role in reward processing. SNr, which receives its input from serotonin, has been reported to control reward-dependent modulation of action in its afferent regions such as PL and ILA (Moukhles, Bosler et al. 1997; Balleine 2005). LDT promotes burst firing of dopamine neurons in VTA, which influences reward processing by increasing dopamine release in ACB (Cornwall, Cooper et al. 1990; Lodge and Grace 2006). LH is thought to be critical for mediating when expected rewards do not occur, as well as behavioral responses to aversive stimuli (Matsumoto and Hikosaka 2007; Hikosaka 2010). HY is an important source of reward information caused by orexin neurons, which activate serotonin release through arousal, feeding and rewarding stimuli (Harris and Aston-Jones 2006; Tao, Ma et al. 2006). LS is an important region involved in reward-oriented behavior when serotonin is released in this region (Kohler, Chanpalay et al. 1982; Clemett, Punhani et al. 2000). Lastly, HIP, through its dense connections with VTA and DR, is reported to strengthen memory encoding of a particular stimulus based on its valence (Amat, Matus-Amat et al. 1998; Fields, Hjelmstad et al. 2007).

Dopamine and Serotonin Receptor Genes

The query in this survey was comprised of dopamine receptors: Drd1a, Drd2, Drd3, Drd4, and Drd5; and serotonin receptors: Htr1a, Htr1b, Htr1d, Htr1f, Htr2a, Htr2b, Htr2c, Htr3a, Htr4, Htr5a, Htr5b, Htr6 and Htr7 (Table 5.1). Experiments for each gene was found in the ABA. For any particular gene that returned multiple experiments (SectionDataSetIDs), the experiment that contained the highest sum of expression energy within brain regions of interest (Chapter 5, Brain Structures Associated with the Reward Circuit) was used in this survey for analysis.

Previous Literature Reporting of Dopamine and Serotonin Receptor Gene Expression

Before analyzing any data from the ABA, levels of expression energy for dopamine and serotonin receptors in the reward circuit taken from previous literature were tabulated (Figure 5.2). This was accomplished to generate predictions about the ABA dataset.

Each subplot in Figure 5.2 represents a different family of dopamine and serotonin receptors, separated by their affect on neurotransmission (excitatory or inhibitory). The top right plot represents excitatory serotonin receptors (Htr2a, Htr2b, Htr2c, Htr3a, Htr4, Htr6, Htr7). The top left plot represents inhibitory serotonin receptors (Htr1a, Htr1b, Htr1d, Htr1f, Htr5a, Htr5b). The bottom right plot represents D1 family receptors (Drd1a, Drd5), which are known to mediate excitatory neurotransmission. Lastly, the bottom left plot represents D2 family

receptors (Drd2, Drd3, Drd4), which are known to mediate inhibitory neurotransmission.

Table 5.1. List of Dopamine and Serotonin Receptor Genes. ImageSeriesID is an identification number for the experiment used to analyze gene expression.

Symbol	Name	ImageSeriesID	Receptor Subtype
Drd1a	dopamine receptor D1A	352	G_s-protein coupled
Drd2	dopamine receptor 2	81790728	G_i/G_o-protein coupled
Drd3	dopamine receptor 3	75038431	G_i/G_o-protein coupled
Drd4	dopamine receptor 4	112650336	G_i/G_o-protein coupled
Drd5	dopamine receptor 5	81790728	G_s-protein coupled
Htr1a	5-hydroxytryptamine receptor 1A	79394355	G_i/G_o-protein coupled
Htr1b	5-hydroxytryptamine receptor 1B	79913318	G_i/G_o-protein coupled
Htr1d	5-hydroxytryptamine receptor 1D	71393418	G_i/G_o-protein coupled
Htr1f	5-hydroxytryptamine receptor 1F	69859867	G_i/G_o-protein coupled
Htr2a	5-hydroxytryptamine receptor 2A	81671344	Gq/G11-protein coupled
Htr2b	5-hydroxytryptamine receptor 2B	71664130	G_q/G_{11}-protein coupled
Htr2c	5-hydroxytryptamine receptor 2C	71393424	G_q/G_{11}-protein coupled
Htr3a	5-hydroxytryptamine receptor 3A	70593142	Ligand-gated Na^+/K^+ cation channel
Htr4	5-hydroxytryptamine receptor 4	69257849	G_s-protein coupled
Htr5a	5-hydroxytryptamine receptor 5A	71393430	G_i/G_o-protein coupled
Htr5b	5-hydroxytryptamine receptor 5B	71247644	G_i/G_o-protein coupled
Htr6	5-hydroxytryptamine receptor 6	69257981	G_s-protein coupled
Htr7	5-hydroxytryptamine receptor 7	71393436	G_s-protein coupled

Though the procedure used to retrieve literature data and classify expression energy is similar to Table 3.2 (Chapter 3, Contrast Between ABA Expression Data and Prior ISH mRNA Literature), Figure 5.2 does not include ABA data. In short, the Gene Expression Nervous System Atlas (GENSAT) was used to access prior rodent brain studies. Classifying expression level from these previous studies were taken directly from their reported wording. Some studies may state qualitative values (high, moderate, low), and others may use symbols (-, +, ++, +++) to classify

expression energy. Expression based on this qualitative assessment was mapped to a different color in Figure 5.2 based on reported levels.

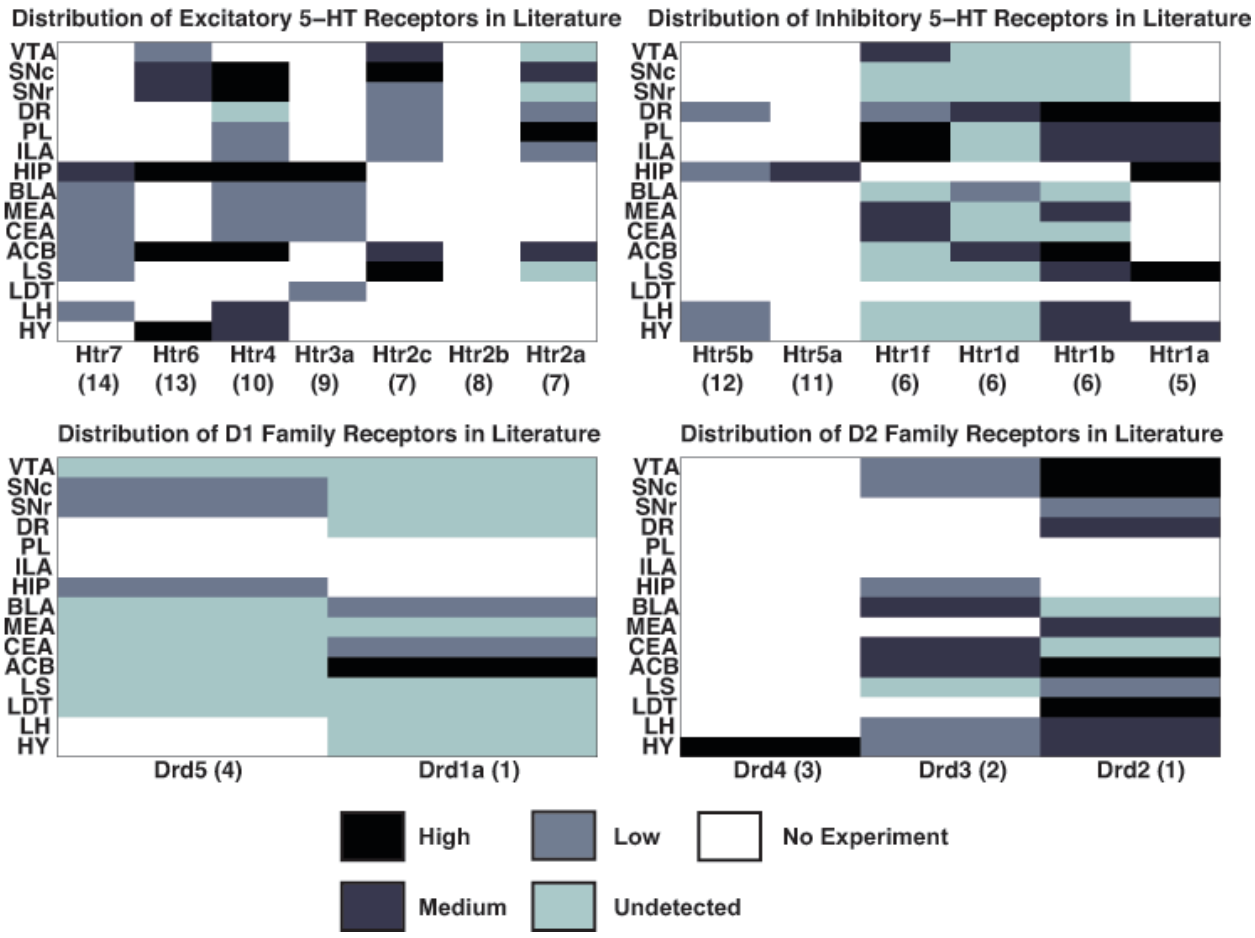

Figure 5.2. Literature Reporting of Dopamine and Serotonin Receptor Gene Expression. Numbers in parentheses next to each receptor gene name correspond to the following literature: 1. (Weiner, Levey et al. 1991), 2. (Bouthenet, Souil et al. 1991), 3.) (O'Malley, Harmon et al. 1992), 4.) (Meador-Woodruff, Mansour et al. 1992), 5.) (Pompeiano, Palacios et al. 1992), 6.) (Duxon, Flanigan et al. 1997), 7.) (Bruinvels, Landwehrmeyer et al. 1994), 8.) (Pompeiano, Palacios et al. 1994), 9.) (Tecott, Maricq et al. 1993), 10.) (Vilaró, Cortés et al. 2005), 11.) (Maroteaux, Saudou et al. 1992), 12.) (Matthes, Boschert et al. 1993), 13.) (Gerard, el Mestikawy et al. 1996), 14.) (Neumaier, Sexton et al. 2001).

In general, many dopamine and serotonin receptors in the reward circuit have neither any documented experimental results nor significant expression energy detection (Figure 5.2, white and light blue cells). Every gene receptor subtype had at least two or more missing data points in every reward-related brain structure (Figure 5.2, white cells), with Htr2b in particular not having any

experiments conducted in the reward circuit (Pompeiano, Palacios et al. 1994), suggesting that perhaps Htr2b may not have influence in modulating activity in the reward circuit (Alex and Pehek 2007).

Total Expression and Individual Receptor Subtypes

Using the ABA to examine receptor subtypes, expression energy of serotonin receptors was observed to be greater than the amount of expression energy of dopamine receptors in the reward circuit brain areas (Figure 5.3). Each bar in Figure 5.3 represents expression energy of a particular receptor subtype combined across all brain structures involved in reward processing (Chapter 5, Brain Structures Associated with the Reward Circuit).

Of all receptor genes assessed, Htr2c had the highest expression energy values within the serotonergic system, followed by Drd1a and Drd2 within the dopaminergic system (Figure 5.3). Htr2c reported as highest in the ABA may be explained its characterized high levels of constitutive activity across the mesolimbocortical pathway (Katsidoni, Apazoglou et al. 2011). As for Drd1a and Drd2, those receptors have been most abundantly expression throughout the brain compared to the rest of the dopamine receptors according to previous reporting (Baik 2013), consistent with ABA results (Figure 5.3).

In the examined brain structures associated with reward processing, dopamine receptor expression energy was more centralized in ACB and serotonin receptor expression energy was more distributed across brain structures (Figure 5.4). Though debatable (Salamone, Correa et al. 2005), a critical portion of reward

processing is encoded in ACB and is mediated through the actions of dopamine (Gale, Shields et al. 2014). This may suggest why there is an abundant amount of dopamine receptor expression energy found in the ACB compared to the other brain structured involved in reward processing (Figure 5.4). In contrast, expression of serotonin receptors was distributed across the studied brain structures (Figure 5.4). While there is evidence to support the functional importance of serotonin in reward-seeking behavior (Cools, Nakamura et al. 2011; Nakamura 2013), developing a formal framework for understanding its precise role remains challenging because, perhaps, its nearly equal, widespread receptor distribution across the reward circuit.

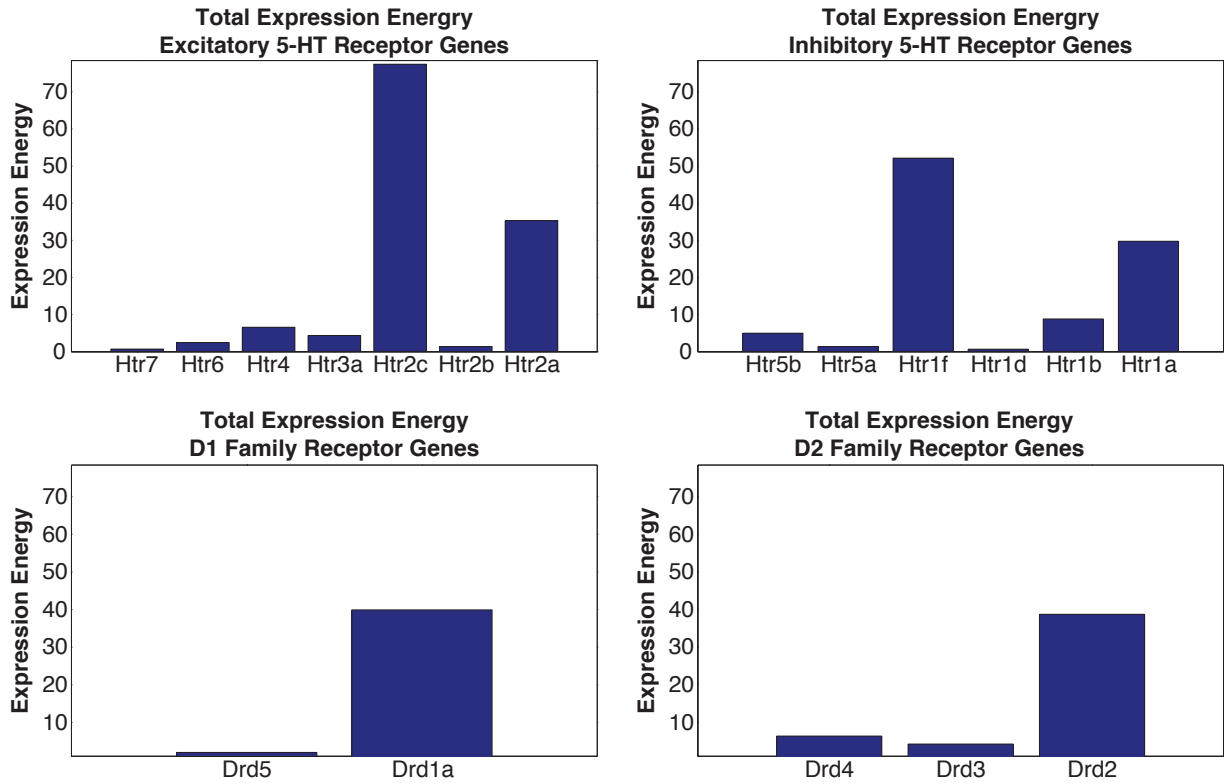

Figure 5.3. Total Gene Expression Energy of Dopamine and Serotonin Receptors Across All Brain Structures Associated with Reward Processing. Gene expression values for each brain structure were collapsed into a single receptor subtype

Individual Receptor Expression

To reveal which receptor subtype is contributing to the expression profiles in Figure 5.3 and 5.4, the expression energy of each gene per brain structure was examined (Figure 5.5).

Though serotonin may seem distributed across all brain structures (Figure 5.4), separating each expression profile by subtype revealed only a few receptors responsible for its distributed profile: Htr1a, Htr1f, Htr2a and Htr2c (Figure 5.5). The remaining serotonin receptors, particularly Htr5a, Htr5b, Htr6 and Htr7, are not contributing much to the overall expression profile (Figure 5.5).

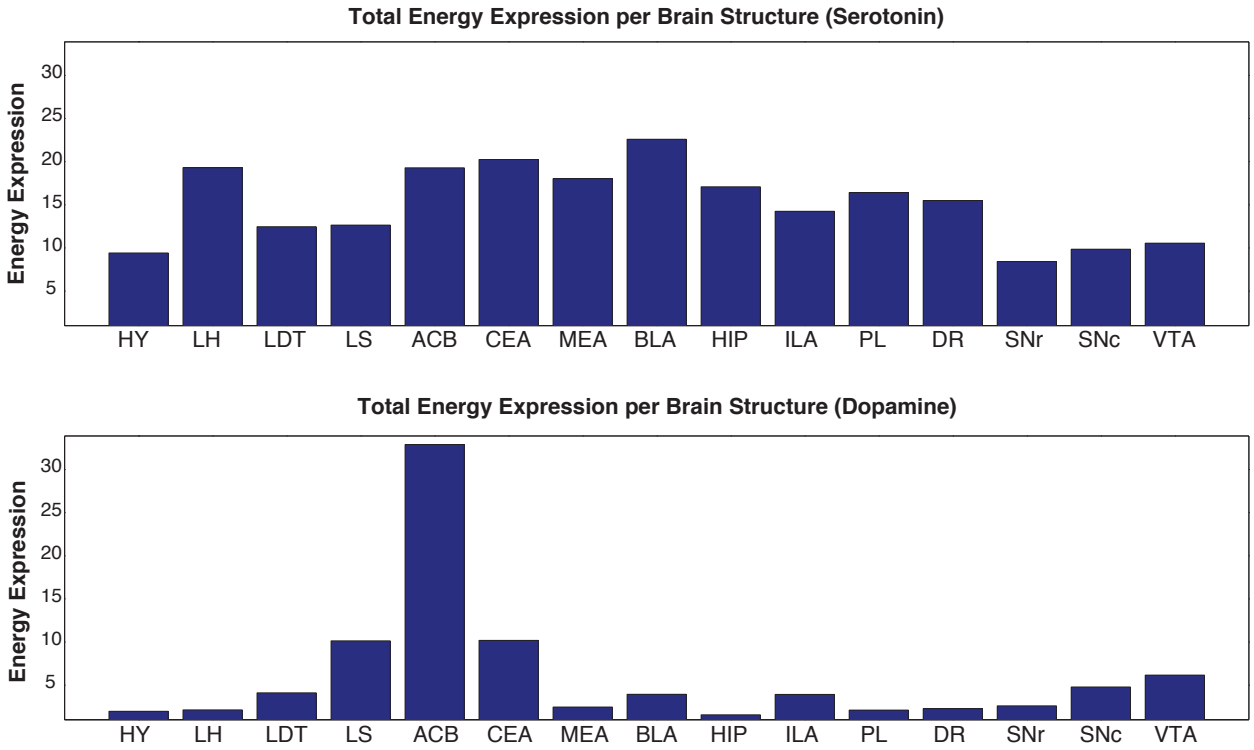

Figure 5.4. Total Gene Expression Energy of Dopamine and Serotonin Receptors per Brain Structure Associated with Reward Processing. Gene expression values for every receptor subtype were collapsed into a single brain structure.

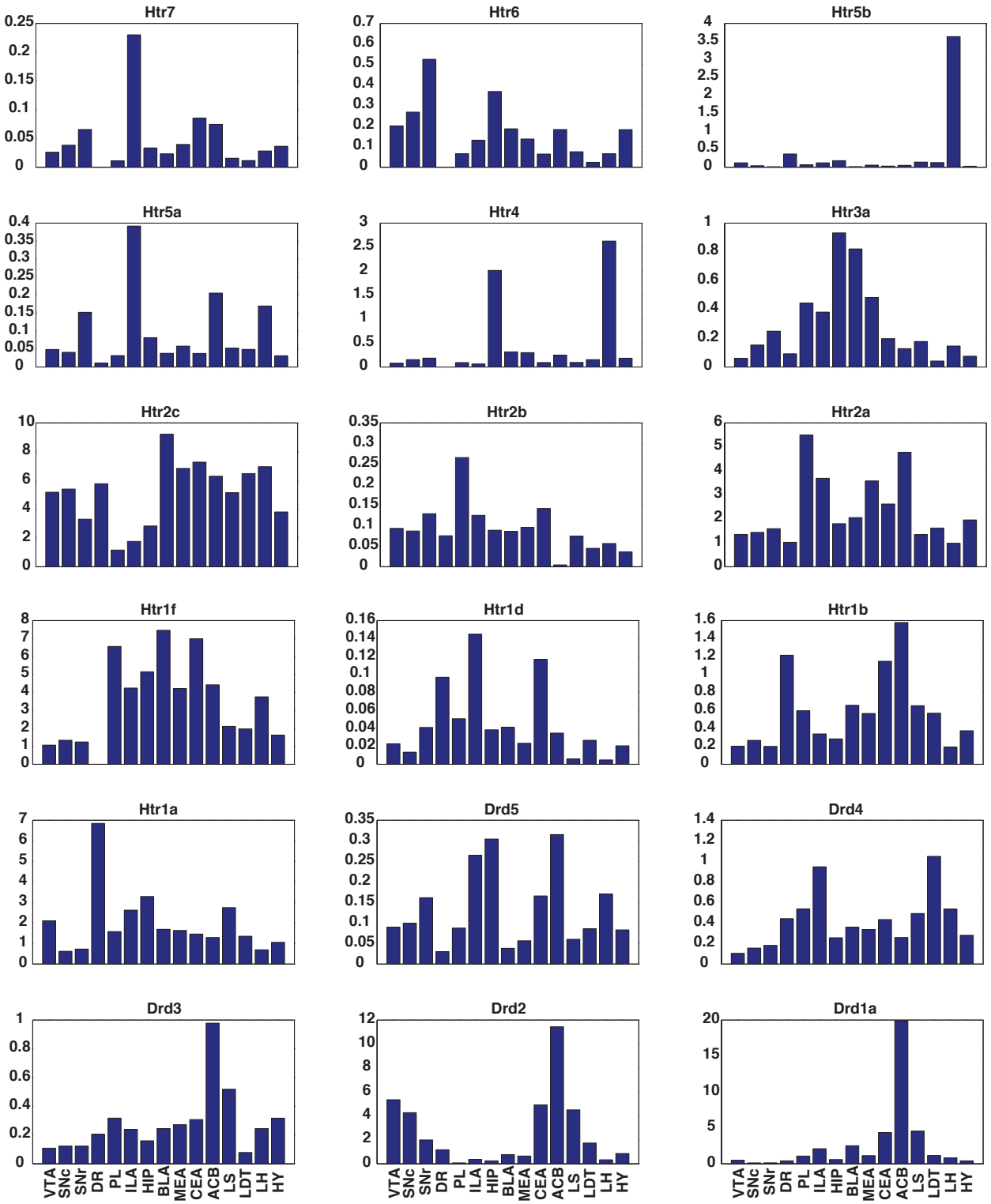

Figure 5.5. Individual Gene Expression Profile of Dopamine and Serotonin Receptors Across Brain Structures Associated with Reward Processing. The brain structures are arranged in the same order across all subplots as displayed in the bottom row. Values on the y-axis represent expression energy.

In regards to dopamine, the expression energy of Drd1a and Drd2 is predominately found in ACB (Figure 5.5). As previously mentioned in Figure 5.3, this observation is in line with evidence that Drd1a and Drd2 are most prevalent throughout the brain, contributing greatly to reward-related behaviors (Baik 2013).

In addition to profiling individual receptor subtypes, proportions of expression energy within reward processing brain structures were visualized using the ABADV introduced in Chapter 4 (Figure 5.6). Each portion (quantity of expression energy in a brain structure) within a chart (gene) is colored differently depending on its parent brain structure according to the Allen Reference Atlas (Dong 2008). This color-coding resulted in five different categories: Interbrain, Midbrain, Cerebral Cortex, Striatum and Pons. Structures in red fall under the Interbrain region, which include HY and LH. Structures in green represent Cerebral Cortex areas, which include BLA, HIP, ILA, and PL. Structures in blue represents regions in the Striatum, which include MEA, CEA, LS, and ACB. Structures in light purple come from the Midbrain, which include VTA, SNc, SNr, and DR. LDT is all by itself in the Pons, colored in light orange.

Overall, the distribution of expression energy varied tremendously within and between each receptor subtype with no emerging patterns. However, brain structures associated with the dopaminergic mesolimbic-cortical pathway stood out in high proportions across several receptors. The mesolimbic-cortical pathway originates in VTA and projects to ACB, ILA, and PL, responsible for value-gained decision-making and processing aversive stimuli (Brooks and Berns 2013;

Nakamura 2013). Drd1a, Drd2, Drd3, Drd5 and Htr1b contained a high proportion of ACB compared to other brain structures. Drd4, Htr1d, Htr5a and Htr7 featured ILA as its highest proportional brain structure. Drd4, Htr1f, Htr2a and Htr2b had a high proportion of expression energy found in PL.

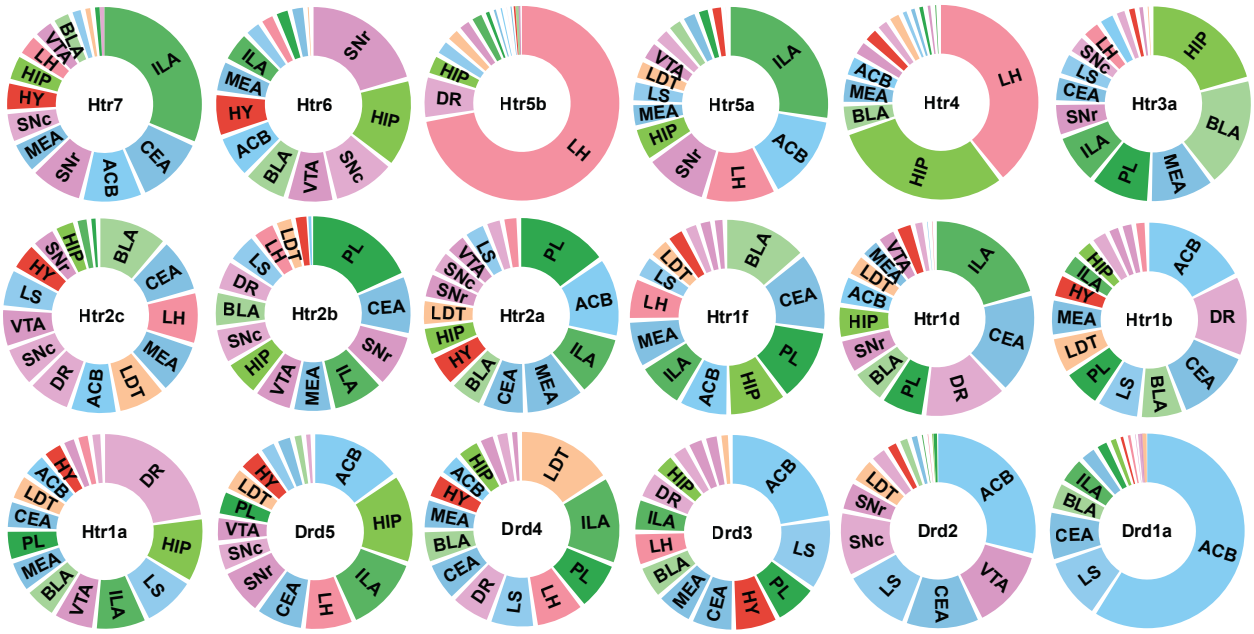

Figure 5.6. Proportions of Brain Structures Associated with Reward Processing Across Dopamine and Serotonin Receptor Gene Expression. Each pie chart represents a receptor subtype and each portion within a pie chart represents a brain structure and the width of each portion represents the total amount of expression energy of the gene relative to other brain structures within the same gene. Brain structures were colored based on their Allen Reference Atlas (Dong 2008).

Hierarchical Clustering Analysis

To identify any functional-structural relationships between dopamine, serotonin and brain structures associated with reward processing, a hierarchical cluster analyses was performed (Figure 5.7). As described in Chapter 3, performing a cluster analysis merges similar groups of brain structures into a binary tree of data that provides a useful summary of similarity within groups and dissimilarity

between groups. New functional-structural relationships about reward processing may surface by joining or "clustering" similar brain structures based on data.

Overall, several structures that clustered together based on expression energy also formed identical clusters based on anatomical location and parent structure (Figure 5.7). VTA, SNc and SNr, as well as PL and ILA, clustered across gene expression, anatomical location, and shared parent structure (Figure 5.7, purple and green). MEA and HY formed a cluster in terms of expression energy and anatomical location, but not based on their shared parent structure (Figure 5.7). CEA and LS, both part of the Striatum parent structure, clustered together based on expression energy, but in terms of anatomical location it was LS and ACB, also part of the Striatum, that clustered (Figure 5.7, blue). In general, these clusters may suggest that the expression profile of dopamine and serotonin receptors in brain structures from Striatum, Cerebral Cortex, and Midbrain are defined by their anatomical location.

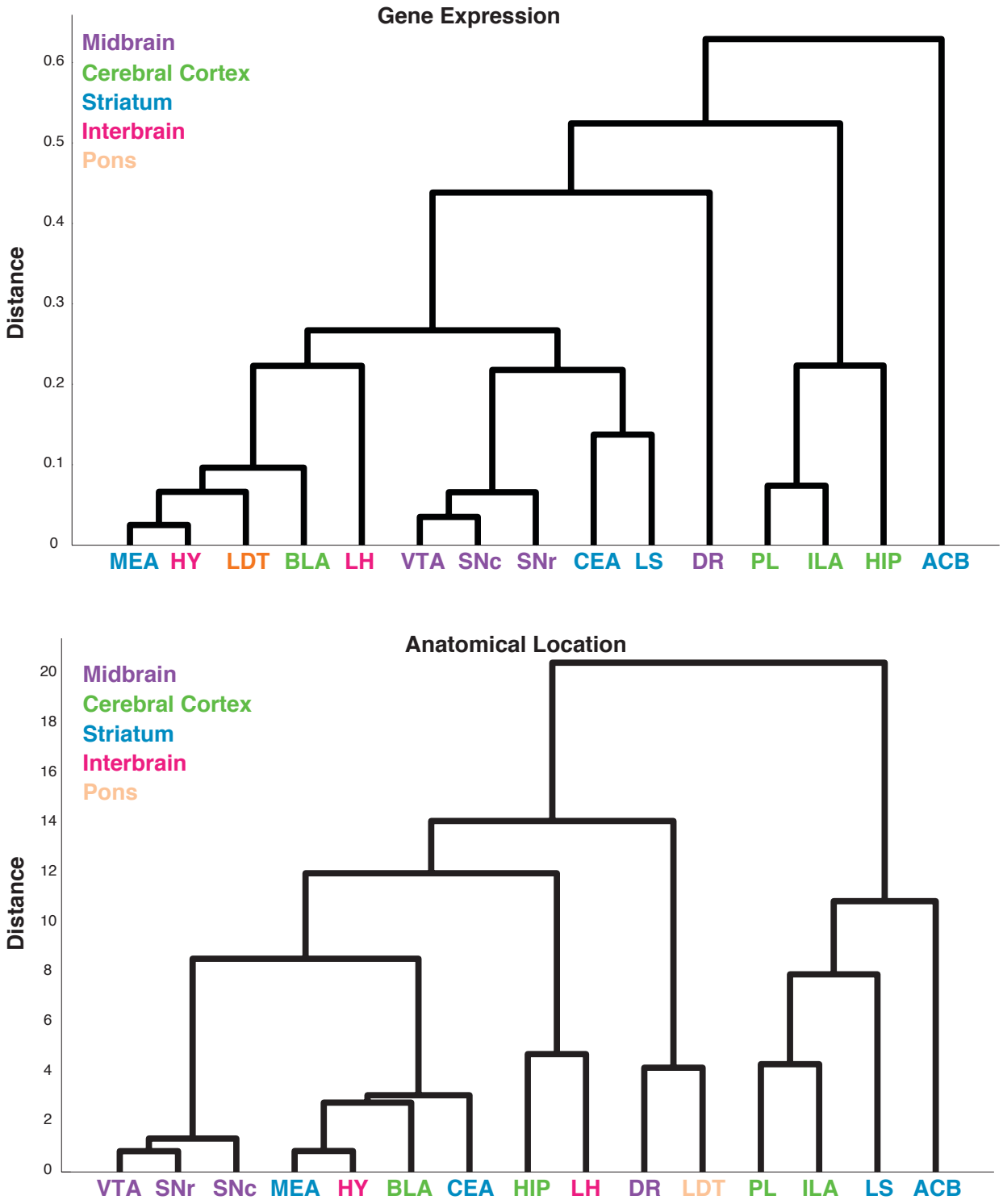

Figure 5.7. Hierarchical Clusters of Dopamine, Serotonin and Centroid Location Based on Brain Structures Associated with Reward Processing. Cluster analysis were performed on energy expression data (top) and anatomical location (bottom). Brain structures were colored based on their shared parent structure according to the Allen Reference Atlas (Dong 2008).

Reward Circuit Network

In order to better analyze a complex network, Cytoscape.js, a Javascript library (Saito, Smoot et al. 2012), was used to visualize potential connectivity relationships between brain regions where dopamine and serotonin originate and brain structures involved in reward processing based on expression data from the ABA (Figure 5.8). Given a dopamine or serotonin source, one can infer the strength of either neuromodulator projection to a target area based on their receptor expression energy, for example by examining at the overall expression energy of D1 family receptor gene expression energy in a target region of interest.

Figure 5.8 is a depiction of the overall relationship between excitatory and inhibitory-mediated dopamine and serotonin receptor genes across brain structures involved in processing reward. Figure 5.8 uses the same coloring scheme featured in Figure 5.6 and 5.7, where brain structures were collapsed together based on their common parent structure, Midbrain, Cerebral Cortex, Striatum, Interbrain and Pons. These categories are encapsulated in nodes, where the Midbrain is the common parent structure for VTA, SNc, SNr and DR; the Cerebral Cortex is the common parent structure for PL, ILA, BLA, and HIP; the Striatum is the common parent structure for MEA, CAE, LS, and ACB; the Interbrain is the common parent structure for HY and LH; and the Pons is the parent structure of LDT. In addition to these five parent structure nodes, there are two source nodes: VTA and DR, which represent the source of dopamine and serotonin, respectively. Between each source node and parent structure node are two edges: an edge that ends with a

triangle, which represents its source node's respective set of expression energy values whose subtype mediates excitatory neurotransmission (Drd1a, Drd5, Htr2a, Htr2b, Htr2c, Htr3a, Htr4, Htr6, Htr7); and an edge that ends with a circle, which represents its source node's respective set of expression energy values whose subtype mediates inhibitory neurotransmission (Drd2, Drd3, Drd4, Htr1a, Htr1b, Htr1d, Htr1f, Htr5a, Htr5b). The width of each edge denotes the total amount of expression energy value.

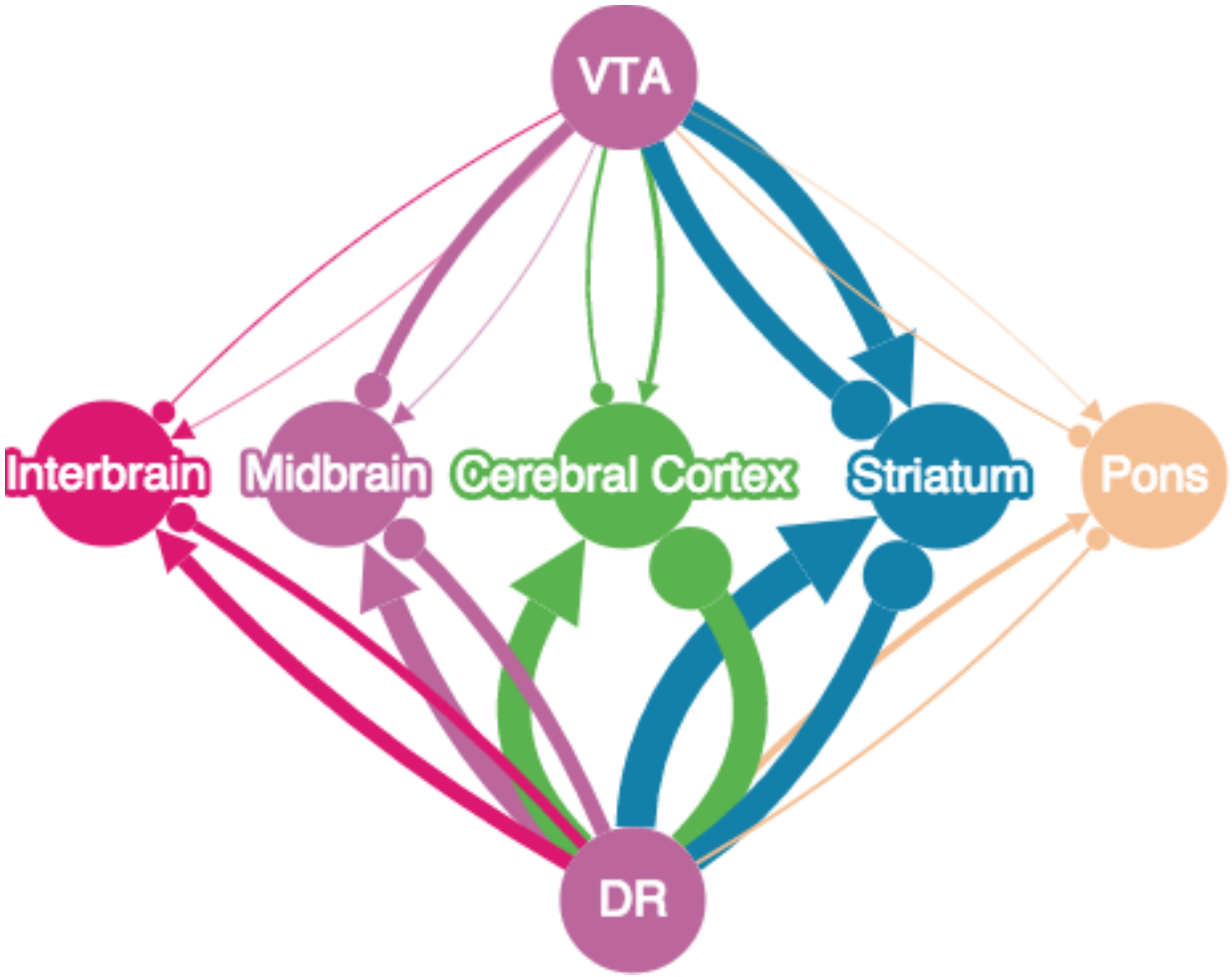

Figure 5.8. Network Graph of the Reward Circuit Based on Dopamine and Serotonin Receptor Gene Expression Energy. Edges with a triangle as its endpoint denote an excitatory connection and edges with a circle as its endpoint denote an inhibitory connection. Size of each edge represents the amount of expression energy. Parent structures were colored according to the Allen Reference Atlas (Dong 2008).

Serotonin has more influence in brain structures associated with reward processing compared to dopamine (Figure 5.8). While excitatory and inhibitory dopamine seems to have the most influence in the Striatum (particularly ACB in Figure 5.4), and to a lesser extent in the Midbrain, where it is mostly mediated by inhibitory DA neurotransmission as opposed to both, excitatory and inhibitory serotonin were more prevalent in not just the Striatum and Midbrain, but also completely dominate in the Cerebral Cortex and Interbrain compared to dopamine (Figure 5.8). Pons, which is only comprised of LDT, received the least amount of expression energy, though excitatory serotonin still favors in its influence compared to inhibitory serotonin and dopamine (Figure 5.8). Compared to dopamine, perhaps serotonin's role in the reward circuit is more important than speculated (Alex and Pehek 2007; Nakamura 2013).

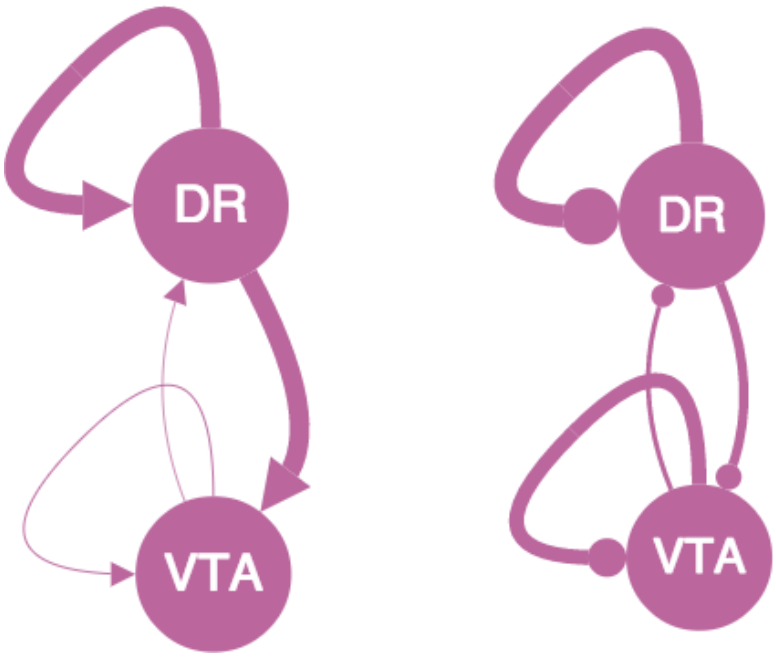

Figure 5.9. Network Graph Between Ventral Tegmental Area and Dorsal Raphe. Edges with a triangle as its endpoint denote an excitatory connection and edges with a circle as its endpoint denote an inhibitory connection. Size of each edge represents the amount of expression energy.

Examining more closely at the interaction of these neuromodulators, the ABA revealed that serotonin has a stronger influence than dopamine between and within their site of origins (Figure 5.9). Excitatory dopamine receptors have low expression in VTA and DR, while excitatory serotonin receptors are more expressed in both (Figure 5.9, left). A similar relationship also exists for their inhibitory counterparts, though inhibitory dopamine receptors are more expressive compared to excitatory dopamine receptors (Figure 5.9, right). The strong presence of serotonin receptor expression energy in these areas suggests that the activity of neurons in these regions is more strongly regulated by serotonin than by dopamine.

Discussion

An exploratory ABA survey of receptor expression energy was conducted using data from the dopaminergic and serotonergic systems in anatomical regions that are associated with reward processing. Under the assumption that the amount of expression energy in a given brain structure is indicative of its function, the ABA results revealed several implications that both support and challenge arguments surrounding the reward circuit.

Both excitatory and inhibitory serotonin receptors expressed high energy across all brain structures investigated. Contrary to the belief that dopamine is the principal neuromodulator for reward-related behavior, serotonin's expression profile suggest that it also plays a principal role in reward processing. On the other hand, expression energy of dopamine receptors was limited to ACB and to a lesser extent in midbrain VTA and SNc. This suggests dopamine is selectively involved in reward

processing, and not across the reward circuit. Moreover, receptor subtypes Htr2c, Drd1a and Drd2 were most expressed, while the remaining subtypes were considerably less expressed. These individual receptor profiles disambiguate the importance of receptor subtype in reward processing regions. In addition, based on expression energy, anatomical location and parent structure, the midbrain VTA, SNc and SNr, as well as cerebral cortex PL and ILA, formed a cluster based on similarity. This clustering of data suggests a structural-functional relationship amongst the midbrain and cerebral cortex regions. Together, the ABA filled in many missing data that was not reported or went undetected in rodent brain ISH studies.

Given the results, there is perhaps an indication that, between the two neuromodulators, it is serotonin driving the overall neuronal activity in the reward circuit (Figure 5.7). This assertion is in support of other studies that challenge the simplified view of DR serotonin neurons and its lack of involvement in reward processing (Balasubramani, Chakravarthy et al. 2014; Liu, Zhou et al. 2014; Macoveanu 2014). Though other methodologies were used to explore serotonin's role in reward, no one has quantitatively reported precisely how much influence each serotonin receptor subtype has in each reward processing brain structure. The quantitative expression energy data presented in this survey contributes by favoring serotonin's involvement with reward from a molecular perspective.

Unexpectedly, expression of dopamine receptors was not as robust as literature would suggest. Perhaps an explanation for the disparity in dopamine receptor expression may stem from its functional connectivity profile, rather than

its level or receptor expression. Chapter 3 explored the interaction between the neuromodulatory system, including dopaminergic, serotonergic, cholinergic and noradrenergic, and identified both substantia nigra (where acetylcholine originates) and ventral tegmental area as a hub, or "rich club" of neuromodulation (van den Heuvel and Sporns 2011). Despite relatively low expression values, the hierarchical clustering analysis in this survey did reveal that VTA, SNc and SNr formed a tight cluster together based on its expression profile, anatomical location and shared parent structure (the Midbrain). This may open up the argument that perhaps dopaminergic innervation may work as an ensemble in order to process rewarding signals, as opposed to separate projections.

Similar to the contribution made in Chapter 3, the comprehensive ABA allowed the present survey to fill in many gaps in the knowledge of ISH dopaminergic and serotonergic receptor gene expression (Figure 5.2). Furthermore, the ABA's standardization and consolidation of numerous ISH experiments more readily allows comparison of gene expression across multiple brain regions. With the ABA and this survey, this information is now curated for other researchers to corroborate results and promote discovery of dopamine and serotonin involvement in reward-related behaviors.

References

Alex, K. D. and E. A. Pehek (2007). "Pharmacologic mechanisms of serotonergic regulation of dopamine neurotransmission." Pharmacol Ther 113(2): 296-320.

Amat, J., P. Matus-Amat, et al. (1998). "Escapable and inescapable stress differentially and selectively alter extracellular levels of 5-HT in the ventral hippocampus and dorsal periaqueductal gray of the rat." Brain Research 797(1): 12-22.

Baik, J. H. (2013). "Dopamine signaling in reward-related behaviors." Front Neural Circuits 7: 152.

Balasubramani, P. P., V. S. Chakravarthy, et al. (2014). "An extended reinforcement learning model of basal ganglia to understand the contributions of serotonin and dopamine in risk-based decision making, reward prediction, and punishment learning." Front Comput Neurosci 8: 47.

Balleine, B. W. (2005). "Neural bases of food-seeking: affect, arousal and reward in corticostriatolimbic circuits." Physiol Behav 86(5): 717-730.

Beaulieu, J. M. and R. R. Gainetdinov (2011). "The physiology, signaling, and pharmacology of dopamine receptors." Pharmacol Rev 63(1): 182-217.

Belova, M. A., J. J. Paton, et al. (2007). "Expectation modulates neural responses to pleasant and aversive stimuli in primate amygdala." Neuron 55(6): 970-984.

Belova, M. A., J. J. Paton, et al. (2008). "Moment-to-moment tracking of state value in the amygdala." Journal of Neuroscience 28(40): 10023-10030.

Bentivoglio, M. and M. Morelli (2005). "Chapter I: The organization and circuits of mesencephalic dopaminergic neurons and the distribution of dopamine receptors in the brain." Handbook of Chemical Neuroanatomy 21: 1-107.

Berridge, K. C. and M. L. Kringelbach (2008). "Affective neuroscience of pleasure: reward in humans and animals." Psychopharmacology (Berl) 199(3): 457-480.

Bjorklund, A. and S. B. Dunnett (2007). "Dopamine neuron systems in the brain: an update." Trends Neurosci 30(5): 194-202.

Bouthenet, M. L., E. Souil, et al. (1991). "Localization of dopamine D3 receptor mRNA in the rat brain using in situ hybridization histochemistry: comparison with dopamine D2 receptor mRNA." Brain Research 564(2): 203-219.

Bromberg-Martin, E. S., M. Matsumoto, et al. (2010). "Dopamine in Motivational Control: Rewarding, Aversive, and Alerting." Neuron 68(5): 815-834.

Brooks, A. M. and G. S. Berns (2013). "Aversive stimuli and loss in the mesocorticolimbic dopamine system." Trends Cogn Sci 17(6): 281-286.

Bruinvels, A. T., B. Landwehrmeyer, et al. (1994). "Localization of 5-HT1B, 5-HT1D alpha, 5-HT1E and 5-HT1F receptor messenger RNA in rodent and primate brain." Neuropharmacology 33(3-4): 367-386.

Camara, E., A. Rodriguez-Fornells, et al. (2009). "Reward networks in the brain as captured by connectivity measures." Front Neurosci 3(3): 350-362.

Clemett, D. A., T. Punhani, et al. (2000). "Immunohistochemical localisation of the 5-HT2C receptor protein in the rat CNS." Neuropharmacology 39(1): 123-132.

Cools, R., K. Nakamura, et al. (2011). "Serotonin and Dopamine: Unifying Affective, Activational, and Decision Functions." Neuropsychopharmacology 36(1): 98-113.

Cornwall, J., J. D. Cooper, et al. (1990). "Afferent and Efferent Connections of the Laterodorsal Tegmental Nucleus in the Rat." Brain Research Bulletin 25(2): 271-284.

Crockett, M. J., L. Clark, et al. (2009). "Reconciling the role of serotonin in behavioral inhibition and aversion: acute tryptophan depletion abolishes punishment-induced inhibition in humans." J Neurosci 29(38): 11993-11999.

De Deurwaerdere, P., L. Stinus, et al. (1998). "Opposite change of in vivo dopamine release in the rat nucleus accumbens and striatum that follows electrical stimulation of dorsal raphe nucleus: Role of 5-HT3 receptors." Journal of Neuroscience 18(16): 6528-6538.

Di Giovanni, G., E. Esposito, et al. (2010). "Role of serotonin in central dopamine dysfunction." CNS neuroscience & therapeutics 16(3): 179-194.

Dong, H. W. (2008). The Allen reference atlas: A digital color brain atlas of the C57Bl/6J male mouse, John Wiley & Sons Inc.

Duxon, M. S., T. P. Flanigan, et al. (1997). "Evidence for expression of the 5-hydroxytryptamine-2B receptor protein in the rat central nervous system." Neuroscience 76(2): 323-329.

Ferre, S. and F. Artigas (1993). "Dopamine D2 receptor-mediated regulation of serotonin extracellular concentration in the dorsal raphe nucleus of freely moving rats." J Neurochem 61(2): 772-775.

Fields, H. L., G. O. Hjelmstad, et al. (2007). "Ventral tegmental area neurons in learned appetitive behavior and positive reinforcement." Annual Review of Neuroscience 30: 289-316.

Fletcher, P. J. and K. M. Korth (1999). "Activation of 5-HT1B receptors in the nucleus accumbens reduces amphetamine-induced enhancement of responding for conditioned reward." Psychopharmacology (Berl) 142(2): 165-174.

Gale, J. T., D. C. Shields, et al. (2014). "Reward and reinforcement activity in the nucleus accumbens during learning." Front Behav Neurosci 8: 114.

Gerard, C., S. el Mestikawy, et al. (1996). "Quantitative RT-PCR distribution of serotonin 5-HT6 receptor mRNA in the central nervous system of control or 5,7-dihydroxytryptamine-treated rats." Synapse 23(3): 164-173.

Groenewegen, H. J. and H. B. Uylings (2000). "The prefrontal cortex and the integration of sensory, limbic and autonomic information." Prog Brain Res 126: 3-28.

Haber, S. N. and B. Knutson (2010). "The Reward Circuit: Linking Primate Anatomy and Human Imaging." Neuropsychopharmacology 35(1): 4-26.

Harris, G. C. and G. Aston-Jones (2006). "Arousal and reward: a dichotomy in orexin function." Trends Neurosci 29(10): 571-577.

Higgins, G. A. and P. J. Fletcher (2003). "Serotonin and drug reward: focus on 5-HT2C receptors." Eur J Pharmacol 480(1-3): 151-162.

Hikosaka, O. (2010). "The habenula: from stress evasion to value-based decision-making." Nature Reviews Neuroscience 11(7): 503-513.

Ikemoto, S. (2010). "Brain reward circuitry beyond the mesolimbic dopamine system: a neurobiological theory." Neurosci Biobehav Rev 35(2): 129-150.

Kapur, S. and G. Remington (1996). "Serotonin-dopamine interaction and its relevance to schizophrenia." Am J Psychiatry 153(4): 466-476.

Katsidoni, V., K. Apazoglou, et al. (2011). "Role of serotonin 5-HT2A and 5-HT2C receptors on brain stimulation reward and the reward-facilitating effect of cocaine." Psychopharmacology (Berl) 213(2-3): 337-354.

Kelley, A. E. (2004). "Ventral striatal control of appetitive motivation: role in ingestive behavior and reward-related learning." Neurosci Biobehav Rev 27(8): 765-776.

Kitahama, K., I. Nagatsu, et al. (2000). "Distribution of dopamine-immunoreactive fibers in the rat brainstem." J Chem Neuroanat 18(1-2): 1-9.

Kohler, C., V. Chanpalay, et al. (1982). "The Distribution and Origin of Serotonin-Containing Fibers in the Septal Area - a Combined Immunohistochemical and Fluorescent Retrograde Tracing Study in the Rat." Journal of Comparative Neurology 209(1): 91-111.

Koob, G. F. and M. Le Moal (2008). "Addiction and the brain antireward system." Annu Rev Psychol 59: 29-53.

Lammel, S., A. Hetzel, et al. (2008). "Unique properties of mesoprefrontal neurons within a dual mesocorticolimbic dopamine system." Neuron 57(5): 760-773.

Lammel, S., B. K. Lim, et al. (2013). "Reward and aversion in a heterogeneous midbrain dopamine system." Neuropharmacology.

LeDoux, J. (2003). "The emotional brain, fear, and the amygdala." Cell Mol Neurobiol 23(4-5): 727-738.

Lee, H. J., D. S. Wheeler, et al. (2011). "Interactions between amygdala central nucleus and the ventral tegmental area in the acquisition of conditioned cue-directed behavior in rats." European Journal of neuroscience 33(10): 1876-1884.

Lee, H. S., Y. J. Eum, et al. (2007). "Projection patterns from the amygdaloid nuclear complex to subdivisions of the dorsal raphe nucleus in the rat." Brain Research 1143: 116-125.

Liu, Z., J. Zhou, et al. (2014). "Dorsal raphe neurons signal reward through 5-HT and glutamate." Neuron 81(6): 1360-1374.

Liu, Z. X., J. F. Zhou, et al. (2014). "Dorsal Raphe Neurons Signal Reward through 5-HT and Glutamate." Neuron 81(6): 1360-1374.

Lodge, D. J. and A. A. Grace (2006). "The laterodorsal tegmentum is essential for burst firing of ventral tegmental area dopamine neurons." Proceedings of the National Academy of Sciences of the United States of America 103(13): 5167-5172.

Macoveanu, J. (2014). "Serotonergic modulation of reward and punishment: evidence from pharmacological fMRI studies." Brain Research 1556: 19-27.

Maroteaux, L., F. Saudou, et al. (1992). "Mouse 5HT1B serotonin receptor: cloning, functional expression, and localization in motor control centers." Proceedings of the National Academy of Sciences of the United States of America 89(7): 3020-3024.

Matsumoto, M. and O. Hikosaka (2007). "Lateral habenula as a source of negative reward signals in dopamine neurons." Nature 447(7148): 1111-U1111.

Matthes, H., U. Boschert, et al. (1993). "Mouse 5-hydroxytryptamine 5A and 5-hydroxytryptamine 5B receptors define a new family of serotonin receptors: cloning, functional expression, and chromosomal localization." Mol Pharmacol 43(3): 313-319.

Meador-Woodruff, J. H., A. Mansour, et al. (1992). "Distribution of D5 dopamine receptor mRNA in rat brain." Neurosci Lett 145(2): 209-212.

Moukhles, H., O. Bosler, et al. (1997). "Quantitative and morphometric data indicate precise cellular interactions between serotonin terminals and postsynaptic targets in rat substantia nigra." Neuroscience 76(4): 1159-1171.

Nakamura, K. (2013). "The role of the dorsal raphe nucleus in reward-seeking behavior." Front Integr Neurosci 7: 60.

Neumaier, J. F., T. J. Sexton, et al. (2001). "Localization of 5-HT7 receptors in rat brain by immunocytochemistry, in situ hybridization, and agonist stimulated cFos expression." J Chem Neuroanat 21(1): 63-73.

O'Malley, K. L., S. Harmon, et al. (1992). "The rat dopamine D4 receptor: sequence, gene structure, and demonstration of expression in the cardiovascular system." New Biol 4(2): 137-146.

O'Connell, L. A. and H. A. Hofmann (2011). "Genes, hormones, and circuits: An integrative approach to study the evolution of social behavior." Frontiers in neuroendocrinology 32(3): 320-335.

Pecina, S., K. S. Smith, et al. (2006). "Hedonic hot spots in the brain." Neuroscientist 12(6): 500-511.

Pentkowski, N. S., F. D. Duke, et al. (2010). "Stimulation of Medial Prefrontal Cortex Serotonin 2C (5-HT2C) Receptors Attenuates Cocaine-Seeking Behavior." Neuropsychopharmacology 35(10): 2037-2048.

Peyron, C., J. M. Petit, et al. (1998). "Forebrain afferents to the rat dorsal raphe nucleus demonstrated by retrograde and anterograde tracing methods." Neuroscience 82(2): 443-468.

Pierce, R. C. and V. Kumaresan (2006). "The mesolimbic dopamine system: the final common pathway for the reinforcing effect of drugs of abuse?" Neurosci Biobehav Rev 30(2): 215-238.

Pompeiano, M., J. M. Palacios, et al. (1992). "Distribution and cellular localization of mRNA coding for 5-HT1A receptor in the rat brain: correlation with receptor binding." Journal of Neuroscience 12(2): 440-453.

Pompeiano, M., J. M. Palacios, et al. (1994). "Distribution of the serotonin 5-HT2 receptor family mRNAs: comparison between 5-HT2A and 5-HT2C receptors." Brain Res Mol Brain Res 23(1-2): 163-178.

Proitsi, P., M. K. Lupton, et al. (2012). "Association of serotonin and dopamine gene pathways with behavioral subphenotypes in dementia." Neurobiol Aging 33(4): 791-803.

Rodd-Henricks, Z. A., D. L. McKinzie, et al. (2002). "Cocaine is self-administered into the shell but not the core of the nucleus accumbens of Wistar rats." Journal of Pharmacology and Experimental Therapeutics 303(3): 1216-1226.

Russo, S. J. and E. J. Nestler (2013). "The brain reward circuitry in mood disorders." Nat Rev Neurosci 14(9): 609-625.

Saito, R., M. E. Smoot, et al. (2012). "A travel guide to Cytoscape plugins." Nat Methods 9(11): 1069-1076.

Salamone, J. D., M. Correa, et al. (2005). "Beyond the reward hypothesis: alternative functions of nucleus accumbens dopamine." Curr Opin Pharmacol 5(1): 34-41.

Schultz, W. (2013). "Updating dopamine reward signals." Curr Opin Neurobiol 23(2): 229-238.

Soubrie, P. (1986). "Reconciling the Role of Central Serotonin Neurons in Human and Animal Behavior." Behavioral and Brain Sciences 9(2): 319-335.

Steinbusch, H. W. (1981). "Distribution of serotonin-immunoreactivity in the central nervous system of the rat-cell bodies and terminals." Neuroscience 6(4): 557-618.

Tao, R., Z. Ma, et al. (2006). "Differential effect of orexins (hypocretins) on serotonin release in the dorsal and median raphe nuclei of freely behaving rats." Neuroscience 141(3): 1101-1105.

Tecott, L., A. Maricq, et al. (1993). "Nervous system distribution of the serotonin 5-HT3 receptor mRNA." Proceedings of the National Academy of Sciences of the United States of America 90(4): 1430.

Tritsch, N. X. and B. L. Sabatini (2012). "Dopaminergic modulation of synaptic transmission in cortex and striatum." Neuron 76(1): 33-50.

Tye, K. M., J. J. Mirzabekov, et al. (2013). "Dopamine neurons modulate neural encoding and expression of depression-related behaviour." Nature 493(7433): 537-541.

Ungless, M. A. and A. A. Grace (2012). "Are you or aren't you? Challenges associated with physiologically identifying dopamine neurons." Trends Neurosci 35(7): 422-430.

van den Heuvel, M. P. and O. Sporns (2011). "Rich-club organization of the human connectome." The Journal of Neuroscience 31(44): 15775-15786.

Vilaró, M., R. Cortés, et al. (2005). "Serotonin 5HT4 receptors and their mRNAs in rat and guinea pig brain: Distribution and effects of neurotoxic lesions." The Journal of comparative neurology 484(4): 418-439.

Weiner, D. M., A. I. Levey, et al. (1991). "D1 and D2 dopamine receptor mRNA in rat brain." Proc Natl Acad Sci U S A 88(5): 1859-1863.

CONCLUSIONS

This dissertation set out to investigate the interaction of neuromodulators and their role in modulating fundamental behaviors by using computational modeling, game theory, embodiment, pharmacological manipulations, and neuroinformatics. While much is known about neuromodulators, their structural and functional implications in fundamental behavior are still not clear. This final chapter will review the research contributions of this dissertation, as well as discuss new directions for future research.

Contributions

Chapter 1 introduced a novel computational model that investigated how dopamine and serotonin shaped competitive and cooperative situations in game theoretic environments. This computational model was based assumptions that dopaminergic activity increases as expected reward increases, and serotonergic activity increases as the expected cost of an action increases. Results from Chapter 1 agreed with proposed theoretical work (Boureau and Dayan 2011), in which the influence of serotonergic and dopaminergic systems are sometimes in opposition. Yet, this opposition is necessary for the model to select appropriate actions. This model was capable of predicting how the neuromodulatory systems shape decision-making and adaptive behavior in competitive and cooperative situations.

Chapter 2 adopted the computational model from Chapter 1 to conduct a human subject experiment. The study put human subjects up against an adaptive model that did not depend on fixed strategies in games of conflict. The study was

designed to gauge subjects' reactions to playing against adaptive agents, as well as measuring the influence of embodied agents on game play. Chapter 2 involved ATD, a dietary manipulation that temporarily lowers serotonin levels in the human central nervous system, resulting in decreased cooperation and lowered harm-aversion (Wood, Rilling et al. 2006; Crockett, Clark et al. 2008). When playing against an aggressive version of the model, there was a significant shift in the subjects' strategy. Subjects also became retaliatory when confronted with agents that tended towards risky behavior. These results highlighted the important interactions between subjects and agents utilizing adaptive behavior. Moreover, like in Chapter 1, the study revealed neuromodulatory mechanism that gives rise to cooperative and competitive behaviors.

Chapter 3 investigated functional activity of these neuromodulatory circuits by exploring the expression energy of cholinergic, dopaminergic, noradrenergic, and serotonergic receptors. Expression energy data from these neuromodulatory receptors were examined in the amygdala, which is thought to be a major target of neuromodulation, and within the sources of neuromodulation themselves, which are all are localized in small subcortical nuclei. Based on these assumptions, connectivity relationships can be inferred by examining the expression energy of receptors specific to those neuromodulatory systems. The survey was conducted using the Allen Mouse Brain Atlas (ABA) as a resource to obtain expression energy data. Results revealed that the substantia innominanta, amygdala and ventral tegmental area all displayed high receptor expression across the classic

neuromodulatory systems. In contrast, the locus coeruleus displayed low receptor expression energy overall. The expression of cholinergic receptors, in particular, was an order of magnitude greater than other neuromodulatory receptors. The comprehensive analysis proposed connectivity relationships, identifying substantia innominanta and ventral tegmental area as the main hubs of neuromodulation activity. The analysis also reported receptor localization in brain regions that were previously undetected according to literature. The methodology presented here may be applied to other neural systems with similar characteristics, and to other animal models as these brain atlases become available.

Inspired by challenges encountered in retrieving and analyzing expression energy data in Chapter 3, a web application called the Allen Brain Atlas-Driven Visualization (ABADV) was implemented in Chapter 4. ABADV was developed to extend the ABA by providing users with a quick and intuitive way to survey large amounts of expression energy data across multiple brain regions of interest. Though the ABA offers their own search engine and software for researchers to view their growing collection of online public data sets, many of their tools limit the amount of genes and brain structures researchers can view at once. Researchers can use ABADV to immediately obtain and survey numerous amounts of expression energy data from the ABA. ABADV was demonstrated by querying available dopamine and serotonin receptor genes. This query helped identify prevalent genes and brain structures that may otherwise be obscured in other types of visualizations. By creating this web application, researchers can immediately obtain and survey

numerous amounts of expression energy data from the ABA, which they can then use to supplement their work or perform meta-analysis.

Chapter 5 continued exploring the interaction of dopamine and serotonin by focusing specifically on the reward circuit. Using similar methodologies from Chapter 3 and 4, dopaminergic and serotoninergic receptor gene expression energy were retrieve from the ABA across available brain structures associated with reward processing. This survey was based on the notion that the ventral tegmental area and dorsal raphe, the site of origin for dopamine and serotonin respectively, both receive common inputs and innervate common output regions that have been shown to process rewards. Between the two neuromodulators, it was a select subset of serotonin receptors that was overall more expressed across the reward circuit, which may suggest serotonin having a principal involvement in reward processing. To the contrary, dopamine receptors were almost exclusively designated in the nucleus accumbens, which may suggest selective involvement in reward processing. However, the ventral tegmental area, substantia nigra pars compacta, and substantia nigra pars reticulata all clustered together based on similar expression profile, as well as anatomical location, suggests a dopaminergic sub-circuit that projects to reward circuit regions. Lastly, much like in Chapter 3, the ABA helped clear up discrepancies from rodent brain-based literature reporting of dopamine and serotonin receptor gene expression data in the reward circuit by filling in the missing gaps of expression energy profile information.

The key findings of each chapter help contribute their share of knowledge on the interaction of neuromodulators and its role in modulating fundamental behaviors. Though each chapter took a very different approach (computational modeling, game theory, embodiment, pharmacological manipulations and neuroinformatics), they all shed new light from their own perspectives. Chapters 1 and 2 provided a more behavioral understanding of how dopamine and serotonin interacts, what that interaction might look like in the brain, and how those interactions transpire in complex situations. Chapters 3, 4, and 5, on the other hand, used an informatics approach to reveal the underlying empirical structure and function behind the interactions of dopamine, serotonin, acetylcholine and norepinephrine in brain regions responsible for the behaviors witnessed in Chapters 1 and 2.

When combined, each perspective provides an additional level of understanding regarding neuromodulators. This is of great importance because neuroscience simply cannot be explained through one methodology. It is going to take a multifaceted effort, like the one presented in this dissertation, to obtain a deeper understanding of the complexity behind neuromodulators and their structural and functional relationship with one another. For instance, Chapters 1 and 2 demonstrated that computational modeling, alongside dietary manipulations, embodiment and game theory, can serve as a great apparatus for investigating complex behaviors. But how can these approaches inform us about the distribution of inhibitory versus excitatory neurotransmitter receptors, which is information

needed in the first place to accurately model the system under study? This is especially crucial to someone conducting a computational modeling study, as they likely want their model to fully adhere to the biological constraints of the mammalian brain. Doing so would lead to more definitive, rather than speculative, predictions about brain phenomena. Thereby, one might want to combine the empirical findings from Chapters 3, 4 and 5 to refine the models from Chapters 1 and 2, which can then help in developing better treatment for patients with brain-related disorders, or technical applications that utilize brain-like computations to perform tasks.

Future Research

Investigating the complexities of neuromodulatory systems using various techniques from various disciplines provides a natural guide to future research. While other researchers may investigate neuromodulatory systems using electrophysiology, pharmacology, genetics, brain imaging, or other techniques in neuroscience, this dissertation took a multidisciplinary approach, emphasizing the combination of neuroscience, computation, embodiment and informatics to answer questions about the interaction of neuromodulators. Other researchers could adopt a similar approach and combine these resources to either study a biological question; develop and evaluate a new method; or integrate, annotate and analyze data to build new data resources (Rung and Brazma 2013). This approach may also accelerate scientific and technological progress, which could result in major clinical and economical benefits. As time and resources are spent more in viewing and

integrating data in novel dimensions, research could become less duplicative and enable more theoretical considerations of these neuromodulatory systems and their underlying structural and functional mechanisms. Utilizing various techniques and publicly accessible data may provide a strong approach toward making predictions about the neurobiology that ties neuromodulators to motivated behavior.

The computational models in Chapter 1 and 2 were rather abstract and could benefit from incorporating additional empirical data collected from the mammalian brain studies (Asher, Craig et al. 2013). For instance, functional data from neuroimaging studies can help turn computational models to more biologically realistic by revealing the specific brain areas active during select behaviors. Single unit recording studies in animals can also inform these computational models on how they dictate the more granular neural behavior within each modeled brain region. Empirical data provides the base assumptions that guide the neural behavior and architecture of computational models, making these models more biologically realistic. Improved biological plausibility can increase the efficacy of theoretical predictions made by our models, resulting in better theories to be tested through future neurophysiological and neuroimaging experiments.

Much research also remains to be done in investigating the role of serotonin and dopamine in the reward circuit. Numerous studies have reported that dopamine activations are primarily driven by reward, which in turn causes dopamine to regulate emotional and motivational behavior through the mesolimbic-cortical pathway (Baik 2013; Schultz 2013). As discussed in Chapter 5, though there

are many arguments that also support the role of serotonin in modulating these same behaviors through the same pathway, the specific mechanisms by which serotonin is having an affect is unclear (Cools, Nakamura et al. 2011; Nakamura 2013). Under the assumption that the more expression found in a particular gene the more functional responsibility that gene has in a brain area, results from surveying the ABA in Chapter 5 suggest that serotonin was responsible for the functional activity of brain areas associated with reward processing. Future work may further this neuroinformatics approach by analyzing other genes involved in the signaling of dopamine and serotonin beyond receptors, such as genes involved in the reuptake or transporting of these neurotransmitters. This may verify the exact quantitative profile of these neuromodulators in the reward circuit.

References

Asher, D. E., A. B. Craig, et al. (2013). "A dynamic, embodied paradigm to investigate the role of serotonin in decision-making." Front Integr Neurosci 7.

Baik, J. H. (2013). "Dopamine signaling in reward-related behaviors." Front Neural Circuits 7: 152.

Boureau, Y. L. and P. Dayan (2011). "Opponency Revisited: Competition and Cooperation Between Dopamine and Serotonin." Neuropsychopharmacology 36(1): 74-97.

Cools, R., K. Nakamura, et al. (2011). "Serotonin and Dopamine: Unifying Affective, Activational, and Decision Functions." Neuropsychopharmacology 36(1): 98-113.

Crockett, M. J., L. Clark, et al. (2008). "Serotonin modulates behavioral reactions to unfairness." Science 320(5884): 1739.

Nakamura, K. (2013). "The role of the dorsal raphe nucleus in reward-seeking behavior." Front Integr Neurosci 7: 60.

Rung, J. and A. Brazma (2013). "Reuse of public genome-wide gene expression data." Nature Reviews Genetics 14(2): 89-99.

Schultz, W. (2013). "Updating dopamine reward signals." Curr Opin Neurobiol 23(2): 229-238.

Wood, R. M., J. K. Rilling, et al. (2006). "Effects of tryptophan depletion on the performance of an iterated Prisoner's Dilemma game in healthy adults." Neuropsychopharmacology 31(5): 1075-1084